Antigen-specific human B cells in viral and autoimmune conditions

Inauguraldissertation

zur
Erlangung der Würde eines Doktors der Philosophie
vorgelegt der
Philosophisch-Naturwissenschaftlichen Fakultät
der Universität Basel

von

Natalie Rose

2020

Genehmigt von der Philosophisch-Naturwissenschaftlichen Fakultät

auf Antrag von

Prof. Dr. Tobias Derfuss

Prof. Dr. Christoph Hess

Prof. Dr. Doron Merkler

Basel, den 17.12.2019

Prof. Dr. Martin Spiess

Dekan

We keep moving forward, opening new doors, and doing new things, because we're curious and curiosity keeps leading us down new paths.

Walt Disney

Table of Contents

Acknowledgements

First and foremost, I would like to thank Professor Tobias Derfuss for giving me the opportunity to pursue a PhD in his Clinical Neuroimmunology group at the Department of Biomedicine. His guidance and scientific expertise were instrumental in completing this work, and his support and patience helped calm down my nerves and motivate me when experiments failed and my frustration was high.

I want to express my gratitude to Professor Raija Lindberg, who tirelessly worked at uniting all of us in lab 302. Thank you for your making the lab a space where everyone enjoys to come to work, and for so graciously opening your home to us for your famous Garden Parties.

My sincere thanks go to the members of my PhD committee, Professor Christoph Hess and Associate Professor Doron Merkler, for fruitful discussions of my research.

I am grateful for the support of Nicholas Sanderson, who never tired of answering my questions and whose enthusiasm for research is simply infectious. I will miss our scientific discussions, hilarious innuendoes, and my shenanigans involving your mug. I apologize for conspiring to kidnap your mug, although I do think it thoroughly enjoyed its little trip to Italy.

I want to thank the past and present members of lab 302 for their encouragement, many delicious souvenirs, and good times in the lab. Thank you Svenya, Maria, Hailey and Ilaria (the Derfuss girlies), Panos, and Zuzanna for your friendship.

I sincerely thank all of my friends in other labs at DBM. Nadine, Julia, Claudi, Lukas, and Jonas never failed to put a smile on my face. I will miss heading to Centrino at 4 pm to get delicious discounted pastries and all the good times in the tissue culture lab with you.

I want to give thanks to the nurses of the neurologic clinic and policlinic who were always willing to take blood from patients or controls for me and who I will remember as some of the friendliest employees of the University Hospital Basel.

My appreciation goes to the doctors of the neurologic clinic and policlinic and in particular to Dr. Eva Kesenheimer for recruiting patients for my research project.

Finally, I am deeply grateful for the willingness of so many patients with myasthenia gravis to donate some of their blood for research purposes and I hope that our work can contribute to the further understanding of the pathogenesis of this disease.

Last but not least, I want to thank my parents, my brothers, and my amazing friends for always being there to support me and build me up. I appreciated when you listened to me excitedly talk about my research, or complain about failed experiments despite the fact that you probably still don’t really understand just what it is that I did in the lab all these years (don’t worry, I feel the same way sometimes).

Abbreviations

α-BTX	α-bungarotoxin
AChR	acetylcholine receptor
AID	activation-induced cytidine deaminase
APC	antigen-presenting cell
BCR	B cell receptor
BSA	bovine serum albumin
CDR	complementarity-determining region
D	diversity
dsDNA	double-stranded deoxyribonucleic acid
EAMG	experimental autoimmune myasthenia gravis
EBV	Epstein-Barr virus
ELISA	enzyme-linked immunosorbent assay
Fab	fragment antigen-binding
FACS	fluorescence-activated cell sorting
FCS	fetal calf serum
FDC	follicular dendritic cell
FR	framework region
GC	germinal center
GMFI	geometric mean fluorescence intensity
HA	influenza haemagglutinin

HC	healthy control
IL	interleukin
J	joining
LPS	lipopolysaccharide
LRP4	low-density lipoprotein receptor-related protein 4
mAb	monoclonal antibody
MAC	membrane-attack complex
MG	myasthenia gravis
MIR	main immunogenic region
MuSK	muscle-specific kinase
NMJ	neuromuscular junction
PBMCs	peripheral blood mononuclear cells
PCR	polymerase chain reaction
rec	recombinant
RIA	radioimmunoassay
SHM	somatic hypermutation
SLE	systemic lupus erythematosus
ssDNA	single-stranded deoxyribonucleic acid
V	variable

Summary

Background and rationale: The low frequency of the antigen specific B cells in the peripheral blood and the complexity of the epitopes they recognize are some of the features of the human immune response that make the isolation and characterization of B cells with a given specificity challenging. While studies of serum and plasma have shown that antibodies that bind to the acetylcholine receptor (AChR) are the main driver of pathogenicity in patients with AChR-myasthenia gravis (MG), little is known about the B cells that secrete these antibodies which hampers the development of more targeted therapeutics.

Results: In the first part of this thesis, we established a novel method for the isolation of B cells recognizing membrane-expressed antigens using influenza haemagglutinin (HA) as a model antigen. We demonstrated that B cells can extract HA together with its intracellular GFP-tag from the plasma membrane of HA-expressing cells and subsequently become activated as evidenced by upregulation of surface-expressed CD69. Most of the HA-specific peripheral B cells after influenza vaccination were somatically hypermutated and their $CD20^{+}CD27^{+}CD71^{+}CD21^{low}$ phenotype matched that of antigen-experienced activated B cells.

In the second part of this thesis, we then adapted the membrane-antigen capture model to isolate B cells that recognize acetylcholine receptor from patients with myasthenia gravis and from healthy controls (HC). From 3 patient with MG, we isolated 6 IgG^{+} AChR-specific B cells: 3 IgG_1, 1 IgG_3, and 2 clonally related IgG_4 B cells. We provided evidence that somatically hypermutated and clonally expanded AChR-specific IgM B cells circulate not only in patients with MG, but also in HCs. AChR-specific IgG B cells were monoreactive, whereas the IgM compartment contained both polyreactive and monoreactive clones.

Conclusion: We have developed a sensitive approach for the isolation of human B cells with a rare antigen specificity that retains conformational epitopes even of large and complex antigens such as multiprotein receptor units. We generated a diverse dataset of AChR-specific BCR sequences from MG patients and HCs that is currently unparalleled. The presence of somatically hypermutated, expanded AChR-specific IgM clones in HCs raises questions on the antigen-experience of these B cells, the pathogenicity of the expressed antibodies, and the presence of an unknown post-germinal center tolerance checkpoint.

Introduction

The generation of B cell receptors

B lymphocytes differentiate from common lymphoid progenitor cells in the bone marrow. The ability of B cells to produce antibodies that bind an antigen with high specificity and affinity makes B cells a key component of the adaptive immune response.

Sequencing of non-B cells revealed that the human genome contains over 30 variable (V) gene segments and 5 to 6 joining (J) gene segments for each of the heavy, and the kappa and lambda light chains. The heavy chain locus further contains more than 20 diversity (D) gene segments. During their development, B cells rearrange these gene segments retaining only 1 segment of each V(D)J in a process called somatic recombination (1).

The combinatorial diversity created by the combinations of a V, a D, and a J gene segment means that a sheer unlimited repertoire of antibodies can be generated. The diversity of the immunoglobulin repertoire is further increased by the addition or deletion of nucleotides at the joints between these gene segments, the pairing of a heavy with a light chain, and finally by the generation of somatic hypermutations once a B cell has recognized its antigen and becomes activated.

The V, D, and J gene segments together form the variable region of the heavy chain while the light chain variable region consists of a V and J gene each. Framework regions (FR) provide the structure of the antibody by forming β sheets and the three complementarity-determining regions (CDR) encode for three hypervariable loops that are exposed at the outer edges of the antibody. The pairing of the three hypervariable loops of the heavy and of the light chain form the paratope whose interaction with its epitope determines the specificity of the antibody. Paratope-epitope interactions are often described in terms of interactions between amino acids or amino acid residues, but the interactions take place at the atomic level, are dynamic and time-dependent (2), which makes them particularly hard to predict with algorithms.

Immune checkpoints

The potential to create B cell receptors (BCR) with virtually any given specificity also bears the risk of creating B cells that recognize self-proteins and are potentially harmful. In 1960, the Nobel prize in medicine was award to Sir Macfarlane Burnet and Peter Medawar for the "discovery of acquired immunological tolerance". They provided evidence that self-discrimination is not pre-determined but instead a gradual process that happens during embryonic development.

Once a B cell has successfully rearranged a heavy and a light chain, it expresses IgM on its surface and enters the stage of an immature B cell. At this point, the BCR's interaction with proteins in the bone marrow determines its fate. Immature B cells whose BCR binds weakly to self-antigens develop into mature B cells that leave the bone marrow and migrate to the periphery. When an immature B cell encounters an antigen in the bone marrow that cross-links its BCRs, the development is arrested. Self-reactive B cells can either be eliminated by apoptosis, perform receptor editing by rearranging a new light chain, or become anergic. This process is called central tolerance. Analyses of the specificities of immature B cells from the bone marrow of humans suggest that up to 75% of the nascent B cells are autoreactive and that this number decreases to about 20% of mature, peripheral blood B cells (3). B cells that bind to a strongly cross-linking self-antigen in the periphery in the absence of infection will become apoptotic. In contrast, B cells that recognize an abundant soluble antigen enter a state of anergy where they do not secrete antibodies and reduce the expression of surface IgM (4). These tolerance mechanisms are referred to as peripheral tolerance because they take place outside of the central lymphoid organs.

The introduction of somatic hypermutations in antibodies during the germinal center reaction can lead to the development of autoreactivity (5). Studies of high-affinity anti-DNA IgG antibodies from patients with systemic lupus erythematosus suggest that the germline precursor forms were not reactive to DNA (6). It is thus assumed that a third, post-GC checkpoint exists and that defects in this checkpoint contribute to the pathogenesis of autoimmunity, but its exact mode of action is still under investigation.

Affinity maturation

It has been observed that the affinity of serum antibodies after immunization increases dramatically over time. The dawn of the sequencing era finally showed that the increase in affinity is due to the introduction of somatic hypermutations (SHM) in the variable region of lower affinity germline V(D)J sequences. This process is called affinity maturation and is thought to take place in germinal centers (GC), specialized structures in secondary lymphoid organs that form approximately one week after the exposure to an antigen. The anatomy of the germinal center is divided into two distinct zones. A light zone containing follicular dendritic cells (FDC), T cells, tingible body macrophages, and B cells forms close to the lymph node capsule or the marginal zone of the spleen. The adjacent dark zone lays above the T cell zone and mostly contains activated B cells that proliferate extensively (7).

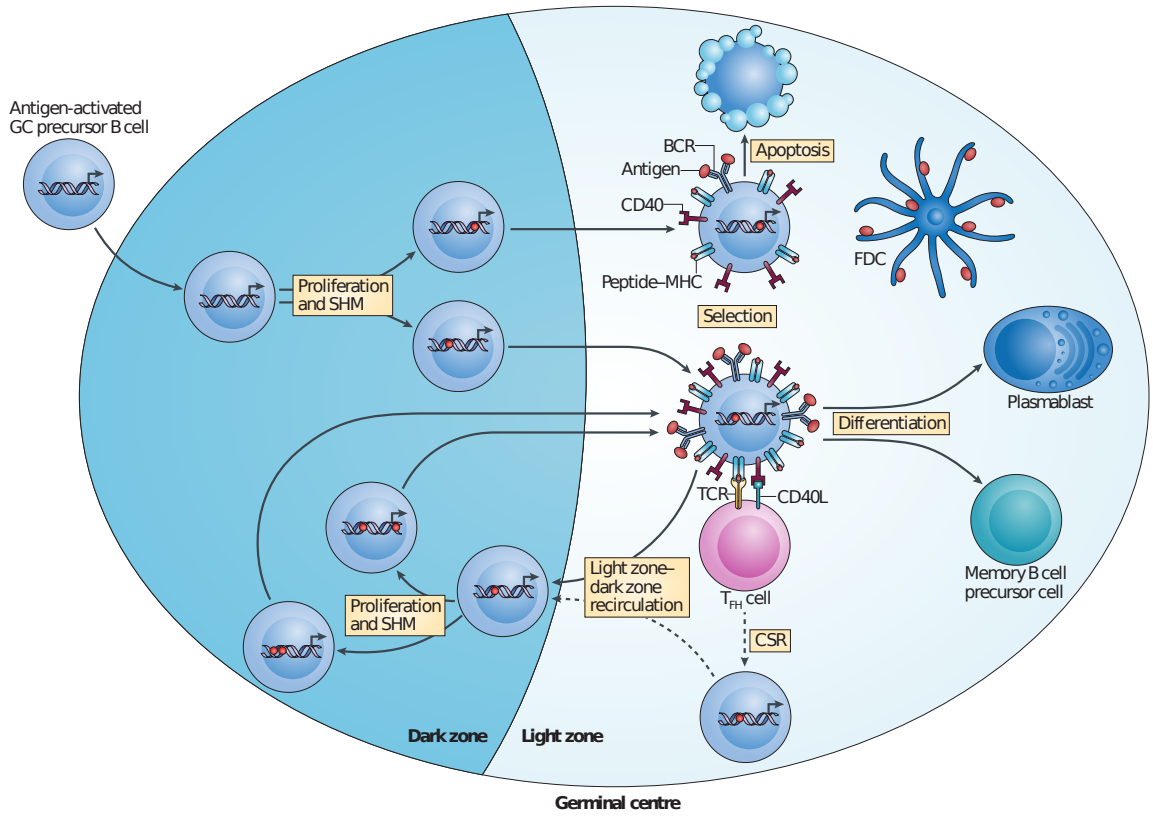

Figure 1 Schematic of the cells and mechanisms involved in the germinal center reaction
Reprinted from Da Silva and Klein, Nature Reviews Immunology, 2015 (7)

GC B cells express the enzyme activation-induced cytidine deaminase (AID). AID can bind to single-stranded DNA only, which means its activity of deaminating cytidine residues is

confined to genes that are being transcribed. AID generates uridine from cytidine which in turn triggers DNA repair mechanisms such as mismatch repair and base-excision repair. These repair mechanisms lead to mutations either due to error prone DNA polymerases or because single-strand nicks are filled in with random nucleotides when the cell divides next. Some of these mutations lead to changes in the amino acid sequence. After a timed cell-intrinsic program changes the phenotype of dark zone B cells, they migrate to the light zone (8) where they are selected for their affinity to the antigen by interactions with FDCs and T cells. A higher affinity results in a higher amount of antigen that is captured from FDCs and in turn a higher density of MHC complexes presenting the peptide to T cells, thus more T cell help. B cells that have a lower affinity for the antigen become apoptotic and are phagocytosed by tingible body macrophages. The process is highly dynamic, with naïve B cells entering, and hypermutated B cells recirculating the GC for further rounds of proliferation, mutation, and affinity testing.

The activity of AID can also change the expression of the constant region of the antibody, a process called class-switch recombination. When single-strand breaks occur in two of the switch-regions that precede the constant region genes, the single-strand breaks can be converted into double-strand breaks. The DNA repair mechanism then joins the 2 switch regions together removing the constant region genes that lie between them and putting a different constant region gene closest to the variable region. The constant region of an antibody determines the effector functions of its secreted form, but the processes that drive the reaction towards a certain isotype or subclass are poorly understood.

High affinity B cells will eventually differentiate into either plasmablasts and plasma cells that secrete large amounts of immunoglobulin, or into precursors of memory B cells that form part of the immunological memory.

Antigen-specific IgM B cells have long been thought of as merely a feature of the early immune response, to be replaced quickly by class-switched high affinity antibody producing B cells. We now know that hypermutated IgM memory B cells circulate in the peripheral blood and can persist for many years after vaccination (9,10), but their role is not yet clear. In some studies, it was shown that IgM memory B cells preferentially enter GCs while IgG memory B cells form plasmablasts (11–14). Other studies have demonstrated the opposite: IgM memory B cells rapidly generated plasmablasts upon secondary challenge whereas IgG memory B cells re-entered GCs (15).

Current technologies for isolating B cells of a given antigen-specificity

One of the main obstacles in the research of antigen-specific B cells and the generation of human monoclonal antibodies is the low frequency of B cells specific for a certain antigen. The frequency of IgG B cells specific for tetanus toxoid among IgG-positive memory B cells ranges from only 0.01% up to 0.11% (16).

Many human monoclonal antibodies (mAb) are derived from phage display libraries. B cells are sequenced in bulk and combinatorial libraries of random pairings of heavy and light chain are expressed as single-chain variable antibody fragments or as antigen-binding fragments (Fabs) by bacteriophages (17). The libraries are then screened for the reactivity to a specific antigen. While this approach can yield high affinity neutralizing antibodies that have therapeutic potential (18), it fails to provide information about the repertoire of antigen-specific B cells that is produced naturally in the human body. Antibodies produced by bacteriophages also might be folded differentially and lack mammalian post-translational modifications.

In order to ensure that the recombinant mAb represents an endogenous pairing of heavy and light chain, the isolation of single B cells with the desired antigen-specificity is essential. The immortalization of bulk B cells with Epstein-Barr virus (EBV) and subsequent generation of monoclonal lines via limiting dilution is a low cost but lengthy approach whose efficiency depends on a high enough percentage of successfully immortalized B cells. The technique is less suited for the isolation of B cells with very rare specificity, but has been used extensively for the production of antiviral human mAbs (19–21).

Antigen peptides or peptide tetramers labeled with fluorescent dyes have been used successfully to fluorescently label and isolate B cells specific for this antigen (16,22,23), but the method is not suitable for large antigens whose epitopes cannot be formed by short peptides or whose epitope is not known. Once a B cells with the desired specificity has been isolated by fluorescence-activated cell sorting (FACS), either the B cell's full transcriptome is sequenced, or the BCR genes are amplified by a reverse-transcription polymerase chain reaction (PCR) with immunoglobulin specific primers (24).

Membrane-antigen capture

It has long been thought that B cells can acquire antigen either in the form of soluble antigen binding to their surface BCR, or by extracting antigen from the surface of specialized antigen-presenting cells (APCs) such as FDCs, dendritic cells or macrophages. Evidence of a third mechanism of antigen uptake through the recognition of membrane-associated antigen was first reported about 20 years ago. Dendritic cells from rats could transfer unprocessed, intact antigen to B cells *in vitro* (25). It was later shown that murine B cells can acquire antigen directly from the membrane of APCs. Intact antigen can be tethered to the membrane of APCs by binding to surface receptors. IgG immune complexes, complexes of soluble antigen and immunoglobulin, bind to Fc-γ receptor II. Antigen that is covered by the complement cascade component C3b is bound to complement receptors such as CD21 (26). When a B cell encounters its cognate antigen in the membrane of a cell, a cluster of BCRs forms at the site of contact (27). The B cell first spreads across the surface of the target cell and subsequently gathers antigen in the center of the immunological synapse by contracting (28). The antigen is then internalized via the BCR, processed, and presented to T cells.

Whether B cells use mechanical forces or enzymes to extract antigen from APCs or plasma membrane has been studied using murine B cells. B cells are able to extract antigen from flexible plasma membrane sheets by pulling on the membrane and invaginating it. The internalization of antigen depends on the high affinity of BCR clusters for the antigen and the fluidity of the antigen-containing membrane (29). While a certain amount of flexibility of the membrane is necessary for the B cell to pinch off the plasma membrane containing the antigen, the stiffness of the membrane of the antigen-expressing cell can contribute to the discrimination of low affinity interactions with the BCR (30).

The recognition of membrane-associated or -expressed antigen by B cells is thought to play an important role in maintaining tolerance. B cells whose BCR bind strongly to membrane-antigens in the bone marrow (31) or the periphery are neutralized by central and peripheral tolerance mechanisms as previously described.

We have recently shown that human B cells that extract their cognate viral antigen from the plasma membrane of antigenic cells can also take up unrelated proteins and subsequently present peptides of these bystander antigens to T cells and receive T cell help (32). This offers an alternative pathway for the development of autoimmune diseases, but whether this process can happen *in vivo* is still under investigation.

Myasthenia gravis – a B cell mediated autoimmune disorder

Myasthenia gravis is a rare neurological autoimmune disease with a prevalence of 138 to 167 cases per million in Northern Europe (33). Autoantibodies that recognize integral proteins at the neuromuscular junction lead to a loss of muscle-type nicotinic acetylcholine receptors (AChR) and thus muscle weakness and fatigability. Patients can be stratified into subgroups according to the target of their autoantibodies or lack of autoantibodies, the age at disease onset, or the presence or absence of thymoma.

Autoantibodies against the AChR are the most common and can be detected in approximately 70% of patients using a commercially available radioimmunoassay (RIA). In a further 5-10% of patients, anti-AChR antibodies can be detected by more sensitive cell-based assays (34). The second most common target of autoantibodies found in 5-8% of patients is the muscle-specific kinase (MuSK) (35), followed by antibodies recognizing low-density lipoprotein receptor-related protein 4 (LRP4) in 1-5% of patients (36). Other autoantibodies such as anti-titin and anti-agrin antibodies are rarely found independently, but in combination with antibodies against the aforementioned targets. The most common autoantibody targets and the proposed pathogenic mechanisms of their binding are illustrated in **Figure *2***.

Thymic changes are often present in patients with AChR-autoantibody mediated MG. An enlargement of the thymus, thymic hyperplasia, is associated with an early onset of the disease, which is defined as onset before 50 years of age. In contrast, an atrophic thymus is more common in patients with a late disease onset (> 50 years). A thymoma is found in 10% of AChR-positive MG patients (37), with an increasing prevalence with increasing age. MG patients with thymoma or thymic hyperplasia are commonly treated with a thymectomy to remove the tumor. Thymectomy has also been shown to improve the outcome of nonthymomatous MG (38).

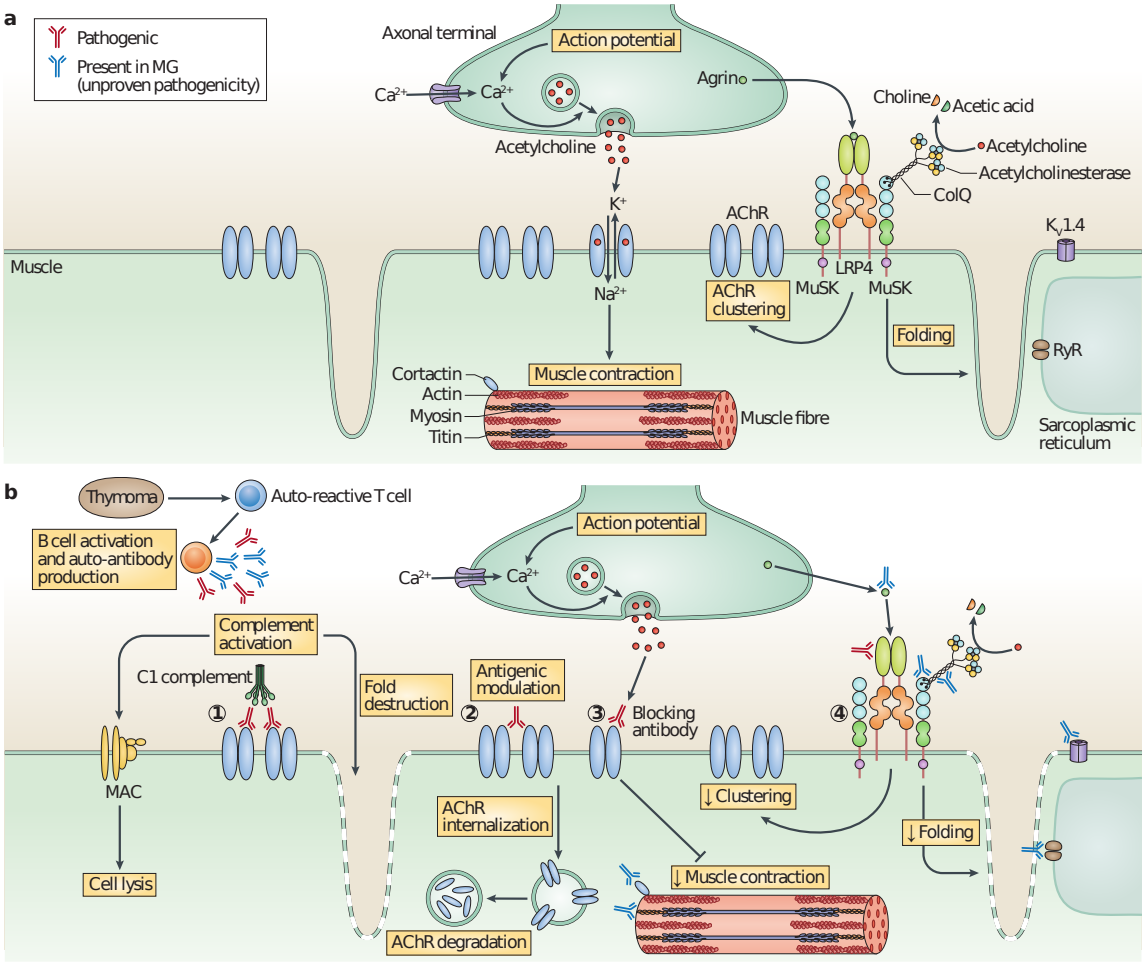

Figure 2 Schematic showing a neuromuscular junction in myasthenia gravis.
The most frequent autoantibodies in myasthenia gravis and their targets at the neuromuscular junction in a. The proposed modes of action that induce the characteristic symptoms of myasthenia gravis are depicted in b.
Adapted from Gilhus et. al., Nature Reviews Neurology, 2016 (39)

Symptoms and diagnosis

The first symptoms typically are restricted to the eye muscles. Intermittent drooping of the eyelid (ptosis) that is usually asymmetrical, and the appearance of double vision (diplopia) define the stage of ocular MG. 85% of MG patients progress to generalized MG and experience weakness and fatigability of all skeletal muscles with pronounced weakness of limbs and muscles needed for swallowing, speech, and in case of myasthenic crisis, breathing (39,40). The condition is diagnosed by a combination of relevant symptoms and positive autoantibody tests. Neurophysiological tests such as electrodiagnostic measurement of muscle innervation (41) and an ice pack test (42) on the drooping eyelid can strengthen the diagnosis particularly in the absence of relevant autoantibodies.

AChR-specific autoantibodies

The AChR is a large, 290 kDa (43) pentameric ion channel consisting of four subunits that each span the plasma membrane four times (44). The fetal form of the receptor consists of two α and one β, γ, and δ subunit each, and is necessary for the proper maturation of the neuromuscular synapse (45). In the early neonatal stages, the γ-subunit is replaced gradually by the adult type ε-subunit in individual endplates (46). Mice deficient for the ε-subunit die two to three months after birth as a result of progressive muscle weakness and atrophy (47).

Antibodies targeting the AChR are the most common and most studied of the autoantibodies in myasthenia gravis. Experiments conducted in the 1980s mostly relied on radio immuno-precipitation of AChR preincubated with ^{125}I-labeled α-bungarotoxin. The AChR used to be commonly purified from the electric organ of the electric ray *Torpedo* and amputated human limbs (48), but has now been replaced by extracting and solubilizing AChR from a human rhabdomyosarcoma cell line. AChR-specific antibodies were found to be polyclonal IgG of all isotypes, with a slight predominance of antibodies of the IgG_1 and IgG_3 subclasses (49). It has been proposed that most of the antibodies in serum are directed against a distinct region on the α-subunit consisting of a number of heterogenous discontinuous epitopes (50,51) which was named main immunogenic region (MIR). Antibodies that bind to the MIR do not directly interfere with the binding of acetylcholine, but can cross-link neighboring AChR and thus facilitate the internalization and subsequent degradation of the receptor in a process called antigenic modulation (52). Reduced availability of complement components in the serum of patients with MG (53), the abundance of the IgG_1 and IgG_3 subclasses that can activate the complement cascade, and complement deposition at neuromuscular junctions (NMJs) (54) point towards a contribution of the complement system to MG pathogenesis by inducing damage to the postsynaptic muscle fiber membrane.

Treatment

Treatment options depend on the subclass of myasthenia gravis and the severity of the symptoms. The first line treatment consists of an acetylcholine esterase inhibitor, immunosuppression with prednisolone and azathioprine, and in case of thymoma or early onset MG, thymectomy. Second line immunosuppressive drugs such as mycophenolate mofetil, cyclosporin, methotrexate, intravenous immunoglobulin, or rituximab are given when first line immunosuppressives do not adequately control the disease. For patients in myasthenic crisis, weakness of the respiratory muscles leading to respiratory failure can become life-threatening, requiring intubation and intensive care. Rapid therapies such as plasma exchange and intravenous immunoglobulin and corticosteroid pulse therapy are recommended in myasthenic crisis (37).

Unmet medical needs

Despite the fact that autoantibodies targeting the NMJ have been determined to be the main cause of pathogenicity in myasthenia gravis nearly 40 years ago (55), how this break in tolerance is generated remains enigmatic and prevents the development of targeted drugs.

Animal models of AChR-MG have indicated that complement-mediated damage to the post-synaptic membrane of the muscle fiber are essential for the induction of EAMG in rodents (56). Complement-deficient mice and rats were resistant to both the passive (57) and the active (58) induction of experimental autoimmune myasthenia gravis (EAMG).

Early studies of human muscle biopsies allege that the terminal lytic component of the complement cascade, the membrane attack complex, is present at 100% of endplates in 30 patients with MG (59). While a phase 2 study showed a significant improvement under eculizumab (60), the results of a recent phase 3 clinical trial, assessing the efficacy of an inhibitor of the complement cascade in patients with refractory MG, were inconclusive (61).

Recently, trials with B cell depleting drugs such as Rituximab have failed to significantly improve the condition in AChR-positive MG (62) but have shown a benefit in MuSK-positive MG (63). This suggests that the titers of pathogenic antibodies are maintained by different mechanisms in the different autoantibody groups of MG.

While thymic changes are often associated with MG, the role of the thymus in MG remains unclear. GCs containing cells reactive to AChR have been found in the thymuses of AChR-positive MG patients with early onset (64), thus far only one human mAb directed against the γ-subunit has been generated from thymic B cells (65). Given that an increased risk of developing another systemic autoimmune disorder later on is associated with thymectomy (66), a clear definition of the subset of MG patients that benefit from this treatment is needed.

While most patients respond well to immunosuppressive drugs, 10-20% of MG patients fail to respond to adequate doses of the available drugs or experience unacceptable adverse reactions to them. These patients continue to require rescue medication and have a higher risk of entering myasthenic crises (67,68). To date, no biomarkers have been associated with refractory MG and new treatments are needed to control the symptoms of these patients.

Aim of the thesis

In the first part of the presented work (Results I), we aimed to establish a suite of techniques that facilitate the isolation of human B cells that recognize membrane antigens from peripheral blood. In contrast to currently available methods for identification of B cells with a given B cell receptor specificity, we hypothesized that the expression of the antigen in the plasma membrane of mammalian cells would be better suited to express the antigen not only in its native conformation, but also with complex mammalian post-translational modifications such as glycosylation. We first demonstrated the validity of the approach with a simple antigen, influenza haemagglutinin. After seasonal vaccination, haemagglutinin specific B cells could be purified from peripheral blood with a specificity of over 90%. The method was however also capable of purifying HA-specific B cells during steady-state. We then characterized B cells isolated by this method to gain further understanding of the phenotype and the BCR repertoire of antigen-specific B cells in a viral vaccine system.

In the second part, we build upon our experiences from isolating haemagglutinin-specific B cells to apply the membrane-antigen capture method to a model with a much higher complexity. In myasthenia gravis, efforts to isolate the AChR-autoantibody producing B cells are impeded in three ways: first, the disease is rare and most patients receive immunosuppressive drugs. Second, the frequency of AChR-specific B cells in the peripheral blood is very low. Third, the antigen is a pentameric membrane protein complex whose epitope depends on correct folding and assembly of the receptor. Furthermore, we did not know whether the forces of the BCR binding to the antigen would be sufficient for B cells to extract this large receptor whose 5 subunits each cross the plasma membrane 4 times. After establishing the method using a cell line expressing GFP-tagged AChR, we performed full RNA repertoire sequencing of the isolated B cells. We then confirmed the specificity of the B cells by producing recombinant human monoclonal antibodies, testing their binding to AChR in a cell-based assay, and performing a polyreactivity ELISA. Sequence analyses provided us with unique insight into the V(D)J gene usage, clonal relations, and presence of somatic hypermutations in peripheral blood AChR-specific B cells.

Results I

frontiers in Immunology

METHODS
published: 16 April 2019
doi: 10.3389/fimmu.2019.00829

Antigen Extraction and B Cell Activation Enable Identification of Rare Membrane Antigen Specific Human B Cells

Maria Zimmermann[1†], Natalie Rose[1†], John M. Lindner[2,3], Hyein Kim[1], Ana Rita Gonçalves[4], Ilaria Callegari[5], Mohammedyaseen Syedbasha[1], Lukas Kaufmann[1], Adrian Egli[1,6], Raija L. P. Lindberg[1], Ludwig Kappos[7], Elisabetta Traggiai[2], Nicholas S. R. Sanderson[1‡] and Tobias Derfuss[8*‡]*

[1] Department of Biomedicine, University Hospital Basel, University of Basel, Basel, Switzerland, [2] Novartis Institute for BioMedical Research, Basel, Switzerland, [3] BioMed X Innovation Center, Heidelberg, Germany, [4] Laboratory of Virology, Geneva University Hospitals, Geneva, Switzerland, [5] Neuroscience Consortium, Monza Policlinico and Pavia Mondino, University of Pavia, Pavia, Italy, [6] Division of Clinical Microbiology, University Hospital Basel, University of Basel, Basel, Switzerland, [7] Departments of Medicine, Neurologic Clinic and Policlinic, Clinical Research and Biomedical Engineering, University Hospital and University of Basel, Basel, Switzerland, [8] Department of Medicine, Neurologic Clinic and Policlinic, University Hospital and University of Basel, Basel, Switzerland

OPEN ACCESS

Edited by:
Michael R. Gold, University of British Columbia, Canada

Reviewed by:
Maria-Isabel Yuseff, Pontificia Universidad Católica de Chile, Chile
Katelyn Spillane, King's College London, United Kingdom

***Correspondence:**
Nicholas S. R. Sanderson
nicholas.sanderson@unibas.ch
Tobias Derfuss
tobias.derfuss@usb.ch

[†]These authors have contributed equally to this work

[‡]These authors share senior authorship

Specialty section:
This article was submitted to B Cell Biology, a section of the journal Frontiers in Immunology

Received: *21 December 2018*
Accepted: *28 March 2019*
Published: *16 April 2019*

Citation:
Zimmermann M, Rose N, Lindner JM, Kim H, Gonçalves AR, Callegari I, Syedbasha M, Kaufmann L, Egli A, Lindberg RLP, Kappos L, Traggiai E, Sanderson NSR and Derfuss T (2019) Antigen Extraction and B Cell Activation Enable Identification of Rare Membrane Antigen Specific Human B Cells. Front. Immunol. 10:829. doi: 10.3389/fimmu.2019.00829

Determining antigen specificity is vital for understanding B cell biology and for producing human monoclonal antibodies. We describe here a powerful method for identifying B cells that recognize membrane antigens expressed on cells. The technique depends on two characteristics of the interaction between a B cell and an antigen-expressing cell: antigen-receptor-mediated extraction of antigen from the membrane of the target cell, and B cell activation. We developed the method using influenza hemagglutinin as a model viral membrane antigen, and tested it using acetylcholine receptor (AChR) as a model membrane autoantigen. The technique involves co-culturing B cells with adherent, bioorthogonally labeled cells expressing GFP-tagged antigen, and sorting GFP-capturing, newly activated B cells. Hemagglutinin-specific B cells isolated this way from vaccinated human donors expressed elevated CD20, CD27, CD71, and CD11c, and reduced CD21, and their secreted antibodies blocked hemagglutination and neutralized viral infection. Antibodies cloned from AChR-capturing B cells derived from patients with myasthenia gravis bound specifically to the receptor on cell membrane. The approach is sensitive enough to detect antigen-specific B cells at steady state, and can be adapted for any membrane antigen.

Keywords: autoimmunity, membrane protein antigens, trogocytosis, human monoclonal antibodies, myasthenia gravis

INTRODUCTION

A cardinal characteristic of the humoral immune response is that only a minuscule fraction of the total B cell pool recognizes a given antigen. Understanding these cells is therefore hindered by the practical difficulty of identifying them. The immunoglobulin ELIspot (1) enables quantification of B cells of a given specificity, but for live cell assays, immunoglobulin gene cloning, and single cell technologies such as RNA sequencing, isolation of intact cells is key.

Flow cytometric methods are an obvious solution, enabling immediate *ex vivo* phenotyping, and live cell sorting for further analysis or cloning. For some antigens, labeling cells with fluorochrome-conjugated soluble antigen is a powerful approach (2–4). However, many important antigens are not easily generated in native conformation in soluble form. Conformation can be a critical determinant of epitopes for both anti-virus (5) and autoimmune (6) antibodies. Furthermore, numerous antigenicity-determining features of membrane antigens like glycosylation, interaction with other membrane components, and assembly into multi-subunit complexes such as ion channels depend on expression in the membrane of a suitable cell. Autoantibodies, for example in myasthenia gravis and NMDA receptor encephalitis, bind to complex ion channels whose structures depend on their orientation in the plasma membrane (7). The pathology of Graves' disease is caused by autoantibodies that stimulate the thyrotropin receptor, but studies with monoclonal antibodies suggest that these agonistic antibodies recognize discontinuous, conformation-dependent epitopes, while antibodies that recognize linear epitopes usually do not affect receptor signaling (6). This phenomenon is thought to be the reason why cell-based assays offer superior sensitivity for detection of clinically relevant autoantibodies compared to recombinant protein-based methods like ELISA or immunoprecipitation assays (8).

Our previous studies of the capture of membrane proteins by antigen-specific B cells (9) suggested an approach that would solve several of the problems inherent in assessing B cell specificity for membrane antigens. When a B cell encounters its cognate antigen expressed in the membrane of another cell, it first binds to and then extracts the antigen. This process was first described by Batista et al. (10), and has since been studied in molecular detail (11). During the interaction, the B cell internalizes large quantities of antigen and rapidly becomes highly activated. If the antigen is rendered fluorescent, this enables highly specific sorting of the antigen-specific B cells. The first advantage of this system is that it enables the use of antigens in their native conformation and natural cellular environment. The second advantage is that because antigen capture leads to activation of the B cell, markers such as CD69 can be used to distinguish between a B cell that has internalized antigen and a B cell that is bound by the antigen for some other reason. The third advantage is that adherent cells can be used as antigen donors, and after antigen-specific B cells have contacted their target antigen and bound the donor cells with high avidity, the majority of non-specific cells can be washed away.

We developed this approach using transgenic mouse B cells of known specificity, and then used it to identify, phenotype and clone human peripheral blood B cells specific for the influenza protein hemagglutinin (HA), and the autoantigen acetylcholine receptor (AChR). Hemagglutinin was chosen as a clinically relevant, viral membrane antigen, B cells specific for which are relatively abundant in the blood of vaccinated donors. Hemagglutinin-binding B cells can be labeled with fluorescent soluble antigen, enabling us to compare the efficiency of the new technique with an established method. The complex membrane protein AChR was chosen as a clinically important autoantigen, B cells specific for which are present in the blood of patients suffering from myasthenia gravis, but are rare and difficult to isolate with available methods.

MATERIALS AND METHODS

Mice and Primary Immune Cells

C57Bl/6 mice were bred in the University of Basel Mouse Core Facility. FluBI mice were bred from founders provided by Hidde Ploegh and Stephanie Dougan (Whitehead Institute, Cambridge, Mass). IgH MOG mice (12) were bred from founder members provided by Guru Krishnamoorthy and Hartmut Wekerle, Max-Planck-Institut für Neurobiologie, Martinsried, Germany.Primary immune cells were obtained from spleens by mechanical disruption followed by brief settlement under gravity to remove tissue fragments. B cells were obtained by negative selection using Pan B Cell Isolation Kit II (Miltenyi, cat 130-104-443). All procedures involving animals were authorized by the Cantonal Animal Research Commission.

Human Samples

Healthy donors between 25 and 65 years old gave written informed consent according to procedures reviewed by the institutional ethics committee (49/06). Some were vaccinated with the 2013, 2014, 2015, or 2016 seasonal influenza vaccine Agrippal®, containing inactivated influenza virus surface antigens (hemagglutinin and neuraminidase) from type A/H1N1 (A/California/07/2009). Blood was drawn into S-Monovette tubes (Sarstedt, 7.5ml K3E, REF 01.1605.100, 1.6 mg EDTA/ml blood) before the vaccination and 7–14 days after vaccination, as specified in figure legends. Peripheral Blood Mononuclear Cells (PBMC) were separated over Ficoll-Paque (Axon Lab, Switzerland) according to the manufacturer's instructions and frozen in 1 ml FCS-10% DMSO (FCS from Gibco, DMSO from Sigma Aldrich). Blood for serum was drawn into S-Monovette tubes containing clotting activator (Sarstedt, 7.5 ml Z, REF 01.1601.100) and left at room temperature for 30–60 min, before centrifuging at 2,000 g for 10 min at room temperature. Serum was aliquoted and frozen at −80°C. B cells were isolated from frozen PBMC by rapid thawing in 10 ml pre-warmed complete RPMI medium, incubation for 1 h at 37°C, centrifugation and resuspension in ice-cold separation buffer, followed by negative isolation with magnetic beads from Miltenyi (human B cell Isolation Kit II, cat no. 130-091-151). This kit includes anti-CD43 among the negative selection antibodies, and therefore depletes plasmablasts. Yields of B cells varied from 2 to 8% of total PBMC depending on the donor.

Plasmids and Cell Lines

A fragment encoding amino acids 1–529 (Genbank ACP41105.1) was amplified from VG11055-C encoding influenza A/California/04/2009 hemagglutinin (Sino Biological, Beijing, China), and fused to an oligonucleotide (Microsynth, Switzerland) encoding amino acids 530–566. The mutation tyrosine-to-phenylalanine (Y98F) in the sialic acid binding site of hemagglutinin (HA) was incorporated by template switching PCR and cloned into the PigLIC expression vector, which

confers puromycin (Gibco) resistance. To make the plasmid encoding the fusion protein HA-Y98F-GFP, we amplified GFP from pcDNA6.2C-EmGFP-DEST (Invitrogen) and fused it to the mutated HA construct described above between amino acid 566 and the STOP codon. MOG-mCherry expressing cells were prepared by stably transfecting TE671 cells with a plasmid made by inserting the N-terminal 204 amino acids of rat myelin oligodendrocyte glycoprotein into the cloning site of pcDNA3 mCherry LIC cloning vector (a gift from Scott Gradia, Addgene plasmid # 30125).

TE671 rhabdomyosarcoma cells (referred to as "TE cells" throughout the text, and as "TE 0" when not transfected with additional antigens) were from ATCC (LGC, Wesel, Germany). TE cells were cultured in complete RPMI medium (10% heat-inactivated fetal calf serum (FCS), 100 units/ml of penicillin and 100 ug/ml of streptomycin; all from Gibco), at 37μC in 5% carbon dioxide. TE671 cells were chosen because they grow adherently in a monolayer, are easily transfectable, and being of a muscle cell type, support the expression of the multi-subutnit acetylcholine receptor (AChR). TE cells were transfected with the HA-Y98F-GFP construct and selected with puromycin. Positive transfectants were identified by GFP fluorescence and extracellular immunolabeling against A/California/07/2009 hemagglutinin and sorted to yield the TE CA09HA-GFP cell line. Predicted intracellular location of the GFP moiety and extracellular location of HA were verified by protease sensitivity assay, as follows: TE0 cells and TE-HA-GFP cells were trypsinized, washed three times with PBS, resuspended in HBSS with 5 mM CaCl, and incubated with or without Pronase (Sigma Aldrich, 2 mg/ml) for 4 h at 37°C. Cells were then washed and incubated with human anti-HA IgG primary antibody then PE-conjugated goat anti-human IgG (Jackson ImmunoResearch, 109-116-098) for 30 min on ice and resuspended in PBS. Fluorescence in GFP and PE channels was measured on a CytoFLEX flow cytometer (Beckman Coulter) and results are shown in **Supplementary Figure 1**. Cells were tested for mycoplasma infection (LookOut Mycoplasma PCR Detection Kit, Sigma Aldrich). Mouse fibroblasts transfected with human CD40 Ligand (Edgar Meinl, Ludwig-Maximilians-Universität, Munich, Germany), used as feeder cells for EBV transformation, were cultured in complete DMEM medium supplemented with 0.5 mg/ml of G418 Sulfate (cat no. 10131-035, Gibco). For irradiation, cells were washed in PBS, trypsinized, resuspended in ice-cold FCS and kept on ice during irradiation (75 Gy).

Live Cell Imaging

TE671 cells stably transfected with GFP-fused hemagglutinin (from influenza A/WSN/1933) were plated in 8-well chambered coverslips (Ibidi cat no. 80826) and allowed to adhere overnight in an incubator at 37°C in 5% carbon dioxide. The next day, B cells isolated from a FluBI mouse were labeled with Lysotracker Deep Red (Thermo Fisher) according to the manufacturer's instructions, washed and kept in complete RPMI on ice. The chambered coverslip was put in a temperature-, CO_2-, and humidity-controlled chamber (INU-TIZ-F1 controller, Tokai Hit) into a Nikon A1R confocal microscope with a 60x, 1.40 NA oil immersion objective. The pinhole was opened to 5.0 Airy units and laser power, PMT voltages, and voxel dimensions were optimized to minimize laser light exposure. One stack of confocal sections per minute was captured, and stacks were assembled into frames with Nikon Elements software.

FACS Isolation of Antigen-Specific B Cells

B cells were isolated from PBMC after influenza vaccination, co-cultured for 3 h with CTV-labeled TE CA09HA-GFP cells, retrieved and incubated with PerCP-Cy5.5-conjugated anti-human CD19 (for IgG ELISpot experiments) diluted 1:20 in cold separation buffer (PBS 2% FCS, 1 mM EDTA) or with APC-conjugated anti-human CD45 (for EBV transformation experiments and high-throughput B cell activation) diluted 1:50 in cold separation buffer and sorted into Eppendorf tubes (FACSAria III Cell Sorter, BD Biosciences). Cells were gated on scatter to select live, single cells; then in two ways to exclude antigen-donor TE cells: CTV negative, and CD19 or CD45 positive. From these putative single, viable B cells, subgates were used for sorting "GFP-capturing," i.e., GFP-positive, and "GFP-non-capturing," i.e., GFP-negative. Non-specific surface membrane labeling of adherent cells by bioorthogonal click chemistry was achieved by incubating the cells overnight with 50 μM L-azidohomoalanine in methionine free medium, then washing and incubating for 1 h with 5 μM A647-tagged DIBO-derivative in HBSS at 37°C. The procedure for isolating AChR-binding B cells was similar, but stable transfection with the HA-GFP antigen was replaced by transient transfection with the multi-subunit AChR, including a GFP-variant of the alpha subunit described by Leite et al. (13). Transient transfection resulted in AChR expression by about half the cells, and for subsequent screening of antibody binding to AChR, we always compared binding to the transfected vs. untransfected cells to normalize for antigen-independent binding. Also, for sorting AChR-specific B cells, the antigen independent labeling with A647 was omitted, and instead a second positive (i.e., specific antigen-dependent) label was added with alpha-bungarotoxin conjugated to A647.

ELISpot for Detection of HA-Specific, IgG-Secreting Human B Cells

96-well plates (Human IgG B cell ELISpot kit (Mabtech, Sweden, Code: 3850-2A) were coated overnight at 4°C with hemagglutinin (Sino Biological, Influenza A H1N1 (A/California/04/2009) hemagglutinin (HA) Protein (His Tag), cat no. 11055-V08B) at 5 μg/ml, or anti-IgG capture-antibody at 15 μg/ml to enumerate total IgG-producing cells, or bovine serum albumin at 5 μg/ml to enable assessment of specificity, washed with sterile PBS and blocked with complete RPMI medium. B cells were isolated, co-cultured with TE mHA-GFP, labeled with anti-human CD19, and GFP-capturing and non-capturing CD19-positive B cells were sorted as described above into coated plates containing 200 μl/well complete RPMI medium supplemented with 1 μg/ml R848 and 10 ng/ml recombinant human IL-2. After culturing for 3 days, the cells were discarded, the plates were washed five times with PBS, and developed by incubating with biotinylated anti-human IgG, followed by streptavidin-AP and BCIP/NBT substrate solution

to visualize IgG spots. Antibodies, IL-2, R848, and solutions were provided with the kit and all steps followed the Mabtech protocol. Plates were imaged and read by AID ELISpot reader (software version 7.0, build 14790, AID GmbH, Strassberg, Germany). Results are shown as number of counted spots.

EBV Transformation of FACS-Isolated Hemagglutinin-Specific B Cells

GFP-capturing and non-capturing B cells were sorted into 1.5 ml Eppendorf tubes containing 200 μl complete RPMI medium, mixed gently with 500 μl of pre-warmed EBV supernatant (ATCC-VR-1492 Epstein-Barr virus, strain B95-8, used neat) and incubated for 1 h at 37°C. Flat-bottomed 96WP were prepared containing 30,000 irradiated CD40L mouse fibroblasts per well in RPMI medium containing 20% non-heat-inactivated FCS, 100 units/ml of penicillin, 100 μg/ml of streptomycin and 1 μg/ml of R848 (Mabtech, Sweden, REF 3611-5X), referred to as "RPMI-20" throughout the text. B cells were added to plates at 30 cells per well and cultured for at least 2 weeks. Proteins, Antibodies and Vital Dyes

Bovine serum albumin (cat no. A4503) was obtained from Sigma Aldrich. Influenza A H1N1 hemagglutinin (A/California/04/2009) protein (cat no. 11055-V08B) and rabbit monoclonal anti-HA antibody RM10 (cat no. 11055-RM10) were obtained from Sino Biological. PerCP-Cy5.5 anti-human CD19 (clone HIB19, BD Biosciences, cat no. 561295), BV510 anti-human CD20 (clone 2H7, BD Biosciences, cat no. 563067), APC anti-human CD45 (clone HI30, BD Pharmingen, cat no. 555485), PerCP-Cy5.5 anti-mouse CD69 (clone H1.2F3, Biolegend, cat no. 104521), APC-Cy7 anti-mouse B220 (clone RA3-6B2, BD Biosciences, cat no. 552094), PE anti-human IgG (Jackson Immunoresearch, cat no. 109-116-098), Alexa Fluor 488 anti-human IgM (Jackson Immunoresearch, cat no. 109-545-129), PE anti-rabbit IgG (Jackson Immunoresearch, cat no. 111-116-144). Anti-human IgG/HRP (cat no. P0214) and anti-human IgM/HRP (cat no. P0215) both obtained from Dako. Cell Trace Violet was obtained from Thermo Fisher Scientific (cat no. C34557) and DAPI from Sigma Aldrich. BV421 anti-human CD27 (clone M-T271, BD Horizon, cat. 562513), BV510 anti-human CD20 (clone 2H7, BD Horizon, cat. 563067), BV605 anti-human IgM (clone G20-127, BD Horizon, cat. 562977), BV711 anti-human CD21 (clone B-ly4, BD Horizon, cat. 563163), PE anti-human CD69 (clone FN50, Biolegend, cat. 310906), PE CF594 anti-human CD138 (clone MI15, BD Horizon, cat. 564606), PE-Cy7 anti-human IgD (clone IA6-2, BD Pharmingen, cat. 561314), PerCP-Cy5.5 anti-human CD19 (clone H1B19, BD Pharmingen, cat. 561295), Alexa Fluor 700 anti-human IgG (clone G18-145, BD Pharmingen, cat. 561296), APC-eFluor 780 anti-human CD38 (clone HIT2, eBioscience, cat. 47-0389-42), APC-Cy7 anti-human CD11c (clone Bu15, Biolegend, cat. 337217), BUV395 anti-human CD71 (clone M-A712, BD Biosciences, cat. 743308).

Phenotyping of Human Peripheral Blood B Cells

PBMC samples collected before and 7 days after influenza vaccination from each of 9 donors were thawed, and B cells isolated by negative magnetic isolation. TE CA09HA-GFP cells were incubated overnight with 50 μM L-azidohomoalanine in methionine free medium, then washed and incubated for 1 h with 5 μM A647 tagged DIBO-derivative in HBSS at 37°C. B cells were co-cultured with these cells for 3 h, retrieved, and incubated with either an antibody panel containing anti-human CD138 (donors 1–5), or an antibody panel lacking anti-human CD138 and containing anti-human CD11c and anti-human CD71 (donors 6–9) for 20 min on ice. B cells were then washed and acquired on a LSRFortessa cytometer (BD Biosciences) configured with five excitation lasers (355, 405, 488, 561, 640 nm) and 20 detectable parameters. Data in.fcs format were exported from the FACSDIVA operating software of the cytometer and either processed directly using FlowJo (version 10.1, FlowJo, LLC) or re-exported and read into R using the flowCore package (14), and clustered with the k-means algorithm. Heatmaps were generated with the heatmap algorithm of base R. Gating strategies for flow cytometry experiments are shown in **Supplementary Figure 3**.

Flow Cytometric Antibody Assay

One hundred microliter of flow buffer containing 50,000 each of unlabeled TE mHA and CTV-labeled TE 0 cells were mixed and incubated with 25 μl of supernatant from EBV transformed B cell clones for 30 min on ice, washed three times with cold flow buffer, labeled with PE-conjugated anti-human IgG and Alexa Fluor 488-conjugated anti-human IgM for 20 min on ice, washed twice with cold flow buffer and measured by flow cytometry. A similar technique was used to measure anti-AChR antibodies in sera and culture supernatants, but using TE cells transiently transfected with AChR-GFP. A647-conjugated α-bungarotoxin (1 μg/ml Thermo Fisher cat. B35450) was used as a positive control.

ELISA

Bovine serum albumin and Tween were from Sigma Aldrich, PBS from Gibco, TMB for chromogenic development from KPL (SureBlue RESERVE, TMB Microwell Peroxidase, 53-00-00). 96 well-plates (Corning Costar 3590 96well EIA/RIA plate flat bottom without lid) were coated with hemagglutinin and BSA, each at 5 μg/ml, overnight at 4°C with shaking, then washed three times with PBS-0.05% Tween and blocked with PBS-2% BSA at room temperature for 2 h with shaking. Supernatants from FACS-isolated, EBV-transformed, putatively hemagglutinin-specific B cell clones, and from GFP-non-capturing, putatively non-hemagglutinin-specific, negative control B cell clones, were diluted 1:3 in PBS-0.5%BSA. Plates were incubated with diluted supernatants for 2 h at room temperature with shaking, washed three times with PBS-0.05% Tween and incubated with rabbit anti-Human IgG HRP (1:6,000) or rabbit anti-human IgM HRP (1:1,000) in PBS-0.5% BSA for 1 h at room temperature with shaking. Plates were washed three times with 250 μl/well PBS-0.05% Tween and developed with TMB until a blue color was visible. The reaction was stopped with 1N HCl and the plates read at 450 nm immediately after stopping.

Hemagglutination Inhibition and Virus Neutralization Assays

The titer of influenza A/California/04/09 (H1N1) antibody in B cell culture supernatant samples was measured by HI assay according to the World Health Organization (WHO) protocol manual on animal Influenza diagnosis and surveillance (WHO/CDS/CSR/NCS/2002.5 Rev. 1), following our previously described procedure (15). The neat supernatant samples were pre-treated with 3-fold of cholera filtrate (cat no. C8772-1VL, Sigma-Aldrich) overnight at 37°C to remove non-specific inhibitors. The samples were 2-fold serial diluted in V-shaped 96-well microtiter plate (cat no. 3897, Corning Costar) with PBS. Twenty-five microliter of corresponding influenza antigen A/California (H1N1) antigen (4 HA units) (cat no. 14/134, NIBSC) was added to each well. After 30 min incubation, 50 μl of 1% of chicken erythrocytes (cat no. CLC8800, Cedarlane) was added to each well for 30 min. The antibody titer was measured by tilting the plate based on erythrocyte agglutination and non-agglutination reactions. The positive serum and back titration controls were included in the assay plate.

For neutralization assays, supernatants were incubated with live influenza A/California/2009 virus at various dilutions and then the pre-incubated virus was added to susceptible MDCK cells. After 16 h at 37°C, the cells were fixed and productive infection was detected with an anti-influenza nucleoprotein primary antibody, an enzyme-conjugated secondary antibody, and a colorigenic substrate and the optical density at 450 nm measured by spectrometry. Values <0.15 were considered to indicate viral inhibition.

High-Throughput B Cell *in vitro* Expansion and ELISA

High-throughput B cell activation and supernatant screening by ELISA (16) followed the method published by Huang et al. (17). FACS-isolated, GFP-capturing and non-capturing B cells were plated at approximately 1.6 cells per well into 384 well plates containing IL-2, IL-21, and irradiated mouse CD40L cells to induce activation and expansion of the B cells. After 12 days, supernatants from these B cell clones were assayed as described above (see section ELISA) with the addition of tetanus toxoid, anti-IgM, and anti-IgG capture antibody-coated wells. cDNA encoding heavy and light chains were cloned from 35 GFP-capturing B cell cultures producing anti-HA antibodies, and expressed recombinantly using standard methods. In later experiments, we replaced the irradiated PBMC with irradiated TE671 cells stably expressing CD40L, and omitted the IL-2.

Assessment of Specificity and Sensitivity of GFP-Antigen Capture by Transgenic B Cells

Wild type and FluBI mouse B cells were isolated using mouse CD19 microbeads from Miltenyi (cat no. 130-052-201). FluBI B cells were labeled with cell trace violet, diluted with unlabeled wild type B cells at 1:100, 1:1,000 and 1:10,000 and co-cultured for 2.5 h with TE cells expressing HA-GFP. B cells were retrieved, labeled with anti-B220 and anti-CD69 antibodies and subjected to flow cytometry. The population of putatively antigen-specific, i.e., CD69-high and GFP-high cells was then examined for CTV labeling to determine the numbers of true and false positives and negatives, and thus the sensitivity and specificity of the technique. The effect of extracellular antigen quenching used a similar experiment, but with a 1 h co-culture time, no CD69-labeling, and flow cytometric measurements of GFP acquisition in the presence or absence of 0.1% trypan blue. The influence of membrane stiffness was assessed with a similar experiment, with the addition of a pretreatment step exposing the antigen-expressing cells to 0, 1, 3, or 10 μM mycalolide B (AG Scientific, San Diego, California), followed by washing with medium before adding the B cells. The proportion of internalized antigen was studied by comparing immunolabeling following fixation and permeabilization of the B cells, or fixation without permeabilization. After retrieving from the co-culture, B cells were fixed in 4% paraformaldehyde for 15 min at room temperature, then permeabilized in 0.1% saponin in PBS. HA was detected with a rabbit polyclonal antibody (Sino Biological, Beijing, China; 11692-T54) and an A657-conjugated goat polyclonal secondary (Jackson 111-605-003).

Statistics

Statistical treatments are specified in each figure legend. We used GraphPad PRISM 6 and various algorithms in R/Bioconductor to graph and analyze the data. Numerical results that passed appropriate tests of normality were analyzed by analysis of variance, and otherwise by appropriate non-parametric tests.

RESULTS

Membrane Antigen Capture Enables Identification of Mouse and Human Hemagglutinin-Specific B Cells

The phenomenon of membrane antigen capture by B cells is illustrated by the live cell imaging sequence in **Figure 1A**. Upon contacting cognate antigen expressed in the membrane of another cell, B cells rapidly extract and internalize large quantities of antigen. In the experiment shown, B cells from FluBI mice (18), which are specific for influenza hemagglutinin (HA), were exposed to adherent cells expressing hemagglutinin fused to GFP (TE HA-GFP cells).

We measured the time course of HA-GFP uptake by antigen-specific FluBI and antigen-irrelevant C57Bl/6 B cells. Hemagglutinin-specific B cells avidly extracted the HA-GFP fusion protein, with GFP uptake reaching a maximum between 45 and 90 min, while antigen-irrelevant B cells capture almost no GFP (**Figure 1B**). We further expected that CD69 expression after exposure to cognate antigen-expressing adherent cells would be time-dependent (9). We confirmed this in FluBI mouse B cells, and also showed that CD69 induction depends on expression of the antigen. The total duration of the co-culture

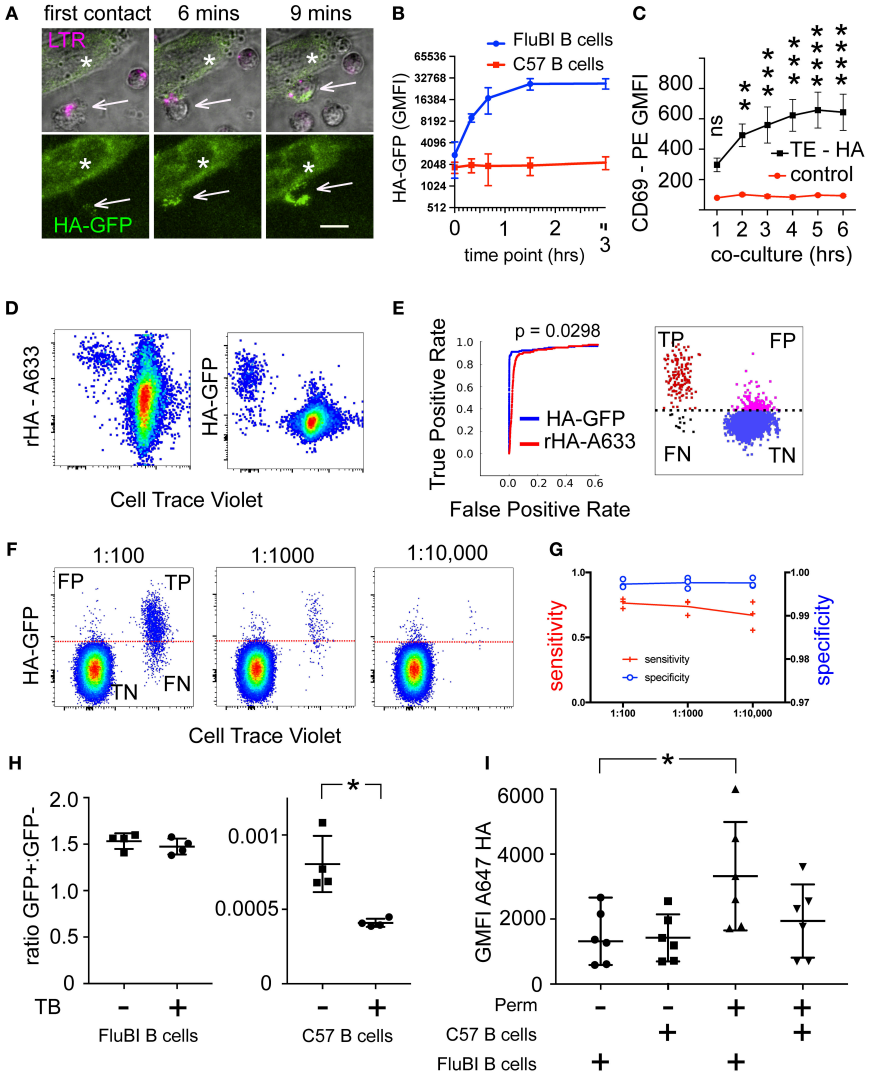

FIGURE 1 | Identification of Hemagglutinin-Specific Transgenic Mouse B Cells by Capture of Membrane-Expressed HA-GFP. **(A)** Live Cell Imaging of membrane antigen capture. Hemagglutinin-specific FluBI B cells (white arrows) labeled with Lysotracker Deep Red (LTR, magenta) are added to cells (white asterisks) expressing a fusion protein comprising the transmembrane and antigenic extracellular domains of hemagglutinin, with a cytoplasmic GFP moiety (HA-GFP, green). Extracellular location of the HA epitope, and the intracellular location of GFP were confirmed by examining sensitivity to extracellular protease (**Supplementary Figure 1**). Images show the initial contact between a B cell and an antigenic target cell, then the same location at 6 and 9 min later. The upper three micrographs show both fluorescent channels merged with a transmitted light channel to show the morphology of the cells (single confocal planes). The lower panels show only the GFP channel (maximum intensity projections) to show capture of antigen (scale bar = 10 um). **(B)** Extraction of membrane-expressed HA-GFP by antigen-specific or antigen-irrelevant B cells. HA-specific FluBI B cells were labeled with Cell Trace Violet (CTV), mixed with unlabeled, antigen-irrelevant, C57 mouse B cells at a ratio of 1:10, and added to an adherent layer of TE671 cells stably transfected with membrane-expressed HA-GFP. At the indicated time points, the B cells were retrieved, immunolabeled with anti-B220 antibody, and interrogated by flow cytometry. The FluBI cells were separated from the C57 B cells by CTV label, and GFP levels were compared between the two cell types. Points and bars show mean and standard deviation of the geometric mean GFP fluorescence. **(C)** Time-course of CD69 upregulation. HA-specific FluBI mouse B cells were exposed to HA-expressing TE HA, or HA-non-expressing TE cells (TE 0) for the indicated times, and then retrieved, immunolabeled for B220 and CD69 and measured by flow cytometry. Vertical axis shows the geometric mean immunofluorescence intensity and SEM of the anti-CD69 signal on B cells exposed to TE HA (black lines and squares), or TE 0 (red lines and circles). Asterisks show significant difference between TE 0 and TE HA conditions at each time point (two-way ANOVA, followed by Sidak's multiple comparison test, (ns = not significant, $^{**}p < 0.01$, $^{***}p < 0.001$, $^{****}p < 0.0001$). **(D)** Comparison of techniques for labeling antigen-specific B cells. CTV-labeled, polyclonal C57 mouse B cells were spiked with 1% unlabeled HA-specific FluBI B cells, and the mixture subjected either

(Continued)

FIGURE 1 | to labeling with Alexa-633-labeled soluble hemagglutinin (left), or to co-culture with adherent TE HA-GFP cells (right). Dot plots show flow cytometric measurements of CTV on the horizontal axis (CTV-negative, HA-specific FluBI cells appear to the left of the C57 cells), and the antigen labels on the vertical axes. The frequency of B cells recognizing this hemagglutinin is more than 90% in FluBI mice, but <1 per 100,000 among polyclonal B cells from naïve, wild-type C57 mice (18), implying that the majority of the wild-type C57 B cells that bind antigen in this context can be considered false positives, whose binding is BCR-independent. **(E)** Receiver Operating Characteristic (ROC) Curves comparing the two methods shown in **(D)**. For three experiments like **(D)**, true- and false positive rates were calculated for each method at various thresholds. The red curve shows the resulting ROC curve for the soluble hemagglutinin label and the blue curve for the membrane-expressed hemagglutinin-GFP fusion protein. Areas under the curves were calculated for each method for three experiments, and compared by two-tailed, paired *t*-test. The schematic on the right shows the four populations, true positives (TP, red), false positives (FP, magenta), false negatives (FN, black), and true negatives (TN, blue) at a given threshold (example threshold shown here by a broken black line). **(F)** Discriminating antigen-specific cells using membrane capture at different target cell frequencies. 10^6 unlabeled C57 mouse B cells were spiked with 1, 0.1, or 0.01% of CTV-labeled HA-specific FluBI B cells [note that the CTV labels the spike in this paradigm, opposite to the paradigm shown in **(D)**], and the mixture co-cultured with adherent TE HA-GFP cells. A threshold was set at approximately 0.1% false positives, the FluBI and C57 cells were distinguished using the CTV label. Then, we calculated the sensitivity [true positives/(true positives + false negatives)] and specificity [true negatives/(true negatives + false positives)]. **(G)** Performance of antigen-capture labeling at different target cell frequencies. Data from three experiments like **(E)** are plotted on two vertical axes, at the target cell frequencies shown on the horizontal axis. Specificity is plotted with open blue circles on a blue line on the right axis (0.97–1.0), and sensitivity is plotted with red crosses on a red line on the left axis (0.0–1.0). **(H)** Effect of extracellular fluorphore quenching on apparent antigen signal. After co-culture with TE HA-GFP cells, FluBI B cells (left column scatter graph) or wild-type C57 B cells (right column scatter graph) were measured by flow cytometry in the presence or absence of 0.1% trypan blue. The vertical axis shows the ratio of GFP+ cells to GFP negative cells. Asterisk shows significant difference between trypan blue treatment conditions (*$p < 0.05$, unpaired, two-tailed *t*-test). Pooled data from two independent experiments. **(I)** Effect of permeabilization on antigen immunodetection. After co-culture with TE HA-GFP cells, FluBI B cells (1st and 3rd columns) or wild-type C57 B cells (2nd and 4th columns) were fixed, and either permeabilized with saponin or not, before immunolabeling with a rabbit anti-HA antibody and an A647-conjugated anti-rabbit secondary antibody. The vertical axis shows the flow cytometric geometric mean fluorescence intensity of the secondary antibody. Asterisk shows significant difference between permeabilization conditions within the FluBI condition (*$p < 0.05$, unpaired, two-tailed *t*-test). Pooled data from three independent experiments.

is also important; CD69 expression increases with longer exposure (**Figure 1C**).

To explore the possibility of exploiting this phenomenon for identifying antigen-specific B cells from among a polyclonal population, we spiked polyclonal mouse B cells from wild type C57Bl/6 mice with varying numbers of FluBI B cells. The two kinds of B cells were pre-labeled before mixing, to enable their separation later. To compare the performance of the antigen capture method with the soluble fluorescent antigen labeling method, one sample was co-cultured with an adherent layer of TE HA-GFP cells and the second sample was labeled with fluorochrome-conjugated recombinant HA. Both methods resulted in sensitive detection of the hemagglutinin-specific FluBI B cells (**Figure 1D**). To make a more quantitative comparison, we extracted a Receiver Operating Characteristics (ROC) curve from the results of three such experiments and compared the curves obtained by labeling with fluorescent soluble antigen or by antigen extraction (**Figure 1E**). The antigen-extraction method performed significantly better than the soluble fluorescent antigen method, with comparable sensitivity but better specificity. To assess the performance of the antigen-capture technique at physiologically realistic frequencies of antigen-specific B cells, we repeated the experiment with serial dilutions of FluBI B cells in wild type C57Bl/6 B cells (**Figure 1F**) and detected HA-specific B cells down to a frequency of 1/10,000. This is in the range of naturally occurring influenza-specific B cells in humans (19). Specificity was always above 99%, and sensitivity varied between 55 and 80% (**Figure 1G**).

We observed a small number of HA-GFP-positive wild type B cells, for example in **Figures 1D,F**. We hypothesized that these are false positives, generated by superficial association of donor cell debris with the B cell membrane surface. To test this, we compared the signal in the presence and absence of trypan blue, which has been reported to quench fluorophores with the spectral characteristics of GFP (20). We reasoned that antigen internalized by the BCR-dependent pathway would be physically separated from the quencher and therefore protected from the quenching effect. As shown in **Figure 1H**, the GFP signal on wild type B cells was approximately halved by quenching, while the signal from FluBI cells was unaffected.

To confirm that the increase in GFP fluorescence in FluBI B cells was due to internalized antigen, rather than superficially membrane-associated debris, we compared the intensity of immunofluorescence after immunolabeling the captured antigen with an anti-HA antibody in permeabilized or unpermeabilized cells. Results are shown in **Figure 1I**. Immunofluorescence was significantly increased after permeabilization in FluBI but not in wild type B cells.

The supposition that the GFP-positive cells among the wild type C57 B cells are antigen-non-specific also predicts that a similar number would be seen among FluBI and C57 B cells if the fluorescent antigen were non-cognate for both cell types. We tested this prediction using myelin oligodendrocyte glycoprotein (MOG) fused to GFP or mCherry as a non-cognate membrane antigen. B cells from IgH MOG BCR transgenic mice do capture this antigen and served as a positive control. The ratio of antigen-acquiring to non-acquiring B cells was consistently 1,000-fold higher for cognate B cells than for antigen-mismatched B cells. There was no significant difference between different mismatched B cell–antigen combinations (**Supplementary Figure 4**).

Since physical properties of the antigen donor cell membrane, such as stiffness and compliance, have an impact on the capture of antigens in immune complexes from follicular dendritic cells (21), we examined the effect of manipulating membrane stiffness with the actin depolymerizing agent mycalolide B. As shown in **Supplementary Figure 5**, as membrane stiffness is reduced, acquisition of antigen by non-cognate B cells increases, while cognate antigen capture decreases.

The strong adherence of B cells to other cells expressing their cognate antigen also offers another possibility for isolating antigen-specific B cells in co-culture with adherent antigen-expressing cells. This can be exploited by washing off non-binding B cells after a short period of co-culture. We examined the effect of the length of the pre-wash co-culture (**Supplementary Figure 2A**), and discovered that a time of about 20 min is optimal. Using this technique, which we call "panning," significant increases in efficiency can be achieved (**Supplementary Figures 2B,C**).

The steps of the technique, as optimized using transgenic mouse B cells, and model antigens, are shown schematically in **Figure 2**. To test the system in the context of a natural immune response, we exposed B cells from human peripheral blood mononuclear cells (PBMC) to adherent TE671 cells stably expressing a GFP-tagged version of the hemagglutinin from influenza A/California/2009, the H1N1 strain included in influenza vaccines from 2010 until 2016 (TE CA09HA-GFP). We introduced the point mutation Y98F in the hemagglutinin to eliminate sialic acid mediated binding (22). After 3 h of co-culture, B cells were retrieved and the GFP-capturing B cells were isolated by FACS (**Figure 3A**). We assessed the antigen-specificity of the sorted cells by anti-HA IgG ELIspot (**Figure 3B**). Comparing unselected B cells and HA-GFP-capturing B cells from the same donor, the technique enriches the hemagglutinin-specific B cells by approximately 100-fold (**Figure 3C**). To obtain clones for characterization of the secreted antibodies, the experiment was repeated, and 5,000 GFP-high, CD45-positive cells, and a similar number of GFP-non-capturing cells were transformed with Epstein Barr Virus (EBV). Four weeks later, the culture supernatants were assayed for HA-binding activity by ELISA and flow cytometry. Out of 46 clones derived from HA-GFP-capturing B cells, 13 produced HA-specific IgG as measured by flow cytometry, and 1 produced hemagglutinin-specific IgM (**Figure 3D**). None of the supernatants from 49 non-GFP-capturing clones bound specifically to hemagglutinin. To verify that hemagglutinin binding measured by these assays corresponds to antigen-specific immunoglobulin binding, we assayed IgG from the 13 hemagglutinin-binding supernatants for hemagglutination inhibition and virus neutralization. Three clones showed neutralizing activity, of which one showed strong virus-neutralizing activity (**Figure 3E**), and also hemagglutination inhibition, confirming the potential of the technique to select and identify B cells of relevant affinity and specificity. We also examined the effect of panning on the efficiency of isolation of human influenza-specific B cells, and showed that more than 80% of sorted B cells secrete HA-specific antibodies in subsequent culture (**Supplementary Figures 2B,C**).

In vitro Single Cell B Cell Cultures of Sorted Cells for Immunoglobulin Cloning

The EBV cloning immortalization efficiency was too low to give informative coverage of immunoglobulin genes of the antigen-extracting population, so we adopted the protocol for expansion of single human B cells described by Huang et al. (17). HA-GFP-capturing and non-capturing B cells from a donor 2 months after immunization (**Figure 4A**) were put into 384-well plates containing irradiated PBMC, anti-CD40, IL-2 and IL-21 to induce proliferation and plasma cell differentiation. Antibodies in the supernatants of these B cell cultures were measured by ELISA for total IgM, total IgG, and specific IgM or IgG against hemagglutinin (**Figure 4B**). From 1920 supernatants of HA-GFP-capturing B cell cultures and 1920 from non-capturing controls 39.6% of the GFP-capturing B cells (761 supernatants) and 38.9% of the non-capturing B cells (747 supernatants) produced IgG (**Supplementary Figure 6**). Thirty-five of the supernatants from GFP-capturing B cells and none of the supernatants from GFP-non-capturing cells bound specifically to hemagglutinin. From those 35 wells (which initially contained 1.6 cells per well on average), 27 recombinant antibodies were recovered which bound specifically to hemagglutinin. Hemagglutinin binding of some of the antibodies is dependent on both the heavy and light chains, and in some cases only on the heavy chain (**Supplementary Figure 7**), as has been reported previously ((23–25)). The sequences had a significant number of mutations from germline V gene segment sequences, with mutations enriched in the complementarity-determining regions (**Figure 4C**). This suggests that the B cells, which captured the antigen *ex vivo*, had an antigen-experienced history, had received T-cell help, and undergone affinity maturation. In parallel, we examined the mutation rate in 33 HA-non-binding heavy chains cloned from the same donor, and the number of clones with unmutated immunoglobulin genes was significantly higher than in the hemagglutinin-capturing cells (**Figure 4D**). All of the 27 heavy and light chain pairs of the HA-binding antibodies were unique. This suggests that the number of available hemagglutinin-specific clones is at least at the higher end of the serum antibody clonotypic diversity, which has been estimated to be between 50 and 400 clones (26, 27). However, we found an over-representation (5/27, 19%) of antibodies with the combination of VH1-18 and VK2-30. According to DeKosky et al. (28), VH1-18/VK2-30 pairings comprise <0.1% of total clones identified for any of the donors, suggesting that in the donor we examined, the VH1-18/VK2-30 pair has some germline-encoded affinity for hemagglutinin.

A Second, Antigen-Independent Label Reports BCR-Independent Binding

Sorting the HA-GFP-capturing cells enriched hemagglutinin-specific B cells by a factor of 100. However, the sorted population still contained 90% of B cells not specific for hemagglutinin. We hypothesized that this is due BCR-independent binding of antigen-donor cell fragments to irrelevant B cells, and that this non-specific signal could be distinguished by adding a second, antigen-independent membrane label. To test this hypothesis, we labeled exposed membrane proteins on the TE CA09HA-GFP antigen-donor cells with Alexa Fluor 647 (A647) using bioorthogonal click chemistry before co-culturing with human B cells. We reasoned that BCR-mediated capture of cognate antigen would result in the uptake of a large amount of

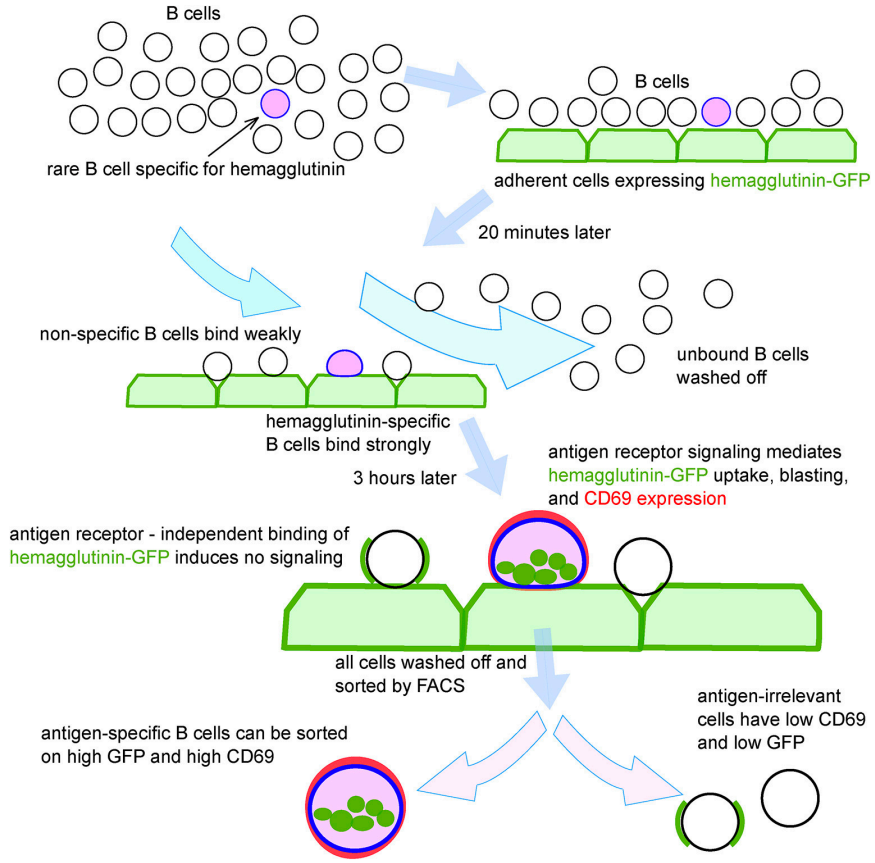

FIGURE 2 | Schematic depiction of process for isolation antigen-specific B cells using adhesion to antigen-expressing cells, fluorescent antigen capture, upregulation of B cell activation markers, and fluorescence-activated cell sorting.

antigen-GFP, and a small amount of antigen-associated A647, proportional to the GFP signal. BCR-independent mechanisms of uptake, such as adhesion of donor-cell-derived vesicles, would result in a higher ratio of A647 to GFP. As is clear from **Figure 5A**, both kinds of events indeed occur–there is one GFP-high, A647-intermediate population that we hypothesize are membrane antigen-capturing B cells (MACB); and one population with a lower GFP:A647 ratio similar to the donor cells. We tested our hypothesis that antigen-specific cells would be contained in the GFP-high, A647 intermediate population in two ways: by tracking the size of the populations before and after influenza immunization, and by examining the activation of this population after exposure to antigen.

B cells from 9 donors, from blood drawn before or 1 week after influenza vaccination, were co-cultured with A647-labeled TE CA09HA-GFP cells for 3 h, then retrieved and immunolabeled for flow cytometry. In all 9 donors, the number of cells in the MACB population increased following immunization, while no consistent increase or decrease was seen in the false positive population (**Figure 5B**).

We also compared the expression of CD69 in the two populations of B cells, as well as the global expression level of CD69 expression. The false positive population had levels of CD69 indistinguishable from the global population, while the MACB population showed a bimodal distribution, with a lower peak like the global population and a CD69-high peak (**Figure 5C**). The MACB population was the only population with the second peak, and the only one whose CD69 expression was influenced by immunization (**Figure 5D**). We concluded that the combination of these three directly antigen-capture-related markers is sufficient to identify antigen-extracting B cells.

Phenotypic Characterization of Influenza-Specific B Cells

Having reliable flow cytometric markers of antigen specificity allowed us to characterize the hemagglutinin-specific B cell subset and compare it to the overall population of B cells.

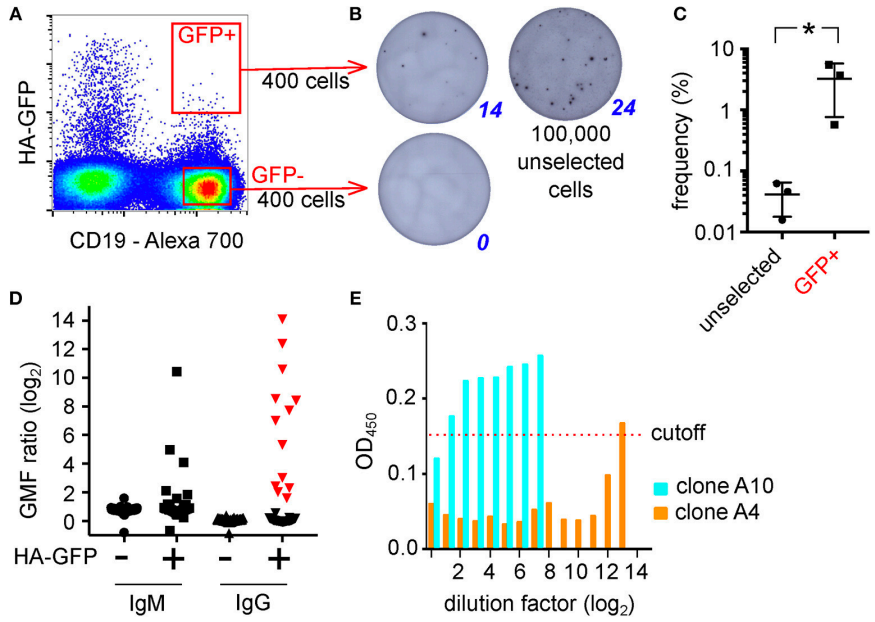

FIGURE 3 | Isolation of Human Hemagglutinin-Specific B Cells by Capture of Membrane-Expressed HA-GFP. **(A)** Gating of HA-GFP-capturing B cells. Polyclonal human B cells were cultured for 3 h on an adherent layer of TE HA-GFP cells, then retrieved and labeled with an anti-CD19 antibody and the CD19-positive, GFP-high cells were sorted by FACS. **(B)** Enumeration of HA-specific antibody-secreting cells by ELIspot. 400 GFP-capturing B cells sorted as shown in **(A)**, or the same number of GFP-negative cells, or 100,000 unsorted polyclonal B cells from the same donor were incubated in ELIspot wells coated with hemagglutinin for 3 days, then the spots of antibody were visualized with anti-human IgG secondary antibody. **(C)** Enrichment of antigen-specific B cells by membrane antigen capture. Three experiments like the one described in **(B)** were completed, using B cells from donors 2 weeks after immunization, and for each the frequencies of HA-specific IgG-producing cells among the GFP-capturing population and the unsorted population were calculated and compared by two-tailed paired *t*-test. The mean frequency was enriched by ~100-fold from 0.04 to 3% (*$p < 0.05$). **(D)** EBV-immortalized clones derived from HA-GFP-capturing B cells. GFP-capturing or non-capturing B cells were sorted as in **(C)**, immortalized with Epstein Barr Virus (EBV), and cultured for 4 weeks. The supernatants were screened by flow cytometry for anti-HA IgM and IgG. Vertical axis shows the log ratio of immunofluorescence on HA-expressing cells divided by the same value for non-expressing control cells: i.e., a value of 0 implies no specific binding. Supernatants plotted with red triangles in the 4th column (HA-specific IgG-containing supernatants clones derived from GFP-capturing B cells) were screened for hemagglutination inhibition and virus neutralization. **(E)** Neutralization of influenza virus by supernatants from EBV clones. Supernatants from the clones shown with red triangles in **(D)** were incubated with live influenza A/California/2009 virus at the indicated dilutions and then the virus was added to MDCK cells. After 16 h, the cells were fixed and productive infection detected by immuno-colorimetry. Vertical axis shows optical density at 450 nm, and values <0.15 imply viral inhibition. Here, clone A10 exhibits minimal neutralization, and clone A4 shows neutralization down to a dilution factor of 212 (1:4,096, or 50 ng/ml).

A longitudinal follow-up also enabled us to track phenotypic changes of this population induced by vaccination (**Figures 6**, **7**). All examined markers except CD138 were differently expressed in the hemagglutinin-specific B cells compared to the overall population of B cells (**Figure 6**). IgM, IgD, and CD21 were significantly reduced in the hemagglutinin-specific population, whereas CD11c, CD19, CD20, CD27, CD38, CD71, and IgG were increased. For most of these markers the differences were more pronounced at the timepoint after vaccination (**Figure 6**). However, higher CD20 and lower CD21 were also seen in the hemagglutinin-specific population before vaccination. The only marker showing opposing trends before and after vaccination was CD11c; before vaccination, CD11c was lower in the hemagglutinin-specific cells than in the overall B cell population, whereas after vaccination it was higher.

We hypothesized that the clearest population differences between hemagglutinin-specific and other B cells seen after immunization were driven by increases in the numbers of recently activated, vaccine-specific B cells, because patterns associated with memory cells (CD27-high, IgG-high, IgD-low) also characterize the post-vaccination, hemagglutinin-specific population. Based on CD27 and IgD expression (**Figure 7A**), we plotted the numbers of naïve and memory B cells as fractions of the global, or fractions of the hemagglutinin-specific B cell populations (**Figure 7B**). Before immunization, about 80% of the global B cell population have a naïve phenotype (IgD-positive, CD27-negative), and about 10% have an IgD-negative, CD27-positive memory phenotype. Hemagglutinin-specific B cells before immunization include about 40% each of naïve and memory cells. Following immunization, the proportions in the global B cell pool remain unchanged from before immunization, while the proportion of hemagglutinin-specific cells with the memory phenotype rises to almost 80%. We hypothesize that these changes reflect an expansion of

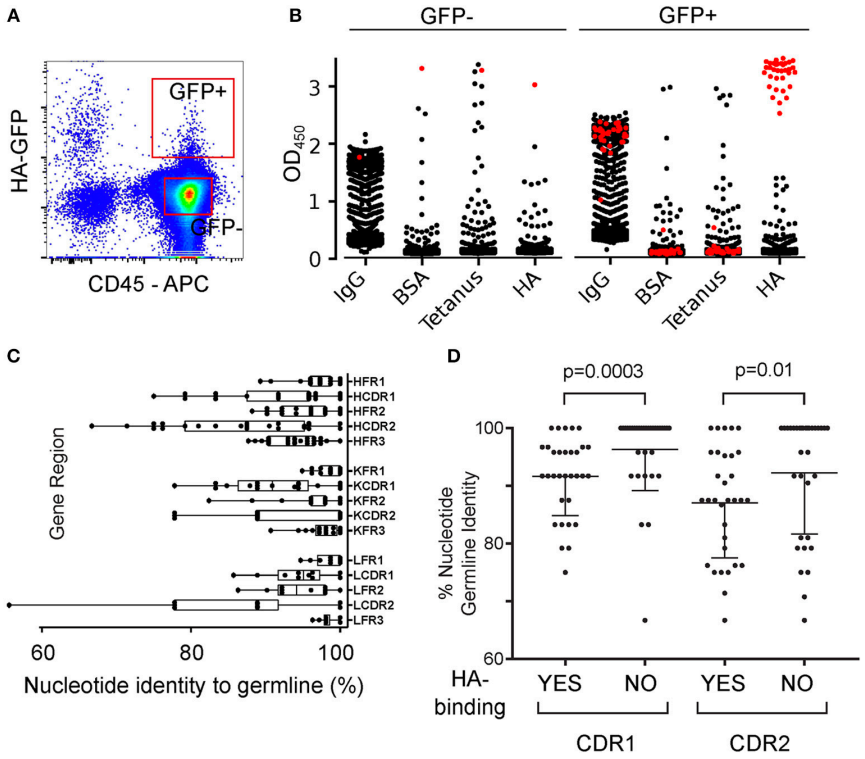

FIGURE 4 | Single Cell Cloning and Immunoglobulin Sequencing of Hemagglutinin-Extracting Human B Cells. **(A)** Gating of HA-GFP-capturing B cells. Human B cells were cultured for 3 h on an adherent layer of TE HA-GFP cells, then retrieved and labeled. CD45-positive, GFP-high cells were sorted by FACS and dispensed into wells of 384-well plates at 1.6 cells per well. **(B)** Specificities of IgG in supernatants from high-throughput B cell cultures. GFP-high and GFP-negative B cells were sorted and distributed into wells as in **(A)**, and expanded for 18 days with irradiated PBMC and cytokines. The supernatants were then screened by ELISA for total IgM, total IgG, and binding to hemagglutinin (HA), tetanus toxoid (Tetanus), or Bovine Serum Albumin (BSA). Vertical axes show the optical density at 450 nm. Red symbols correspond to supernatants binding to HA, of which there are 34 derived from GFP-high cells and one from a GFP-negative cell. IgG from the single GFP-negative cell-derived clone also bound to other antigens and was deemed non-specific. Raw numbers, and ELISA optical densities of IgG-producing, and HA-specific IgG-producing clones are shown in **Supplementary Figure 6**. **(C)** Distribution of mutations in the immunoglobulin genes of hemagglutinin-capturing B cells. RNA from the cultures described in **(B)** was reverse-transcribed and segments corresponding to variable regions of heavy, lambda, and kappa chains were amplified by PCR. We examined antigen binding of the recovered recombinant antibodies to confirm the correct pairing of heavy and light chains, and compared sequences of the cloned gene segments with the closest germline sequences from publicly available databases. Germline conservation is indicated by the percentage of nucleotide identity to the nearest-match V gene segment for each of the germline-encoded structural components: FR1, framework 1; CDR1, complementarity-determining region 1; FR2, framework 2; CDR2, complementarity-determining region 2; FR3, framework 3. Amino acid sequences and inferred V, D, and J gene segments are shown in **Supplementary Table 1**. **(D)** Comparison of somatic hypermutation in heavy chain immunoglobulin sequences isolated from HA-enriched (HA-GFP-capturing) and HA-binding (in first-round screen) hits vs. hemagglutinin-non-binding control sequences. Hemagglutinin-specific VH sequences ($n = 32$) represent antibodies that were verified to bind HA after cloning and re-expression. HA-non-binding VH sequences ($n = 33$) represent heavy chains that were cloned from wells containing HA-binding antibodies, but did not contribute to a hemagglutinin-binding heavy-light chain pair in the validation screen. *p*-values from Mann-Whitney test. Germline identity was assessed with IgBLAST using the IMGT germline database.

hemagglutinin-specific memory B cells following immunization, rather than a change in phenotype, because the absolute numbers of naïve cells in the hemagglutinin-specific pool are not changed by immunization (**Figure 7C**).

The increased abundance following vaccination, and the diminished CD21 expression characterizing the post-vaccination hemagglutinin-capturing B cells led us to hypothesize that this population might be related to the vaccination-induced "activated B cells" (ABC) described by Ellebedy et al. (29). The cardinal features of these B cells are minimal IgD, and high CD71 expression. Plotting IgD against CD71 for the global B cell pool, or for the hemagglutinin-capturing B cells, we see that cells with these features are rare (~0.1%) in the global B cell pool, but comprise 40% of the post-vaccination hemagglutinin-capturing B cells (**Figure 7D**). Before vaccination, most of the hemagglutinin-capturing B cells are CD71-negative. To examine the relationships between the four populations of cells (global pool, ABC, and the pre-, and post-vaccination HA-capturing B cells) quantitatively and without the assumptions of manual gating, we used the automated clustering algorithm k-means

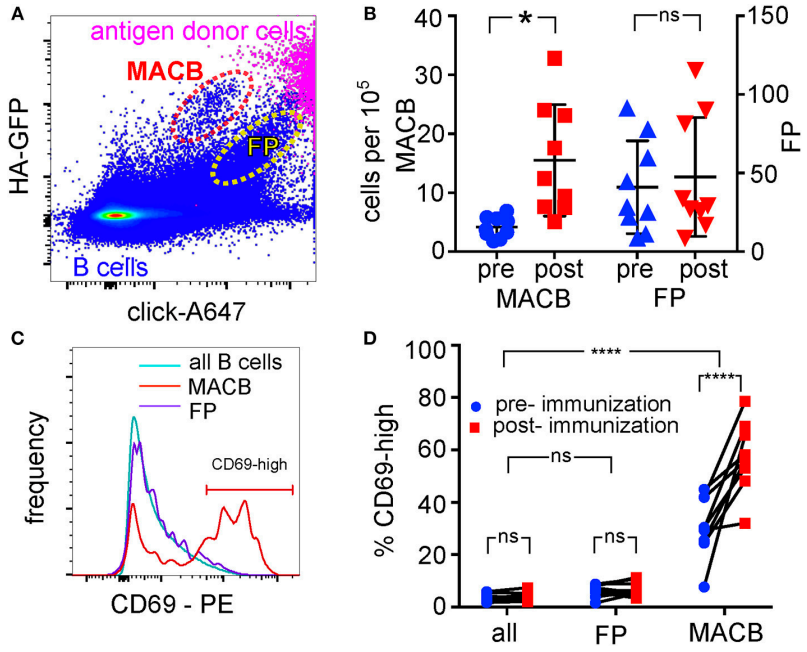

FIGURE 5 | Identification of Antigen-Specific Population with Antigen-Associated and Antigen-Independent Labels. **(A)** BCR-dependent and non-specific antigen uptake. B cells were co-cultured for 3 h with TE HA-GFP cells, of which the extracellular domains of membrane proteins had been additionally labeled with Alexa 647 (A647) by click chemistry. B cells were then retrieved and immunolabeled for CD19, measured by flow cytometry, and gated on single B cells. The plot shows GFP intensity plotted against A647 intensity, both for the B cell population (blue pseudocolor, lower half of the figure), and, for comparison, the antigen-expressing TE cells (magenta, upper right corner). Most B cells capture neither HA-GFP, nor other proteins (bottom left corner of plot). Two populations of B cells acquire HA-GFP: those that acquire high GFP and intermediate A647 ("MACB"–membrane antigen-capturing B cells, broken red oval); and those that also acquire large quantities of A647 (labeled "FP"–false positive, broken yellow oval). Gating is shown in **Supplementary Figure 3**. **(B)** Increase in numbers of HA-GFP capturing cells after immunization. B cells from nine donors were collected before and 1 week after influenza immunization, and then all 18 samples were assayed as above. Numbers of cells falling in the MACB gate (1st and 2nd scatter columns, left vertical axis), and the FP gate (3rd and 4th scatter columns, right vertical axis) shown in **(A)** were compared before and after immunization for each donor by two-way ANOVA followed by Sidak's test. Vertical axes show numbers of cells in the gates per 100,000 B cells measured. Bars show means and standard deviations $^{*}p < 0.05$. **(C)** Histograms of CD69 expression by the cells in the three populations. CD69 expression on cells in populations MACB, FP, and the global B cell pool was measured by flow cytometry. The horizontal bar on the right of the plot marked "CD69-high" shows the gate used to determine the percentages shown in **(D)**, and also in analyses hereafter of the "CD69-high" sub-population of antigen-extracting cells. **(D)** CD69 expression, and response to immunization by the cells in the three populations. Samples from nine donors taken before and after immunization were measured and gated as in **(C)**, and the levels of CD69 compared between populations and between time points by two-way ANOVA, followed by Dunnett's test to compare the two populations with the whole B cell pool, and Sidak's test to compare pre- vs. post-immunization within each population ($^{****}p < 0.0001$).

to classify B cells into nine clusters, based on their expression of eight markers (**Figure 7E**). These markers were chosen to avoid the GFP, A647, CD69, and CD71 that were used to define the cell populations. We then assessed the frequencies of the four cell populations in each of the nine clusters. The highest frequency of ABC was seen in the CD19-high, CD20-high, CD21-low cluster (cluster 5 in **Figures 7E,F**). This cluster also contained the highest frequency of hemagglutinin-capturing B cells post vaccination, corroborating the hypothesis that these cells are related. Across all nine clusters, the frequencies of post-vaccination hemagglutinin-capturing B cells were low in clusters that contained few ABC, and high in clusters enriched for ABC. The cluster (cluster 8 in **Figures 7E,F**) characterized by low CD20, low IgD, low CD138 and high IgM was unique in containing equally low frequencies of ABC and post-vaccination hemagglutinin-capturing B cells, but a frequency of pre-vaccination hemagglutinin-capturing B cells almost as high as among the global B cell pool (**Figure 7F**). These results are consistent with the hypothesis that hemagglutinin-specific B cells circulating in peripheral blood at steady state include naïve cells as well as memory cells, and that following vaccination, one or both of these populations gives rise to the activated B cells described by Ellebedy et al. (29).

Since expression of these markers differs between antigen-capturing B cells and the global B cell pool, we examined the possibility that these markers might be enough to identify the antigen-capturing population without the fluorescent antigen marker. In samples taken post vaccination, this does indeed enable more than 100-fold enrichment, but at steady state, the most promising combination of markers only offers about 10-fold enrichment (**Supplementary Figure 8**).

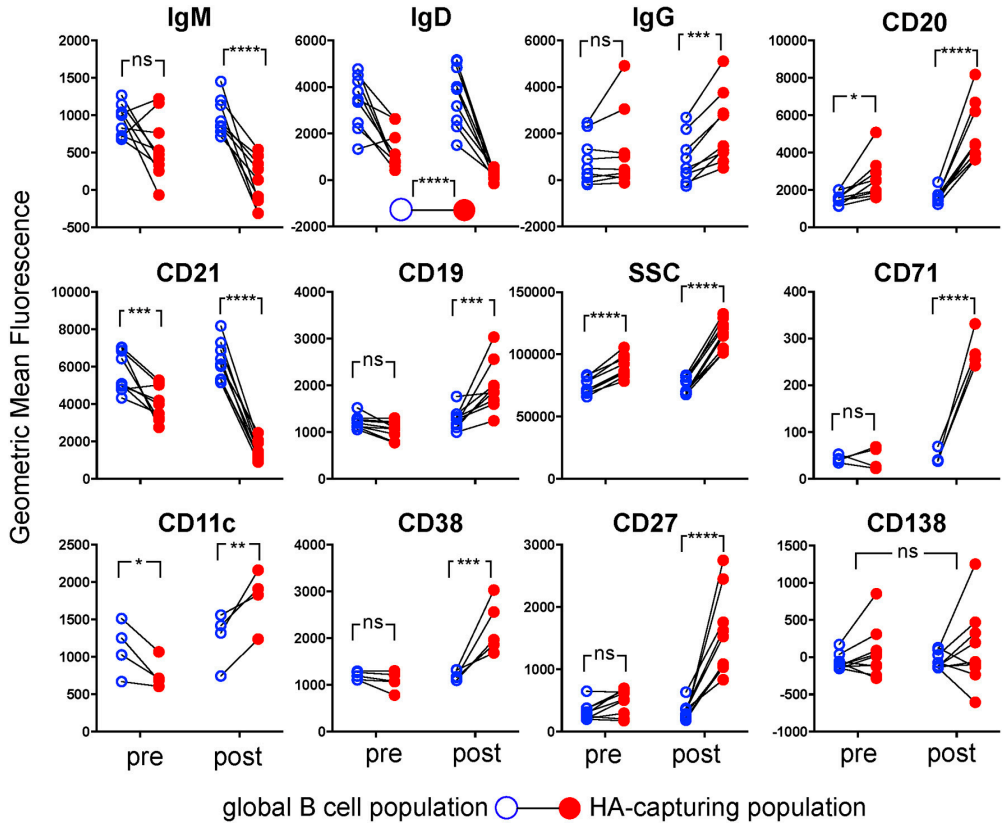

FIGURE 6 | Phenotypes of Hemagglutinin-Specific B Cells from Peripheral Blood. For the nine donors shown in **Figure 5D**, expression of markers was compared between MACB cells (solid red circles) and the whole B cell population (open blue circles), before (left on each plot) and after (right on each plot) immunization, by two-way repeated measures ANOVA. Paired samples from each donor are linked by black lines. Four donors were assessed with an antibody panel including CD11c and CD71, and 5 donors assessed with a panel including CD38 instead. For all parameters shown except IgD and CD138 there was a significant interaction between population and time-point, so the antigen-extracting population was compared to the whole population at the two time-points independently with Sidak's test (*$p <$ 0.05, **$p < 0.01$, ***$p < 0.001$, ****$p < 0.0001$).

Adapting the Method to Isolate Autoantigen-Specific B Cells

Having optimized the paradigm using influenza hemagglutinin as a model membrane antigen, we examined its applicability to isolating B cells specific for a more complex membrane protein, for which the fluorescent soluble antigen approach is less suitable. We chose the ligand-gated ion channel nicotinic acetylcholine receptor (AChR), antibodies against which can cause the pathology of myasthenia gravis. The receptor is comprised of five protein subunits, each with four transmembrane domains, and despite recent advances in isolating AChR-specific B cells, they remain a challenging target (30). As antigen-donor cells we used TE671 cells transiently transfected with the alpha, beta, delta and epsilon subunits of human AChR. The alpha subunit was modified by the insertion of GFP in the cytoplasmic loop between its third and fourth transmembrane domains (13) (**Figure 8A**). Binding of IgG from serum of a patient diagnosed with myasthenia gravis to AChR-transfected cells is shown in **Figure 8B**. Peripheral blood B cells from this donor were co-cultured for 3 h with AChR-GFP-transfected cells. As an additional specificity marker, transfected cells were labeled with A647-conjugated α-bungarotoxin (a high affinity AChR-binding toxin). B cells were then sorted on scatter, IgD, CD69, and antigen capture, as shown in **Figure 8C** and **Supplementary Figure 3**. Single B cells sorted from the antigen-capturing gate were cultivated in 384-well plate wells with IL-21 and feeder cells as described for the culture of HA-specific B cells, and after 13 days, their supernatants were tested for AChR-binding specificity. Examples of negative and positive clones are shown in **Figure 8D**. Using this technique, the frequency of antigen-specific clones is lower than observed for vaccine-induced

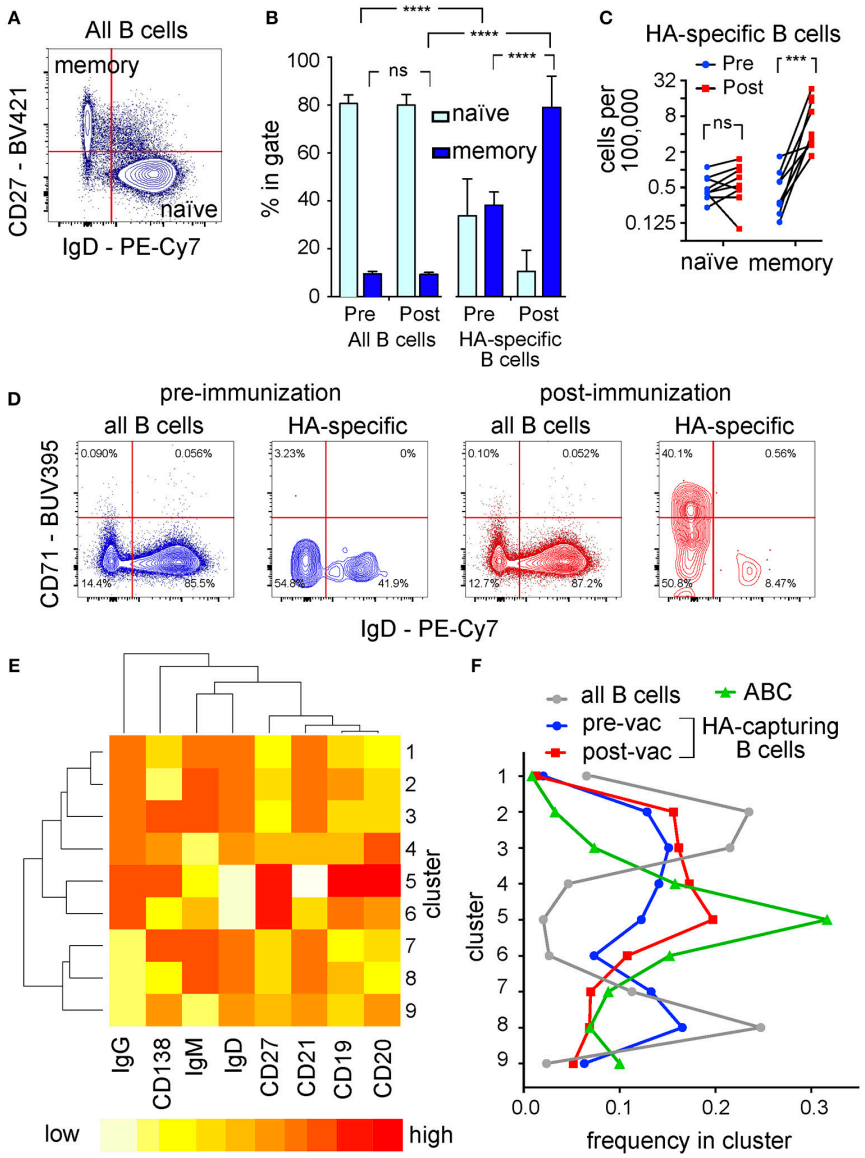

FIGURE 7 | Antigen Experience Profiles of Hemagglutinin-Specific B Cells Detected in Human Blood. **(A)** Representative dot plot of IgD vs. CD27 expression. Human peripheral blood B cells were co-cultured and analyzed by flow cytometry as described in **Figure 5**. The plot shows IgD immunofluorescence on the horizontal axis and CD27 immunofluorescence on the vertical axis, for the whole B cell population. Percentages of events in the "memory" and "naïve" quadrants shown were used to generate **(B)**, and absolute numbers of cells in these quadrants were used to generate **(C)**. **(B)** Proportions of events in the naïve (light blue bars) and memory (dark blue bars) quadrants in samples taken before and after immunization. Left half of bar chart shows proportions of naïve and memory cells in the whole B cell pool; right half shows proportions among the hemagglutinin-specific fraction. In each sub-chart, the two bars on the left correspond to samples taken before immunization, and the two bars on the right to samples taken after. Following two-way, repeated measures ANOVA, the differences between frequencies of memory cells before and after immunization were subjected to Sidak's test; and the differences between frequencies of memory cells in hemagglutinin-specific vs. the total B cell population to Dunnett's test (****$p < 0.0001$). **(C)** Absolute numbers of naïve and memory cells in the hemagglutinin-specific population. Numbers of cells corresponding to the "memory" phenotype [upper left quadrant in **(A)**], and "naïve" phenotype [lower right quadrant in **(A)**] in the hemagglutinin-specific population per 100,000 total B cells are plotted on a log scale. Pre-immunization values are plotted with blue circles, and post-immunization with red squares, and paired samples from each donor are linked by black lines. Following significant two-way ANOVA, the values were compared between the two time points within the two populations by Sidak's test (***$p <$ 0.001). **(D)** Contour plots of IgD vs. CD71 expression. Plots show either the whole B cell pool (1st and 3rd plots), or the CD69-high, hemagglutinin-capturing

(Continued)

FIGURE 7 | cells (2nd and 4th plots), taken from one donor, either before vaccination (blue contour plots on left), or 1 week after (red contour plots on right) vaccination. Cells from nine donors falling in the top left quadrants (IgD-negative, CD71-high) of plots corresponding to the 4th plot here were used as the "Activated B Cells" in **(E,F)**. **(E)** Heat map showing the characteristics of 9 phenotypic clusters. Flow cytometry results for the 8 markers shown, for cells taken before and after vaccination from 9 donors were subjected to automated clustering using the k-means algorithm in R/Bioconductor. Dendrogram to the left of the plot shows the hierarchical relationships between the clusters, and the dendrogram above the plot the relationships between the markers. Red color encodes the highest level of expression, and yellow-to-white the lowest. **(F)** Fractions of different cell populations falling in the clusters shown in **(E)**. Gray circles (connected by gray line) show the distribution of all B cells among the clusters. Blue circles show the fractions of hemagglutinin-capturing, CD69 high (HA-specific) B cells from donors before vaccination, and red squares the corresponding population one week after vaccination. Green triangles show the fractions of vaccination-induced "Activated B Cells," as defined by the IgD-negative, CD71-high quadrant in the 4th plot of **(D)**. Cluster numbers on the vertical axis correspond to cluster numbers shown in **(E)**. Fractions shown on the horizontal axis were calculated by dividing the total number of cells (pooled from all 9 donors) in a given cell population, in a given cluster, by the total number of cells in that population.

hemagglutinin-specific B cells; in this donor, about 0.5% of sorted clones were AChR-binding.

DISCUSSION

The approach of exposing polyclonal B cells to cell-expressed membrane antigens and then sorting the antigen-capturing cells is a powerful technique for B cell research and antibody engineering. Its advantages include the ability to present antigens in their native state and environment, the possibility to exploit the activation of the B cells themselves to increase specificity, and the gain in efficiency offered by panning the B cells that adhere to the antigenic cell layer. The technique is only appropriate for B cells recognizing integral membrane proteins, but this includes many important antigens including viral glycoproteins, autoantigens, and tumor antigens. We assume that there is a lower limit on the affinity of the BCR-antigen interaction required to enable antigen capture, but for many purposes, the preferential isolation of higher affinity clones is a positive feature.

During optimization of the technique, we cloned and phenotyped hemagglutinin-specific B cells from human peripheral blood. The phenotypic characteristics of antigen-capturing B cells characterized after co-culture can reflect either *in vivo* developmental changes, or changes induced by the capture process. The strong induction of CD69 and the differences in light scattering properties that are seen before and more so after vaccination are probably at least partly a consequence of B cell activation following antigen capture *ex vivo*. We assume that when a significant difference is observed between the hemagglutinin-specific and global B cell populations, following vaccination, but not at steady state, that this is likely to reflect the *in vivo* response to vaccination. Elevated expression of IgG, CD19, CD71, CD38, and CD27 fit this pattern. On the other hand, low IgD, low CD21, and high CD20 appear to be characteristics of hemagglutinin-specific B cells irrespective of recent vaccination. A plausible interpretation of this pattern of results is that a small population of hemagglutinin-specific memory B cells, possibly resulting from previous infections or vaccinations, circulates in blood at steady state. Following vaccination, some of these cells proliferate strongly, and their progeny produce the post-vaccination-typical population we observe, characterized by high CD27, CD38, and CD71 expression. Not all the hemagglutinin-capturing B cells from donors before vaccination had this memory-like phenotype. The membrane-capture technique also identifies a small number of hemagglutinin-specific naïve B cells, and it remains possible that descendants of these cells contribute to the post-vaccination expanded memory pool.

Having developed the method using influenza hemagglutinin as a model antigen, we moved on to AChR, a multi-subunit membrane antigen, and the major autoantigen in myasthenia gravis. The isolation of AChR-specific human B cells remains difficult because the most commonly recognized epitope is dependent on the receptor's native conformation (31). We were able to isolate anti-AChR reactive B cells from 6/6 tested patients. As reported by others (30), the frequency of these B cells was much lower than that of B cells directed against influenza hemagglutinin after vaccination. Because the goal of this project was to obtain patient-derived AChR-specific monoclonal antibodies, sensitivity was a higher priority than specificity. We therefore did not use an antigen-independent label to reject likely false positives, and this may also have depressed our specificity.

These two applications of the technique both involved known target antigens, but the method should be adaptable to isolating B cells that recognize antigens whose identity is not yet known, but that are known to be expressed in the membrane of a particular adherent cell line. For this purpose, membrane components of the antigen-expressing cell line would be chemically labeled with a fluorophore before adding B cells. After co-culture, all B cells that have upregulated CD69 and taken up the fluorophore are sorted and cultured. Antigen-specificity of the secreted antibodies in the B cell culture supernatant can then be tested against the antigen-expressing cell line. Heavy and light chain genes can be cloned from the cultured B cells, and used to prepare monoclonal antibodies for identification of the target antigen by immunoprecipitation and mass spectrometry.

The seminal study of antigen acquisition by B cells from the membranes of other cells by Batista et al. (10) used hen egg lysozyme (HEL) as a model antigen, in one of two forms. Either the antigen was complexed with antibodies and loaded onto an Fcγ receptor-expressing myeloid cell line, or antigen-donor cells were transfected with a construct encoding a transmembrane domain and an extracellular HEL moiety. HEL-specific B cells were seen to form stable contacts or "synapses" with either kind of antigen donor cell, and gather the antigen into the synapse. Since then, evidence has accumulated supporting the idea that B cells in the germinal center acquire antigen in the form of immune complexes (32) from specialized antigen-proffering

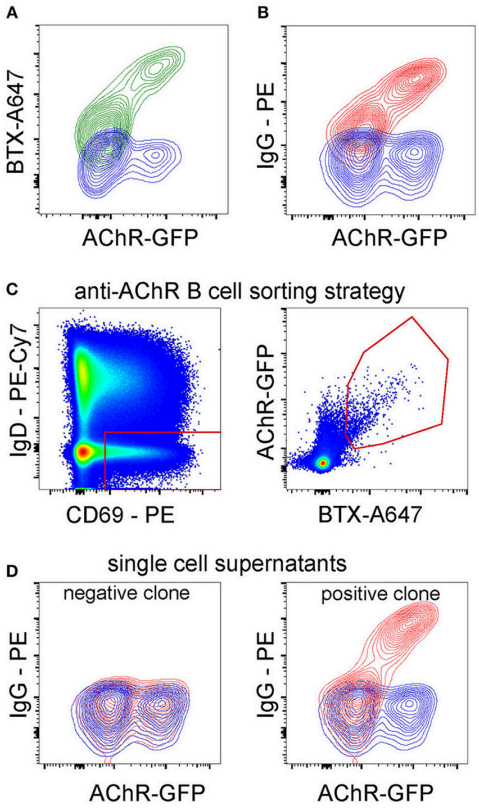

FIGURE 8 | Optimized Sorting Using Membrane-Antigen-Capture Enables Near-Complete Purification of Antigen-Specific Cells. **(A)** A647-labeled alpha-bungarotoxin (BTX) binds to AChR-GFP transfected TE671 proportionally to GFP intensity. TE cells were transiently transfected with the alpha, beta, delta and epsilon subunits of human AChR with a GFP moiety between third and fourth transmembrane helices of the alpha subunit. After 24 h, cells were labeled with A647-alpha-bungarotoxin and analyzed by flow cytometry. **(B)** AChR-binding IgG from patient serum. Serum from a patient diagnosed with myasthenia gravis was diluted to 1:200 and incubated with TE671 cells transiently transfected with AChR-GFP, then with PE anti-human IgG. **(C)** Application of antigen-capture sorting to the isolation of AChR-specific B cells from a human donor. Magnetically isolated peripheral blood B cells from a patient diagnosed with myasthenia gravis were cultured for 3 h with TE cells expressing AChR. The AChR alpha subunit has a GFP moiety fused in-frame in the large cytoplasmic loop between the third and fourth transmembrane helices, and the antigen-donor cells are additionally labeled with A647-conjugated bungarotoxin (BTX). After co-culture, B cells were retrieved by washing, labeled with fluorescent antibodies, and CD69-high, IgD-low, GFP- and A647- double positive cells (gating strategy in **Supplementary Figure 3**) were sorted. **(D)** Confirmation of AChR-specificity of B cell clone from patient. Single B cells sorted as in C were cultured for 13 days with CD40L-expressing feeder cells and IL-21 as described in Methods. Culture supernatants were then assayed for specific antibodies by incubating with AChR-GFP-transfected (GFP-expressing) or non-transfected (GFP-negative) cells, washing, and detecting with fluorescent secondary antibodies against human IgM, IgA, or IgG. The contour plot on the left shows results from a clone considered negative (similar IgG binding to transfected and untransfected cells), and the plot on the right a positive (higher binding to transfected than untransfected cells) anti-AChR IgG-producing clone.

cells such as follicular dendritic cells (FDC), and studies of the subcellular details of how B cells acquire antigen have focused on this mechanism. The extraction of membrane integral protein antigens demonstrated by Batista et al., has received much less attention, and there are important differences between the two scenarios. In both cases, the ability of the B cell to remove the antigen from the donor cell is dependent on a high enough BCR-antigen binding affinity, but the forces retaining the antigen on the donor cell differ. In the case of FDC-proffered immune complexes, the outcome of the "tug-of-war" between the B cell and the donor cell is dependent on the affinities of several non-covalent interactions between antigen, antibodies, complement components and receptors on the FDC. *In vitro* experiments suggest that when B cells acquire cognate antigen in the form of immune complexes from FDC, they capture the antigen without co-capturing the tethering moiety, i.e., without removing any transmembrane protein from the membrane of the FDC, suggesting that in these circumstances, extraction of the integral membrane protein is energetically less favorable than rupturing one of the protein-protein adhesions in the tethering chain of proteins (21). In the case of an integral membrane antigen, extracting the antigen from the membrane (possibly together with some quantity of the associated membrane) is the only option, unless the antigen is enzymatically cleaved. Enzymatic cleavage is a possibility because B cells can secrete lysosome hydrolases into the synaptic cleft (33), but this mechanism appears to be restricted in its utilization and not to be employed for acquiring antigen from live cells (21). A more analogous physiological equivalent of the mechanism exploited by our technique might be the capture of viral antigen from infected cells, such as lymph node subcapsular macrophages. These cells act as pathogen sentinels, being particularly susceptible to infection with viruses such as vesicular stomatitis virus (34) and are important for early B cell responses against the pathogen (35). The fact that the specificity of the technique is reduced by depolymerizing the actin cytoskeleton of the antigen-donor cells is, however, perhaps analogous to the reduction in affinity discrimination caused by similar treatment of FDC in the immune complex acquisition scenario described by Spillane and Tolar (21). This result also predicts that cells with stiffer membranes will make the most suitable antigen-donors for this technique.

The fluorescent membrane antigen capture method can thus be used in two ways. By using a short *ex vivo* co-culture with antigen donor cells, and using the combination of an antigen-associated fluorophore and an antigen-independent fluorophore to report antigen specificity, very rare populations of antigen-specific B cells can be precisely characterized. By using adherent antigen-donor cells and a long enough co-culture to allow activation and surface expression of CD69, antigen-specific B cells can be efficiently sorted at very high purity and expanded *in vitro* for antibody screening and immunoglobulin gene cloning. In both cases, the technique is powerful enough to detect antigen-specific cells without the need for pre-selection of memory or IgG-positive B cells. A particularly flexible feature of the membrane antigen capture method we describe is that it

can be used to detect B cells that recognize an antigen that is expressed on a defined cell type, but whose molecular identity is unknown. This is commonly the situation in the search for anti-cancer antibodies, and autoantibodies involved in autoimmunity, and we envisage that this technique will be applied in these fields to search for new antigens.

ETHICS STATEMENT

This study was carried out in accordance with the recommendations of the Federation of European Laboratory Animal Science Associations. The protocol was approved by the Basel Stadt Cantonal Animal Research Commission.

This study was carried out in accordance with written informed consent from all subjects. All subjects gave written informed consent in accordance with the Declaration of Helsinki. The protocol was approved by the Ethikkommission beider Basel.

AUTHOR CONTRIBUTIONS

JL, ET, NS, and TD: conceptualization. MZ, NR, JL, HK, AG, IC, MS, LsK, NS: investigation. AE and LgK: resources. MZ, NR, JL, ET, NS, and TD: writing. RL, LudK, NS, and TD: funding acquisition. RL: supervision.

FUNDING

The project was funded by Swiss National Science Foundation grants 149966 and 169674, the Swiss Multiple Sclerosis Society, Neuromuscular Research Association Basel, and the University Hospital Basel.

ACKNOWLEDGMENTS

We are grateful to patients and staff of the University Hospital Basel, Hidde Ploegh and Stephanie Dougan, Christoph Hess, Glenn Bantug, Christoph Berger, Hélène Rossez, and Anne-Catherine Lecourt, and the animal and flow cytometry facilities of the Department of Biomedicine, University of Basel.

SUPPLEMENTARY MATERIAL

The Supplementary Material for this article can be found online at: https://www.frontiersin.org/articles/10.3389/fimmu.2019.00829/full#supplementary-material

REFERENCES

1. Crotty S, Aubert RD, Glidewell J, Ahmed R. Tracking human antigen-specific memory B cells: a sensitive and generalized ELISPOT system. *J Immunol Methods.* (2004) 286:111–22. doi: 10.1016/j.jim.2003.12.015
2. Scheid JF, Mouquet H, Feldhahn N, Walker BD, Pereyra F, Cutrell E, et al. A method for identification of HIV gp140 binding memory B cells in human blood. *J Immunol Methods.* (2009) 343:65–7. doi: 10.1016/j.jim.2008.11.012
3. Taylor JJ, Martinez RJ, Titcombe PJ, Barsness LO, Thomas SR, Zhang N, et al. Deletion and anergy of polyclonal B cells specific for ubiquitous membrane-bound self-antigen. *J Exp Med.* (2012) 209:2065–77. doi: 10.1084/jem.20112272
4. Andrews SF, Joyce MG, Chambers MJ, Gillespie RA, Kanekiyo M, Leung K, et al. Preferential induction of cross-group influenza A hemagglutinin stem-specific memory B cells after H7N9 immunization in humans. *Sci Immunol.* (2017) 2:13. doi: 10.1126/sciimmunol.aan2676
5. Klein F, Gaebler C, Mouquet H, Sather DN, Lehmann C, Scheid JF, et al. Broad neutralization by a combination of antibodies recognizing the CD4 binding site and a new conformational epitope on the HIV-1 envelope protein. *J Exp Med.* (2012) 209:1469–79. doi: 10.1084/jem.20120423
6. Michalek K, Morshed SA, Latif R, Davies TF. TSH receptor autoantibodies. *Autoimmun Rev.* (2009) 9:113–6. doi: 10.1016/j.autrev.2009.03.012
7. Hughes EG, Peng X, Gleichman AJ, Lai M, Zhou L, Tsou R, et al. Cellular and synaptic mechanisms of anti-NMDA receptor encephalitis. *J Neurosci.* (2010) 30:5866–75. doi: 10.1523/JNEUROSCI.0167-10.2010
8. Waters PJ, McKeon A, Leite MI, Rajasekharan S, Lennon VA, Villalobos A, et al. Serologic diagnosis of NMO: a multicenter comparison of aquaporin-4-IgG assays. *Neurology.* (2012) 78:665–71; discussion 9. doi: 10.1212/WNL.0b013e318248dec1
9. Sanderson NS, Zimmermann M, Eilinger L, Gubser C, Schaeren-Wiemers N, Lindberg RL, et al. Cocapture of cognate and bystander antigens can activate autoreactive B cells. *Proc Natl Acad Sci USA.* (2017) 114:734–9. doi: 10.1073/pnas.1614472114
10. Batista FD, Iber D, Neuberger MS. B cells acquire antigen from target cells after synapse formation. *Nature.* (2001) 411:489–94. doi: 10.1038/35078099
11. Spillane KM, Tolar P. Mechanics of antigen extraction in the B cell synapse. *Mol Immunol.* (2018) 101:319–28. doi: 10.1016/j.molimm.2018.07.018
12. Litzenburger T, Fassler R, Bauer J, Lassmann H, Linington C, Wekerle H, et al. B lymphocytes producing demyelinating autoantibodies: development and function in gene-targeted transgenic mice. *J Exp Med.* (1998) 188:169–80. doi: 10.1084/jem.188.1.169
13. Leite MI, Jacob S, Viegas S, Cossins J, Clover L, Morgan BP, et al. IgG1 antibodies to acetylcholine receptors in 'seronegative' myasthenia gravis. *Brain.* (2008) 131:1940–52. doi: 10.1093/brain/awn092
14. Ellis B, Haaland P, Hahne F, Le Meur N, Gopalakrishnan, Spidlen J, et al. *FlowCore: Basic Structures for Flow Cytometry Data*. R package version 1.40.6. (2017).
15. Kaufmann L, Syedbasha M, Vogt D, Hollenstein Y, Hartmann J, Linnik JE, et al. An optimized hemagglutination inhibition (HI) assay to quantify influenza-specific antibody titers. *J Vis Exp.* (2017) e55833. doi: 10.3791/55833
16. Lindner JM, Cornacchione V, Sathe A, Be C, Srinivas H, Riquet E, et al. Human Memory B Cells harbor diverse cross-neutralizing antibodies against BK and JC polyomaviruses. *Immunity.* (2019) 50:668–76.e5. doi: 10.1016/j.immuni.2019.02.003
17. Huang J, Doria-Rose NA, Longo NS, Laub L, Lin CL, Turk E, et al. Isolation of human monoclonal antibodies from peripheral blood B cells. *Nat Protoc.* (2013) 8:1907–15. doi: 10.1038/nprot.2013.117
18. Dougan SK, Ashour J, Karssemeijer RA, Popp MW, Avalos AM, Barisa M, et al. Antigen-specific B-cell receptor sensitizes B cells to infection by influenza virus. *Nature.* (2013) 503:406–9. doi: 10.1038/nature12637
19. Wrammert J, Koutsonanos D, Li GM, Edupuganti S, Sui J, Morrissey M, et al. Broadly cross-reactive antibodies dominate the human B cell response against 2009 pandemic H1N1 influenza virus infection. *J Exp Med.* (2011) 208:181–93. doi: 10.1084/jem.20101352
20. Vranic S, Boggetto N, Contremoulins V, Mornet S, Reinhardt N, Marano F, et al. Deciphering the mechanisms of cellular uptake of engineered nanoparticles by accurate evaluation of internalization using imaging flow cytometry. *Part Fibre Toxicol.* (2013) 10:2. doi: 10.1186/1743-8977-10-2
21. Spillane KM, Tolar P. B cell antigen extraction is regulated by physical properties of antigen-presenting cells. *J Cell Biol.* (2017) 216:217–30. doi: 10.1083/jcb.201607064

22. Whittle JR, Wheatley AK, Wu L, Lingwood D, Kanekiyo M, Ma SS, et al. Flow cytometry reveals that H5N1 vaccination elicits cross-reactive stem-directed antibodies from multiple Ig heavy-chain lineages. *J Virol.* (2014) 88:4047–57. doi: 10.1128/JVI.03422-13
23. Avnir Y, Tallarico AS, Zhu Q, Bennett AS, Connelly G, Sheehan J, et al. Molecular signatures of hemagglutinin stem-directed heterosubtypic human neutralizing antibodies against influenza A viruses. *PLoS Pathog.* (2014) 10:e1004103. doi: 10.1371/journal.ppat.1004103
24. Lingwood D, McTamney PM, Yassine HM, Whittle JR, Guo X, Boyington JC, et al. Structural and genetic basis for development of broadly neutralizing influenza antibodies. *Nature.* (2012) 489:566–70. doi: 10.1038/nature 11371
25. Pappas L, Foglierini M, Piccoli L, Kallewaard NL, Turrini F, Silacci C, et al. Rapid development of broadly influenza neutralizing antibodies through redundant mutations. *Nature.* (2014) 516:418–22. doi: 10.1038/nature13764
26. Lavinder JJ, Wine Y, Giesecke C, Ippolito GC, Horton AP, Lungu OI, et al. Identification and characterization of the constituent human serum antibodies elicited by vaccination. *Proc Natl Acad Sci USA.* (2014) 111:2259–64. doi: 10.1073/pnas.1317793111
27. Wine Y, Horton AP, Ippolito GC, Georgiou G. Serology in the 21st century: the molecular-level analysis of the serum antibody repertoire. *Curr Opin Immunol.* (2015) 35:89–97. doi: 10.1016/j.coi.2015.06.009
28. DeKosky BJ, Kojima T, Rodin A, Charab W, Ippolito GC, Ellington AD, et al. In-depth determination and analysis of the human paired heavy- and light-chain antibody repertoire. *Nat Med.* (2015) 21:86–91. doi: 10.1038/nm.3743
29. Ellebedy AH, Jackson KJ, Kissick HT, Nakaya HI, Davis CW, Roskin KM, et al. Defining antigen-specific plasmablast and memory B cell subsets in human blood after viral infection or vaccination. *Nat Immunol.* (2016) 17:1226–34. doi: 10.1038/ni.3533
30. Makino T, Nakamura R, Terakawa M, Muneoka S, Nagahira K, Nagane Y, et al. Analysis of peripheral B cells and autoantibodies against the anti-nicotinic acetylcholine receptor derived from patients with myasthenia gravis using single-cell manipulation tools. *PLoS ONE.* (2017) 12:e0185976. doi: 10.1371/journal.pone.0185976
31. Luo J, Taylor P, Losen M, de Baets MH, Shelton GD, Lindstrom J. Main immunogenic region structure promotes binding of conformation-dependent myasthenia gravis autoantibodies, nicotinic acetylcholine receptor conformation maturation, and agonist sensitivity. *J Neurosci.* (2009) 29:13898–908. doi: 10.1523/JNEUROSCI.2833-09.2009
32. Cyster JG. B cell follicles and antigen encounters of the third kind. *Nat Immunol.* (2010) 11:989–96. doi: 10.1038/ni.1946
33. Yuseff MI, Reversat A, Lankar D, Diaz J, Fanget I, Pierobon P, et al. Polarized secretion of lysosomes at the B cell synapse couples antigen extraction to processing and presentation. *Immunity.* (2011) 35:361–74. doi: 10.1016/j.immuni.2011.07.008
34. Iannacone M, Moseman EA, Tonti E, Bosurgi L, Junt T, Henrickson SE, et al. Subcapsular sinus macrophages prevent CNS invasion on peripheral infection with a neurotropic virus. *Nature.* (2010) 465:1079–83. doi: 10.1038/nature09118
35. Junt T, Moseman EA, Iannacone M, Massberg S, Lang PA, Boes M, et al. Subcapsular sinus macrophages in lymph nodes clear lymph-borne viruses and present them to antiviral B cells. *Nature.* (2007) 450:110–4. doi: 10.1038/nature06287

Conflict of Interest Statement: The authors declare that the research was conducted in the absence of any commercial or financial relationships that could be construed as a potential conflict of interest.

Results II

Hypermutated and clonally expanded acetylcholine receptor-specific IgM B cells circulate in myasthenia gravis patients and healthy controls

(Manuscript in preparation)

[1]Natalie Rose, [1]Hyein Kim, [1]Raija Lindberg, [2]Ludwig Kappos, [1]Nicholas Sanderson, [1,3]Tobias Derfuss

[1]Department of Biomedicine, University Hospital Basel, University of Basel, Basel, Switzerland, [2]Departments of Medicine, Neurologic Clinic and Policlinic, Clinical Research and Biomedical Engineering, University Hospital and University of Basel, Basel, Switzerland, [3]Department of Medicine, Neurologic Clinic and Policlinic, University Hospital and University of Basel, Basel, Switzerland

Abstract

Myasthenia gravis is an autoimmune disorder defined by muscle weakness and fatigability due to the binding of pathogenic antibodies to proteins at the neuromuscular junction. The most common autoantibody target is the acetylcholine receptor (AChR). IgG binding to AChR leads to internalization of the receptor, complement-mediated damage of the postsynaptic membrane, or inhibition of acetylcholine binding.

The rarity of the AChR-specific B cells in the peripheral blood and the complexity of the AChR make their isolation and further characterization difficult. We isolated AChR-specific B cells from 4 patients with myasthenia gravis, 1 patient with multiple autoantibodies, and 5 healthy controls (HC) using a membrane-antigen capture assay. Our assay enabled us to isolate not only class-switched IgG B cells, but also IgM B cells that recognize AChR. Specificity of the mAbs was verified in a cell-based assay where the majority of IgM but not of IgG mAbs bound to the main immunogenic region on the alpha-subunit. RNA sequence analyses revealed that anti-AChR IgM B cells can be hypermutated and clonally expanded in patients with MG and intriguingly also in HC, which suggests that anti-AChR germinal center reactions can also take place in healthy people.

Introduction

Myasthenia gravis is widely regarded as a prototypical B cell mediated autoimmune disorder. Patients suffer from muscle weakness and fatigability due to the binding of autoantibodies to proteins at the neuromuscular junction. The most common target is the nicotinic acetylcholine receptor (AChR) located in the postsynaptic membrane of the muscle fiber. Approximately 80% of patients have antibodies binding to AChR in their serum which can be detected using a standard radio immunoprecipitation assay.

Despite the fact that antibodies have been identified as the main pathogenic factor in myasthenia gravis in the late 1950s (1) and have been studied extensively since then, little is known about the epitopes they bind to, the determinants of the pathogenicity of an antibody, and the B cells that produce these antibodies. It has been shown that the titers of AChR-autoantibodies that are measured by the RIA do not correlate with the clinical severity and are not a useful tool for inter-patient comparisons (2) which suggests that some antibodies are less pathogenic than others. In recent years, assays using live cells that express AChR have increased the sensitivity of AChR-antibody detection, but such tests are not yet standardized for use as a diagnostic tool (3–5).

While phage display studies have produced antibodies that recognize AChR (6–8), these antibodies are not guaranteed to represent pairings of heavy and light chains that occur in patients. Despite the claims that the thymus of myasthenia gravis patients contains AChR-specific B cells at high frequencies (9–11), so far only one AChR-gamma-subunit specific recombinant antibody has been sequenced from thymic B cells (12). Recently, a group was able to isolate 8 AChR-specific memory B cells from 5 MG patients using recombinantly expressed extracellular domain of the α-subunit and found diverse usage of V(D)J genes within and between patients (13).

We have recently developed a suite of techniques for the isolation of B cells that are specific for a given membrane antigen (14) and have adapted it to isolate AChR-specific B cells from peripheral blood mononuclear cells. Our method allows for the enrichment of antigen-specific B cells without the need to pre-select a B cell compartment such as memory B cells.

Materials and Methods

Human samples

Peripheral blood samples were collected from 5 healthy controls, 4 patients with AChR-autoantibodies and clinically confirmed myasthenia gravis and 1 patient with AChR-autoantibodies and multiple autoantibodies of unknown etiology.

Peripheral blood was drawn into S-Monovette tubes containing 1.6 mg EDTA per ml blood (01.1605.100) for isolation of PBMCs, and into S-Monovette tubes with clot activator (01.1601.100, both from Sarstedt) for serum preparation. PBMC isolation and serum preparation was performed as previously described (14). PBMCs were stored in liquid nitrogen until use, serum was stored at -20°C.

Plasmids and Cell Lines

TE671 rhabdomyosarcoma cells were obtained from ATCC (LGC, Wesel, Germany) and cultured in complete RPMI medium (10% heat-inactivated fetal calf serum (FCS), 100 units/ml of penicillin and 100 ug/ml of streptomycin; all from Gibco), at 37°C in 5% carbon dioxide. β, δ, and ε-subunits of AChR cloned into pcDNA3.1-hygro, and α-subunit cloned into pEGFP-N1 for a intracellular eGFP tag were a gift from David Beeson (15).

pCMV3 containing human CD40 ligand was purchased from sino biological. TE cells were stably transfected, sorted for CD40L expression, and irradiated at 72 Gy for mitotic inactivation and kept frozen in liquid nitrogen until use.

Cell-based antibody assay

TE671 cells were transfected with 6 µg of plasmid DNA at a ratio of 2:1:1:1 of α-GFP, β, δ, and ε-subunits using Jetprime transfection reagent according to manufacturer's instructions. 24 hours post transfection, TE-AChR-GFP were washed, trypsinized, and resuspended in cold separation buffer (PBS with 2% FCS and 2 mM EDTA).

Flow cytometry and cell sorting

To isolate AChR-specific B cells, B cells were enriched from thawed PBMCs using negative selection (Pan B cell isolation kit, human, Miltenyi). TE-AChR-GFP were stained with Af647-labeled α-bungarotoxin (B35450, ThermoFisher), then washed with complete RPMI medium. B cells were co-cultured for 3 hours with CTB-labeled TE-AChR. B cells were retrieved and

incubated for 20 min on ice with PE-conjugated anti-human CD69 diluted 1:100 in cold separation buffer. B cells were sorted on a FACSAria III Cell Sorter (BD Biosciences). Cells were gated on scatter to select live, single cells and on CTB-negative to exclude TE-AChR cells. Cells that were double positive for GFP and Af647 were sorted into 1.5 ml Eppendorf tubes containing 700 µl B cell medium (RPMI with 40% FCS), 100 units/ml of penicillin and 100 ug/ml of streptomycin, and 50 ng/ml recombinant human IL-21 all from Gibco).

Primary B cell culture

B cells were plated in flat bottom 384 well plates at a density of 1 B cell per well in the presence of 5000 irradiated TE-CD40L and 50 ng/ml recombinant human IL-21 in 75 µl RPMI-40. The outer wells of each plate were filled with 120 µl sterile H_2O. Plates were wrapped lightly in aluminum foil to limit evaporation and placed in a humidified incubator with 5% CO_2 and 8% O_2 at 37°C for 12 days.

Screening of primary B cell culture supernatants

15 µl of B cell culture SN was incubated with 10 µl separation buffer containing 5000 TE-AChR-GFP for 30 min at room temperature in the dark. Cells were washed and incubated with goat PE anti-human IgG at 1:200 (109-116-098), Af647 anti-human IgA at 1:400 (109-605-011), and Af594 anti-human IgM at 1:200 (109-585-129; all from Jackson ImmunoResearch), washed again and fixed in 4% PFA-PBS. Cells were acquired on a Cytoflex flow cytometer (Beckman Coulter).

cDNA generation, Illumina library preparation and sequencing

After the screening, all but 10 µl of cell culture supernatant was removed and transferred to storage plates using the ViaFlo 384 (Integra). B cells were lysed in 20 µl lysis buffer as previously described (16). Plates containing lysed B cells were stored at -80°C, plates containing supernatant at -20°C.

RNA was isolated from lysed samples using the Quick-RNA MicroPrep Kit (Zymo). In brief, samples were thawed at room temperature, then mixed with 100 µl lysis buffer. 130 µl 100% ethanol was added and the mixture transferred to a supplied column. After centrifugation, the column was treated with DNAse for 15 min at room temperature. The column was first washed with RNA prep buffer, then twice with RNA wash buffer before the RNA was eluted in 15 µl H_2O. 4.5 µl RNA was used to generate cDNA using the SMART-Seq® v4 Ultra® Low Input RNA Kit for Sequencing by Takara following the manufacturer's instructions at half the

volume of reaction. Illumina library preparation (Nextera XT DNA Library Preparation Kit) and sequencing on a NexSeq500 (Illumina) were handled by an in-house service.

Extraction and assembly of immunoglobulin gene sequences

Immunoglobulin gene sequences were extracted from the raw sequencing reads using R as described in detail in Supplementary Materials. Fastq files from the sequencer were aligned using the QasR and Rsamtools packages to an artificial mini genome containing the genomic sequences of constant regions from delta, mu, gamma, alpha, and epsilon heavy chain genes, and kappa and lambda light chain genes, and the number of reads aligning to each were used to infer the class and subclass. Variable regions were reassembled using tools from the ShortRead and BioStrings Packages. Assembled variable regions were checked for plausible V(D)J open reading frames using IgBlast (NCBI).

Recombinant human antibody production

DNA constructs encoding the inferred amino acid sequence from leader to several bases into the constant region were synthesized by IDT with restriction sites at the termini to enable in-frame cloning into pUltra plasmids already containing the appropriate constant region. Adherent HEK293T/17 (ATCC) were cultured in DMEM-10 in 12 or 6 well plates. Cells were transiently transfected with 1.5 µg plasmids encoding the heavy and light chain of a recombinant antibody in 1.5 ml DMEM-10 using 150 µl jetprime buffer and 3 µl jetprime reagent (PPLU114-07, Polyplus transfection). For IgM antibodies, we co-transfected the HEK293T/17 cells with a plasmid encoding the human J-chain. After 48-72 hours, the supernatants were harvested.

Quantification of IgG and IgM in HEK cell culture supernatant via ELISA

IgM and IgG in the supernatant was quantified by a sandwich ELISA. Goat anti-human IgG (2014-01) or IgM (2023-01) capture antibody was diluted to 1 µg/ml in PBS and coated onto MaxiSorp ELISA plates (Nunc) overnight at 4°C. Plates were washed with PBS, blocked with PBS-1% BSA for 2 hours at room temperature, then washed with PBS-0.05% Tween20 before incubating with HEK cell culture supernatant for 2 hours at room temperature. After washing with PBS-0.05% Tween20, plates were incubated with either goat anti-human IgG-HRP (2014-05) or goat anti-human IgM-HRP (2023-05, all Southern Biotech) for 1 hour at room temperature. Plates were washed with PBS-0.05% Tween20 and developed with TMB (53-00-

02, Seracare) until a blue color was visible. The reaction was stopped with an equal volume of 1N H_2SO_4 and the plates were read at 450nm within 30 min of stopping the reaction.

Polyreactivity ELISA

dsDNA (D4522, Sigma Aldrich), ssDNA (dsDNA heated to 95°C for 5 min), and LPS (L4391, Sigma Aldrich) were diluted to a concentration of 10 µg/ml in PBS, and insulin (Actrapid 100, Novo Nordisk) and influenza haemagglutinin (11055-V08B, Sino Biological) were diluted to a concentration of 5 µg/ml in PBS and coated onto MaxiSorp ELISA plates (Nunc) overnight at 4°C. The rest of the procedure followed the ELISA protocol for the quantification of Ig as described above. For anti-milk reactivity, plates were incubated with 5% skim milk powder in PBS and secondary antibodies were diluted in 0.5% skim milk powder.

Statistics

We used GraphPad PRISM 8 and FlowJo 10.5.2 to graph and analyze the data. Numerical results that passed appropriate tests of normality were analyzed by t-test or analysis of variance, and otherwise by appropriate non-parametric tests.

Study approval

5 healthy controls, 4 patients with myasthenia gravis and 1 patient with AChR-autoantibodies gave written informed consent in accordance with the Declaration of Helsinki. This study was carried out in accordance with the recommendations of the Federation of European Laboratory Animal Science Associations. The protocol was approved by the Basel Stadt Cantonal Animal Research Commission.

Supplementary methods

Immunofluorescent labeling of rat muscle sections

Lewis rats were transcardially perfused under barbiturate anesthesia with 10 ml PBS followed by 20 ml 4% paraformaldehyde in PBS. Gastrocnemius muscles were dissected and cryoprotected in sequential 10%, 20%, and 30% sucrose solutions in PBS at 4°C, then frozen in OCT (81-0771-00, Biosystems) and sectioned directly onto slides at 45 microns in a Leica cryostat. Sections were blocked in 5% normal goat serum (G6767, Sigma-Aldrich), 0.3% triton-X in PBS for one hour, then incubated overnight at room temperature in a labeling solution consisting of 1 µg/ml AF647-α-BTX (B35450, ThermoFisher), 1 µg/ml DAPI (D9542, Sigma-Aldrich), and either AF488-conjugated goat anti-human IgM (109-545-129), or rhodamine-conjugated goat anti-rat secondary antibody (112-295-003, both Jackson ImmunoResearch) in blocking solution. After washing in PBS containing 0.3% triton-x, slides were coverslipped with Fluoromount (0100-01, Southern Biotech) and imaged with a Nikon Ti2 epifluorescent microscope.

Results

Study participant characteristics.

Three patients with generalized myasthenia gravis (1 female, 2 male), one male patient with ocular myasthenia gravis, and one female patient with multiple autoantibodies of unknown etiology were included in this study. The mean age was 48.4 years (range 35 – 63). At the time of sample collection, all patients tested positive for anti-AChR IgG in the standard radioimmunoassay (RIA) and none of them received immunosuppressive drugs. Manufacturers report that the specificity of the RIA is 95% or higher (RSRLTD; Euroimmun). A recently published paper reported 5 patients who were positive for AChR in a RIA but negative in a cell-based assay (17) and whose clinical courses did not match a myasthenia gravis diagnosis. Similarly, the case history and symptoms of patient MG5 did not match diagnostic criteria of myasthenia gravis.

The AChR autoantibody titers ranged from 16.5 nmol/l to 850.9 nmol/l (mean 290.9 nmol/l, median 193.7 nmol/l). The Besinger score was used to quantify the severity of myasthenia gravis symptoms in the four confirmed MG patients. It ranged from 3 to 8 and did not correlate with AChR autoantibody titers ($P > 0.1$, Pearson r – 0.8997). One MG patient had been thymectomized approximately 17 years before sample collection, one patient had a thymoma and another patient had slight thymic hyperplasia.

Five healthy controls (3 female, 2 male) with no history of autoimmune disorders, no recent inflammatory events, and no AChR autoantibodies in serum were also included (mean age 49.2 years, range 36 – 65 years). Table 1 summarizes the demographic and clinical data of all study participants.

Establishment of a live cell-based flow cytometric assay for AChR autoantibodies.

The advantages of the cell-based assay are that AChR is expressed in its native conformation and with mammalian posttranslational modifications. It offers comparable or even increased sensitivity compared to the RIA (15,18). We transiently transfected the human rhabdomyosarcoma cell line TE 671 with plasmids encoding for the human α, β, δ, and ε-subunits of AChR (15). The α-subunit carried an intracellular eGFP-tag which enabled us to identify successfully transfected cells. We tested serum samples from all study participants and assessed them for binding of IgA, IgG, and IgM to AChR. Representative flow cytometry plots

of patients with a positive AChR RIA (A, top) and HC (A, bottom) are shown in Figure 1. Positive reactivity was measured by dividing the geometric mean fluorescence intensity (GMFI) of binding to AChR-transfected, GFP-positive cells, by the GMFI of binding to untransfected, GFP-negative cells. All four of the confirmed AChR-MG patients showed IgG binding to AChR. The ratio of binding to AChR ranged from 7.1 to 23.9 and did not directly correlate with the titers of the RIA ($P > 0.5$, Pearson r – 0.4321). None of the healthy controls showed any anti-AChR reactivity in their serum. The patient with multiple autoantibodies of unknown etiology was negative in the cell-based assay for anti-AChR antibodies.

Isolation of AChR-specific B cells by membrane-antigen capture assay.

We have previously shown that B cells can capture their cognate antigen directly from the plasma membrane of antigen-expressing cells. When antigen is internalized, antigen-associated fluorophores are taken up with it, and surface expression of the early activation marker CD69 is rapidly upregulated (Figure 2A)(14). TE671 transiently transfected with AChR-GFP (TE AChR-GFP) were incubated with AF647-labelled α-bungarotoxin (α-BTX) to stain AChR. TE AChR-GFP were then co-cultured for 3 hours with B cells from patients or healthy controls. B cells were retrieved, stained with PE-anti CD69 and antigen-capturing B cells were sorted (Figure 2B). Single sorted B cells were expanded for 10-12 days in the presence of irradiated CD40L-expressing feeder cells and IL-21 before their supernatant was screened for anti-AChR antibodies via the cell-based assay we established with serum. Contents of wells with positive reactivity to AChR were lysed, and full transcriptome sequencing was performed.

AChR-specific IgG B cells in MG patients are highly specific and bind to AChR at concentrations below 100 ng/ml.

All recovered immunoglobulin variable sequences were cloned into vectors containing the constant region for heavy and light chain of the originally isolated B cell, and transfected into HEK cells for recombinant expression. Experiments were performed with unpurified cell culture supernatants of transfected HEK cells. In total, we cloned and recombinantly expressed 6 anti-AChR IgG from 3 of the 4 confirmed MG patients (3 IgG_1, 1 IgG_3, 2 IgG_4; Figure 3A). Isotyping of the serum anti-AChR antibodies revealed that the patient from whom we cloned 2 IgG_4 B cells had positive reactivity of all 4 IgG isotypes in his serum and the strongest

reactivity of IgG4. The other two patients only showed IgG_1 serum reactivity to AChR (Figure 3B).

Recombinant IgG bound strongly to AChR in a live cell-based assay even at low concentrations of 60-90 ng/ml, their binding to AChR was not inhibited by pre-incubation with α-BTX, and pre-incubation with the MIR-specific rat monoclonal mAb35 decreased the binding of 2 rec. IgG to 58 or 44% respectively (Figure 3C). A similarly expressed IgG_1 anti-HA was used as negative control and showed no AChR binding. An indirect ELISA was performed to assess the polyreactivity of the cloned antibodies and showed that they were not cross-reacting with any of the tested antigens (Figure 3D).

Variable regions of AChR-specific IgG B cells are hypermutated and comprised of diverse V(D)J gene combinations.

Except for the 2 IgG_4 clones which shared the use of H and L chain V(D)J combinations, there was no particular gene family or allele that was commonly found in AChR-specific IgG. J region family 6 was used in the heavy chain of all 6 IgG, either allele *02 or *03. Table 2 summarizes the use of V(D)J gene family and allele, number of mutations, and the amino acid sequence of the CDR3. All IgG B cells had mutations in their heavy and light chains, with more mutations located in the complementarity determining regions (CDR) than in the framework regions (FR) (Figure 3E).

AChR-specific IgM have a wide range of affinities for AChR.

We also isolated 28 anti-AChR IgM from the 5 patients with MG, and 11 from 2 HC. Of the 11 B cells isolated from HC, 2 expressed identical immunoglobulin heavy and light chains. Variable regions were cloned into plasmids containing the constant regions of the originally isolated B cell and were transfected into HEK cells together with a plasmid containing the construct for human J chain to facilitate the formation of IgM pentamers (19,20). The concentration of IgM in HEK cell supernatants was determined by ELISA and all supernatants were standardized to a concentration of approximately 500 ng/ml. Recombinant IgM differed a lot in their ability to bind to AChR. Representative flow cytometry plots of binding to TE AChR-GFP are shown in Figure 4A. AChR binding ranged from 1.98 to 34.67 for antibodies derived from patients with MG (Figure 4B) and 1.91 to 22.14 for IgM derived from HC (Figure 4C). mAb MG5-C also bound to rat AChR in fixed muscle tissue (Supplementary Figure 3).

None of the recombinant IgM were inhibited by preincubation with α-BTX. Preincubation with mAb35 reduced the binding of 60.7% of IgM derived from patients with MG (17/28) and 30% of HC derived IgM (3/10) to less than half. Interestingly, preincubation with mAb35 increased the binding of 17.9% of MG derived IgM (5/28) and 10% of HC derived IgM (1/10) by more than 50% (Figure 4B, C). This increase was not seen in the same experimental condition using recombinant anti-AChR IgG (Figure 3C).

Clonally expanded, somatically hypermutated AChR-specific IgM B cells circulate in myasthenia gravis patients and healthy controls.

Of the 28 AChR-specific IgM B cells isolated from patients with MG, 17 had sequences identical to germline (60.7%) (Supplementary table 1), while in healthy controls the percentage of unmutated IgM was 36.4% (Supplementary table 2). There was evidence of clonal expansion of AChR-specific IgM B cells both in myasthenia gravis patients and in healthy volunteers. Clones D and G of patient MG4 had identical light chain sequences and only differed in their heavy chain where mAb D had 2 additional mutations. We found clonally related IgM B cells in 2 HC and both expanded clones were somatically hypermutated.

Assessment of polyreactivity of recombinant anti-AChR IgM.

We performed a commonly used indirect ELISA to assess the polyreactivity of our recombinant IgM. Antibodies that bound to 2 or more antigens with an OD450nm above the cut-off were considered to be polyreactive (Figure 5A). There was no significant difference in the proportion of polyreactive B cells in AChR-specific IgM from patients or HC (Figure 5B). There was no correlation between the binding to antigens in indirect ELISA and the strength of binding to AChR (Figure 5C, Supplementary Figure 2A) or the number of mutations in heavy and light chain (Figure 5D, Supplementary Figure 2B). None of the 5 polyreactive IgM from patients with MG shared the same V(D)J gene combinations (Table 3). The 3 polyreactive IgM from HC contained 2 B cells of the same donor that were clonally related (Table 4). We also assessed whether our antibodies bound to the corresponding strain of influenza haemagglutinin that was used in the ELISA when it was expressed natively on the surface of live cells (Figure 5E). None of the antibodies that bound haemagglutinin in ELISA showed positive reactivity in the cell-based assay, while the similarly expressed HA-specific positive control IgM was positive in both assays. Next, we performed a two-way analysis of variance

on the number of mutations in the VH region in polyreactive and non-polyreactive mAbs from MG and HC and found no significant differences (main effect of health status P=0.779, main effect of reactivity P=0.1478, interaction P=0.1294). We compared the length of IgH CDR3, positive charges in IgH CDR3, and grand average of hydropathy (sum of hydropathy values of all amino acids divided by the protein length) and found no significant differences. Interestingly, recombinant HC3-B, that uses the same V(D)J combinations of heavy and light chain as the highly polyreactive antibodies HC3-F and HC3-G, was not polyreactive. It had 2 or 3 mutations respectively more in its heavy, and 1 or 2 in its light chain compared to the other clones, but had an identical IgH CDR3 (Table 4).

Discussion

Extensive characterization of AChR-specific antibodies is hindered by the low frequency of the B cells that produce them and requires either the enrichment of B cells producing the relevant antibodies or the employment of expensive high-throughput technologies.

While we know that the majority of AChR+ MG patients have anti-AChR antibodies of IgG_1 and IgG_3 isotype, isotypes IgG_2 and IgG_4 can also be found and their contribution to the pathogenicity is still unclear (21). With our approach of using a membrane-antigen capture assay, we were able to isolate and sequence not just AChR-specific IgG, but also IgM B cells, thus enabling us to gain insight into the possible mechanisms of how autoreactive B cells arise and become pathogenic. While there is evidence that suggests that the titers of anti-AChR-ab are maintained by long-lived plasma cells because they are less likely to be affected by anti-CD20 treatment (22–24), it is still unclear if this pool of plasma cells is replenished by AChR-specific memory B cells or by newly emerging AChR-specific B cells. We were not able to isolate clonally related IgG and IgM B cells, but the presence of clonally diverse and somatically hypermutated IgM B cells that recognize AChR suggests that the pool of autoreactive B cells is dynamic. Interestingly, we also found clonally expanded, mutated IgM B cells in healthy volunteers suggesting that these B cells are antigen-experienced. This contrasts reports that a third checkpoint eliminates mature naïve autoreactive IgM before they become memory B cells (25). Whether an additional checkpoint prevents these AChR-specific IgM from class-switching and thus becoming pathogenic, or whether antibodies raised in healthy controls bind to epitopes that do not cause disease is subject of ongoing investigation.

It is not clear what the relationship between polyreactive B cells and the emergence of an autoimmune disorder is. It is generally believed that the majority of nascent B cells are self-reactive (26) but that most of the self-reactive B cells are eliminated by the central and peripheral checkpoint before B cells reach the mature naïve state. It has been suggested that both checkpoints harbor defects in MG patients leading to a higher proportion of poly- and self-reactive B cells in the peripheral blood (27).

Our results show that both polyreactive and monoreactive B cells exist among the AChR-specific B cells from patients with AChR-ab and from healthy controls. Polyreactivity also did not correlate with the amount of mutations in the variable regions, suggesting that it is not

merely a characteristic of newly emerged, unmutated IgM B cells. Furthermore, our data from 3 clonally related IgM support the notion that polyreactivity is not easily explained by the length, charge, and hydrophobicity of the heavy chain CDR3 region (28). Finally, we question whether binding to unrelated antigens in a cell-based ELISA proves the polyreactivity of an antibody. Our data show that many of the antibodies that bind to an BSA coated well also show positive reactivity to other antigens. However, since BSA was universally used as a blocking agent except for the condition using skim milk as antigen, we cannot say with certainty whether the positive reactivity is due to genuine binding to the antigen or binding to BSA. Comparing the binding to influenza-haemagglutinin in an indirect ELISA and in a cell-based, flow cytometric assay shows that even the antibodies with a high reactivity in ELISA don't bind to haemagglutinin when it is expressed on cells. A cell-based assay is much more likely to present the antigen in its native conformation and thus preserves discontinuous epitopes better than an ELISA that uses purified, recombinant proteins adhering to a resin. Furthermore, in most studies the polyreactivity of IgM B cells is tested by in vitro switching them to IgG (27–29) despite the fact that a change or loss of affinity can be induced by class-switching from IgM to IgG (30).

We observed that in contrast to IgM, AChR-specific IgG were not polyreactive. Future experiments will focus on investigating the relationship between somatic hypermutation, polyreactivity and affinity for AChR. This could yield valuable clues about the emergence of autoimmunity. If autoimmunity arises due to molecular mimicry, we expect the affinity for the pathogen to increase and the affinity for the autoantigen to decrease with an increasing amount of somatic hypermutation (31).

Mapping the precise location of the epitope of an antibody on its cognate antigen has important implications for basic research and medical applications such as vaccine design.
The concept of an immunodominant region on the acetylcholine receptor was first proposed by Tzartos and Lindstrom in 1980 (32). Using hybridomas created from Lewis rats that were immunized with acetylcholine receptor from eel or torpedo they hypothesized that most of the antibodies bound to a small region on the α-subunits which they named the main immunogenic region (MIR). Later, they used monoclonal antibodies to compete with the binding of serum antibodies from MG patients, and postulated that more than 50% of the patient antibodies were directed against the MIR (33), despite the fact that their data show similar rates of inhibition of serum antibody binding by antibodies directed against the gamma or beta subunits. The

location of the MIR was mapped to residues 67-76 (34) by using short peptides and a solid phase radioimmunoassay, and electron microscopy showed that these residues were located at the extracellular domain and thus highly accessible to antibodies (35).

A careful review of these early papers on the MIR shows several weaknesses that were also addressed by a paper in 1985 (36). Lennon and Griesmann found that while mAb35 is cross-reactive with Torpedo and human AChR, most sera from MG patients are not reactive with Torpedo AChR. Further investigation showed that the binding of mAb35 also inhibited the binding of a monoclonal whose epitope was located in a region of the α-subunit that is unrelated from the MIR. They thus hypothesized that the inhibition of the binding of serum antibodies by preincubation with a MIR-region specific antibody is more likely facilitated by steric inhibition than by competition for the same epitope. Using the previously described method of preincubation with mAb35, we were able to confirm that around 30 - 60% of AChR-specific monoclonal antibodies were blocked by mAb35. Our findings indicate that the binding of mAb35 to AChR can alter the structure of AChR or cluster AChR in the membrane in a way that can even enhance the binding of other antibodies (Figure 4B) suggesting allosteric affects may also play a role. We thus conclude that it is overly simplistic to determine than an antibody binds to the MIR simply because of its inhibition by mAb35.

With sequences of clonally related AChR-specific B cells that only differ in the number of somatic hypermutations that they have acquired, our data set provides unique insight into the development of these B cells. Future investigations about how these mutations affect the antibodies' affinity for AChR will be of clinical relevance by providing essential clues about the pathogenesis of AChR-antibody mediated myasthenia gravis.

Acknowledgements

We are grateful to patients, healthy controls, and staff of the University Hospital Basel. We thank Dr. Eva Kesenheimer for patient recruitment. We acknowledge the animal and flow cytometry core of facilities of the Department of Biomedicine, Basel.

References

1. Nastuk WL, Strauss AJL, Osserman KE. Search for a neuromuscular blocking agent in the blood of patients with myasthenia gravis. The American Journal of Medicine. 1959 Mar;26(3):394–409.

2. Gilhus NE, Skeie GO, Romi F, Lazaridis K, Zisimopoulou P, Tzartos S. Myasthenia gravis — autoantibody characteristics and their implications for therapy. Nat Rev Neurol. 2016 May;12(5):259–68.

3. Jacob S, Viegas S, Leite MI, Webster R, Cossins J, Kennett R, et al. Presence and Pathogenic Relevance of Antibodies to Clustered Acetylcholine Receptor in Ocular and Generalized Myasthenia Gravis. Arch Neurol [Internet]. 2012 Aug 1 [cited 2019 Oct 30];69(8). Available from: http://archneur.jamanetwork.com/article.aspx?doi=10.1001/archneurol.2012.437

4. Rodríguez Cruz PM, Al-Hajjar M, Huda S, Jacobson L, Woodhall M, Jayawant S, et al. Clinical Features and Diagnostic Usefulness of Antibodies to Clustered Acetylcholine Receptors in the Diagnosis of Seronegative Myasthenia Gravis. JAMA Neurol. 2015 Jun 1;72(6):642.

5. Lozier BK, Haven TR, Astill ME, Hill HR. Detection of Acetylcholine Receptor Modulating Antibodies by Flow Cytometry. American Journal of Clinical Pathology. 2015 Feb 1;143(2):186–92.

6. Graus YF, de Baets MH, Parren PW, Berrih-Aknin S. Human anti-nicotinic acetylcholine receptor recombinant Fab fragments isolated from thymus-derived phage display libraries from myasthenia gravis patients reflect predominant specificities in serum and block the action of pathogenic serum antibodies. JI. 1997;158:1919–29.

7. Rey E, Zeidel M, Rhine C, Tami J, Krolick K, Fischbach M, et al. Characterization of Human Anti-acetylcholine Receptor Monoclonal Autoantibodies from the Peripheral Blood of a Myasthenia Gravis Patient Using Combinatorial Libraries. Clinical Immunology. 2000 Sep;96(3):269–79.

8. Fostieri E, Tzartos S, Berrih-Aknin S, Beeson D, Mamalaki A. Isolation of potent human Fab fragments against a novel highly immunogenic region on human muscle acetylcholine receptor which protect the receptor from myasthenic autoantibodies. Eur J Immunol. 2005 Feb;35(2):632–43.

9. Vincent A, Thomas HC, Scadding GlenisK, Newsom-Davis J. IN-VITRO SYNTHESIS OF ANTI-ACETYLCHOLINE-RECEPTOR ANTIBODY BY THYMIC LYMPHOCYTES IN MYASTHENIA GRAVIS. The Lancet. 1978 Feb;311(8059):305–7.

10. Willcox HNA, Newsom-Davis J. Greatly increased autoantibody production in myasthenia gravis by thymocyte suspensions prepared with proteolytic enzymes. Clin exp Immunol. 1983;54:378–86.

11. Hill ME, Shiono H, Newsom-Davis J, Willcox N. The myasthenia gravis thymus: A rare source of human autoantibody-secreting plasma cells for testing potential therapeutics. Journal of Neuroimmunology. 2008 Sep;201–202:50–6.

12. Vrolix K, Fraussen J, Losen M, Stevens J, Lazaridis K, Molenaar PC, et al. Clonal heterogeneity of thymic B cells from early-onset myasthenia gravis patients with antibodies against the acetylcholine receptor. Journal of Autoimmunity. 2014 Aug;52:101–12.

13. Makino T, Nakamura R, Terakawa M, Muneoka S, Nagahira K, Nagane Y, et al. Analysis of peripheral B cells and autoantibodies against the anti-nicotinic acetylcholine receptor derived from patients with myasthenia gravis using single-cell manipulation tools. Saruhan-Direskeneli G, editor. PLoS ONE. 2017 Oct 17;12(10):e0185976.

14. Zimmermann M, Rose N, Lindner JM, Kim H, Gonçalves AR, Callegari I, et al. Antigen Extraction and B Cell Activation Enable Identification of Rare Membrane Antigen Specific Human B Cells. Front Immunol. 2019 Apr 16;10:829.

15. Leite MI, Jacob S, Viegas S, Cossins J, Clover L, Morgan BP, et al. IgG1 antibodies to acetylcholine receptors in 'seronegative' myasthenia gravis†. Brain. 2008 Jul;131(7):1940–52.

16. Huang J, Doria-Rose NA, Longo NS, Laub L, Lin C-L, Turk E, et al. Isolation of human monoclonal antibodies from peripheral blood B cells. Nat Protoc. 2013 Oct;8(10):1907–15.

17. Maddison P, Sadalage G, Ambrose PA, Jacob S, Vincent A. False-positive acetylcholine receptor antibody results in patients without myasthenia gravis. Journal of Neuroimmunology. 2019 Jul;332:69–72.

18. Rodriguez Cruz PM, Huda S, López-Ruiz P, Vincent A. Use of cell-based assays in myasthenia gravis and other antibody-mediated diseases. Experimental Neurology. 2015 Aug;270:66–71.

19. Niles MJ, Matsuuchi L, Koshland ME. Polymer IgM assembly and secretion in lymphoid and nonlymphoid cell lines: evidence that J chain is required for pentamer IgM synthesis. Proceedings of the National Academy of Sciences. 1995 Mar 28;92(7):2884–8.

20. Johansen, Braathen, Brandtzaeg. Role of J Chain in Secretory Immunoglobulin Formation. Scand J Immunol. 2000 Sep;52(3):240–8.

21. Rødgaard A, Nielsen FC, Djurup R, Somnier R, Gammeltoft S. Acetylcholine receptor antibody in myasthenia gravis: predominance of IgG subclasses 1 and 3. Clin exp Immunol. 1987;67(1):82–8.

22. Iorio R, Damato V, Alboini PE, Evoli A. Efficacy and safety of rituximab for myasthenia gravis: a systematic review and meta-analysis. J Neurol. 2015 May;262(5):1115–9.

23. Topakian R, Zimprich F, Iglseder S, Embacher N, Guger M, Stieglbauer K, et al. High efficacy of rituximab for myasthenia gravis: a comprehensive nationwide study in Austria. J Neurol. 2019 Mar;266(3):699–706.

24. BeatMG: Phase II Trial of Rituximab In Myasthenia Gravis - Study Results - ClinicalTrials.gov [Internet]. [cited 2019 Oct 25]. Available from: https://clinicaltrials.gov/ct2/show/results/NCT02110706

25. Tsuiji M, Yurasov S, Velinzon K, Thomas S, Nussenzweig MC, Wardemann H. A checkpoint for autoreactivity in human IgM+ memory B cell development. J Exp Med. 2006 Feb 20;203(2):393–400.

26. Mouquet H, Nussenzweig MC. Polyreactive antibodies in adaptive immune responses to viruses. Cell Mol Life Sci. 2012 May;69(9):1435–45.

27. Lee J-Y, Stathopoulos P, Gupta S, Bannock JM, Barohn RJ, Cotzomi E, et al. Compromised fidelity of B-cell tolerance checkpoints in AChR and MuSK myasthenia gravis. Ann Clin Transl Neurol. 2016 Jun;3(6):443–54.

28. Mouquet H, Scheid JF, Zoller MJ, Krogsgaard M, Ott RG, Shukair S, et al. Polyreactivity increases the apparent affinity of anti-HIV antibodies by heteroligation. Nature. 2010 Sep;467(7315):591–5.

29. Robbiani DF, Bozzacco L, Keeffe JR, Khouri R, Olsen PC, Gazumyan A, et al. Recurrent Potent Human Neutralizing Antibodies to Zika Virus in Brazil and Mexico. Cell. 2017 May;169(4):597-609.e11.

30. Lindner JM, Cornacchione V, Sathe A, Be C, Srinivas H, Riquet E, et al. Human Memory B Cells Harbor Diverse Cross-Neutralizing Antibodies against BK and JC Polyomaviruses. Immunity. 2019 Mar;50(3):668-676.e5.

31. Burnett DL, Langley DB, Schofield P, Hermes JR, Chan TD, Jackson J, et al. Germinal center antibody mutation trajectories are determined by rapid self/foreign discrimination. Science. 2018 Apr 13;360(6385):223–6.

32. Tzartos SJ, Lindstrom JM. Monoclonal antibodies used to probe acetylcholine receptor structure: localization of the main immunogenic region and detection of similarities between subunits. Proceedings of the National Academy of Sciences. 1980 Feb 1;77(2):755–9.

33. Tzartos SJ, Seybold ME, Lindstrom JM. Specificities of antibodies to acetylcholine receptors in sera from myasthenia gravis patients measured by monoclonal antibodies. Proceedings of the National Academy of Sciences. 1982 Jan 1;79(1):188–92.

34. Tzartos SJ, Kokla A, WALGRAVEt SL, CONTI-TRONCONIt BM. Localization of the main immunogenic region of human muscle acetylcholine receptor to residues 67-76 of the a subunit. :5.

35. Beroukhim R, Unwin N. Three-dimensional location of the main immunogenic region of the acetylcholine receptor. Neuron. 1995 Aug;15(2):323–31.

36. Lennon VA, Griesmann GE. Evidence against acetylcholine receptor having a main immunogenic region as target for autoantibodies in myasthenia gravis. Neurology. 1989 Aug 1;39(8):1069–1069.

Figure legends

Figure 1: Serum IgG binding to AChR by myasthenia gravis patients in a cell-based assay (CBA).

A. Representative flow cytometry plots showing binding of serum IgG to the surface of live cells transfected with AChR-GFP. The x-axis depicts the fluorescence intensity of GFP and the y-axis the fluorescence intensity of the secondary anti-human IgG PE antibody. AChR-GFP expressing cells are in Q2 and Q3, transfected cells bound by IgG in Q2. The top row shows serum samples from patients with MG and the bottom row serum samples from healthy controls. **B.** Summary of CBA data from 5 AChR-RIA positive patients and 5 healthy controls. Serum was serially diluted and incubated with TE AChR-GFP before incubation with anti-human IgA, IgG, and IgM secondary antibodies. GMFI ratio = Geometric Mean Fluorescence Intensity (GMFI) of secondary antibody binding to AChR-GFP transfected cells (Q2 + Q3) / GMFI of secondary antibody binding to non-transfected cells (Q1 + Q4). Dots represent means of 3 independent experiments.

Figure 2: A membrane-antigen capture technique for purifying AChR-specific B cells.

A. TE671 transfected with AChR-GFP are labeled with AF647-α-bungarotoxin (α-BTX) and cell trace blue (CTB). B cells are isolated from peripheral blood mononuclear cells via negative magnetic selection and co-cultured with antigen-donor cells. B cells specific for AChR bind to the receptor on the surface of transfected cells and extract AChR and the associated fluorophores from the plasma membrane. AChR is internalized, surface immunoglobulin is downregulated and the activation marker CD69 is upregulated. After 3 hours of co-culture, B cells are retrieved and stained for CD69 expression. **B.** Representative FACS plots showing the gating strategy for membrane-antigen capturing B cells from a HC (top) and a patient with MG (bottom). After gating on lymphocytes and doublet exclusion, $CD69^{+}$ CTB^{-} cells that have taken up both antigen-associated fluorophores are sorted.

Figure 3: Characteristics of recombinant antibodies produced from isolated anti-AChR IgG B cells.

After enrichment of antigen specific B-cells by antigen capture B cells were single cell expanded in vitro and sequenced. Variable Ig regions were cloned into plasmids containing the constant regions of the originally expressed isotype. Cell culture supernatants of HEK cells transfected with heavy and light chains were assessed for AChR binding and polyreactivity. **A.** 6 IgG B cells could be cloned from 3 myasthenia gravis patients. 3 IgG_1, 1 IgG_3, and 2 IgG_4 B cells were recombinantly expressed in their native isotypes. Four IgG clones (2 IgG_1 and 2 clonally related IgG_4) were cloned from patient MG2, one IgG_3 from patient MG3, and one IgG_1 from patient MG4. **B.** Representative flow cytometry plots showing the isotyping of anti-AChR serum IgG. Patient MG2 showed binding of IgG of all 4 isotypes to AChR and the highest binding of IgG_4, while patients MG3 and MG4 only showed anti-AChR IgG_1. **C.** Recombinant IgG bound strongly to AChR, whereas a similarly expressed anti-influenza haemagglutinin control antibody 8B4 did not bind. Binding was quantified as described in Fig. 1. Binding of rec. IgG to AChR was not reduced by pre-incubation with bungarotoxin (AF647-α-BTX). Preincubation of the main immunogenic region-specific rat monoclonal antibody mAb35 strongly reduced the binding of 2 out of the six recombinant IgG. **D.** None of the recombinant anti-AChR IgG bound to ubiquitous, non-related antigens as assessed by ELISA. **E.** All of the isolated anti-AChR IgG B cells showed signs of somatic hypermutation in their heavy and light chains.

Figure 4: Characteristics of recombinant antibodies produced from isolated anti-AChR IgM B cells.

28 anti-AChR IgM B cells were isolated from the 5 patients with MG, and 11 from HC. The 11 IgM from HC included 2 B cells with identical heavy and light chain, for which we recombinantly expressed 1 mAb. HEK cells were transfected with plasmids containing constructs of the heavy, light, and J chain. Cell culture supernatants of transfected HEK cells were harvested and used to determine AChR binding characteristics and polyreactivity. **A.** Representative flow cytometry plots showing binding of recombinant human IgM derived from patients with MG (top) and HC (bottom). **B.** GMFI ratio of AChR binding, fold change of AChR binding after pre-incubation with either α-BTX or mAb35 of recombinant IgM derived from patients with MG. **C.** Characteristics of HC-derived recombinant IgM analogous to B.

Figure 5: Assessment of polyreactivity of recombinant anti-AChR IgM

A. ELISAs measuring the reactivity of recombinant AChR-specific IgM from MG (top) and HC (bottom) against double-stranded DNA, single-stranded DNA, insulin, lipopolysaccharide (LPS), bovine serum albumin (BSA), milk, and influenza haemagglutinin (HA). Horizontal lines show cut-off for positivity. Donut charts summarize the frequency of polyreactive (black) and non-polyreactive (grey) recombinant IgM, the center denotes the total number of IgM for a given study participant. **B.** Comparison of the proportion of polyreactive IgM from MG and HC. **C.** Correlation of reactivity in anti-insulin ELISA and binding to AChR in a live cell-based assay of IgM derived from HC (blue circles) or MG patients. **D.** Correlation of reactivity in anti-insulin ELISA with the number of amino acid changes in variable regions of heavy and light chain of recombinant anti-AChR IgM derived from HC or MG. **E.** Correlation of reactivity in anti-haemagglutinin ELISA with the binding to haemagglutinin in a live cell-based assay of anti-AChR IgM derived from HC or MG. Green arrow depicts the recombinant anti-haemagglutinin IgM mAb 3G16 that serves as positive control. **F.** Plots showing the number of mutations in the heavy chain variable region and the length, positive charges and hydropathy of the heavy chain CDR3.

Table 1: Study participant clinical, laboratory, and demographic data

Myasthenic symptoms quantified by Besinger score, immunotherapy, and serum AChR-autoantibody levels were assessed at the time of sample collection or within 6 months of sample collection. All serum AChR-antibody levels were assessed by radio-immuno-precipitation assay in the same study center.

Table 2: V(D)J gene usage, number of mutations, and amino acid sequence of the CDR3 of anti-AChR IgG B cells.

† denote B cells that are clonally related.

Table 3: Molecular characteristics of polyreactive anti-AChR IgM from patients with MG.

V(D)J gene usage, number of mutations, amino acid sequence of the CDR3, CDR3 positive charges and hydropathy of polyreactive anti-AChR IgM B cells derived from patients with MG.

Table 4: Molecular characteristics of polyreactive anti-AChR IgM from HC.

V(D)J gene usage, number of mutations, amino acid sequence of the CDR3, CDR3 positive charges and hydropathy of polyreactive anti-AChR IgM B cells derived HC.

‡ denotes B cells that are clonally related. A clonally related, not polyreactive IgM is depicted in blue.

Supplementary Figure 1: V and J gene allele usage.

Heat maps showing the usage of alleles of variable vs joining gene segments in anti-AChR B cells from patient with MG (left) and HC (right) in heavy chains (**A**) and light chains (**B**).

Supplementary Figure 2: Correlation of polyreactivity ELISA vs AChR-binding or number of mutations in variable regions of heavy and light chain.

A. There was no correlation between the reactivity to any antigen in the polyreactivity ELISA and the binding to AChR for recombinant antibodies derived from patients MG or from HC.

B. There was no correlation between the number of amino acids changes in variable regions of heavy and light chain and the reactivity to any unrelated antigen in ELISA.

Supplementary Figure 3: Exemplary staining of fixed rat muscle tissue with mAb35 and a recombinant human anti-AChR IgM.

A. 4%-PFA-PBS fixed gastrocnemius muscles of Lewis rats were sectioned and stained with AF647-α-BTX and rat mAb35. Binding of mAb35 was detected by a FITC anti-rat IgG secondary antibody. The merged image shows overlap of AF647-α-BTX and AF488-anti-rat IgG. **B.** A rat muscle section was incubated with HEK cell culture supernatant containing mAb MG5-C, and with AF647-α-BTX. Binding of human IgM was detected by an AF488-anti-human IgM secondary antibody. The merged image shows that staining of AF488-anti-human IgM and AF647-α-BTX are co-localized.

Supplementary Table 1: Isotype, V(D)J gene usage, and number of mutations of all anti-AChR B cells isolated from patients with MG.

† and ‡ denote B cells that are clonally related.

Supplementary Table 2: Isotype, V(D)J gene usage, and number of mutations of all anti-AChR B cells isolated from HC.

† and ‡ denote B cells that are clonally related.

Figure 1

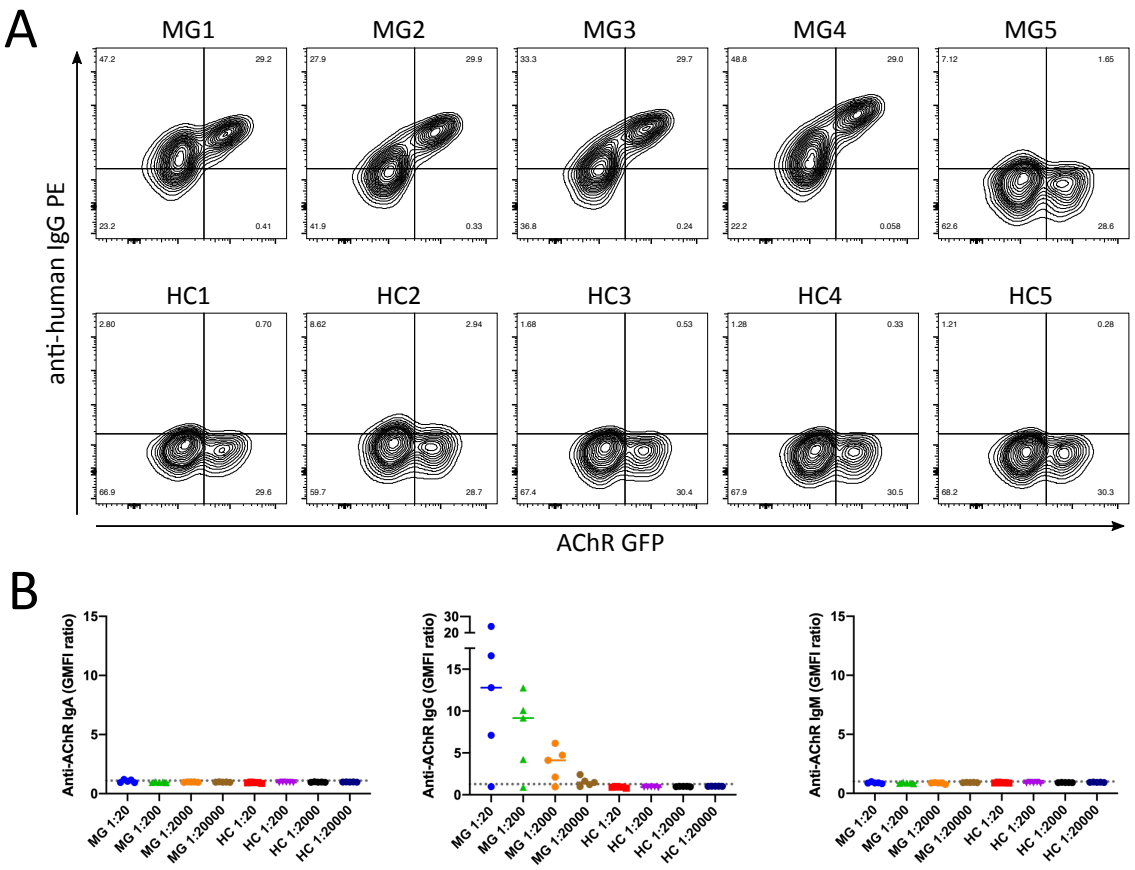
A
MG1
MG2
MG3
MG4
MG5
HC1
HC2
HC3
HC4
HC5
anti-human IgG PE
AChR GFP
B
Anti-AChR IgA (GMFI ratio)
Anti-AChR IgG (GMFI ratio)
Anti-AChR IgM (GMFI ratio)
MG 1:20
MG 1:200
MG 1:2000
MG 1:20000
HC 1:20
HC 1:200
HC 1:2000
HC 1:20000

Figure 2

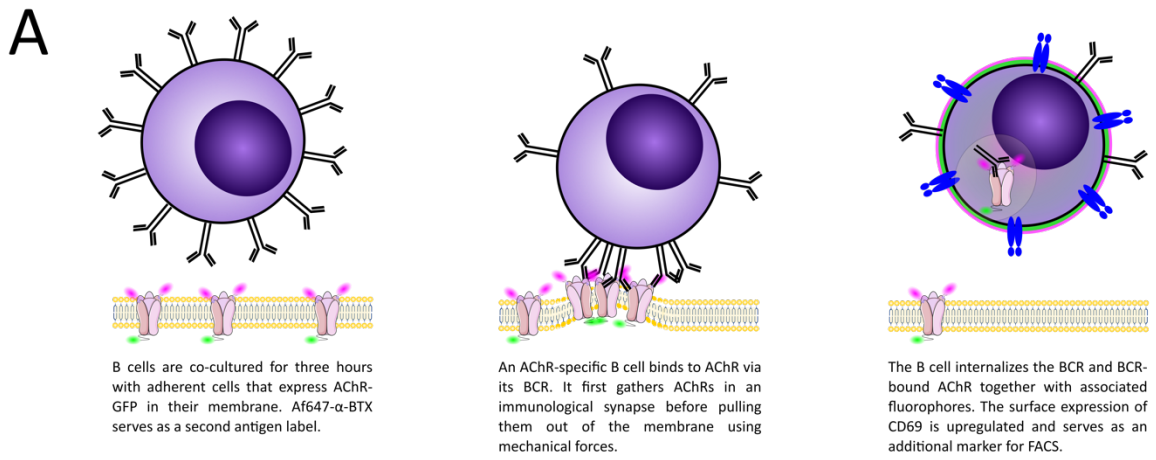
A
B cells are co-cultured for three hours with adherent cells that express AChR-GFP in their membrane. Af647-α-BTX serves as a second antigen label.
An AChR-specific B cell binds to AChR via its BCR. It first gathers AChRs in an immunological synapse before pulling them out of the membrane using mechanical forces.
The B cell internalizes the BCR and BCR-bound AChR together with associated fluorophores. The surface expression of CD69 is upregulated and serves as an additional marker for FACS.

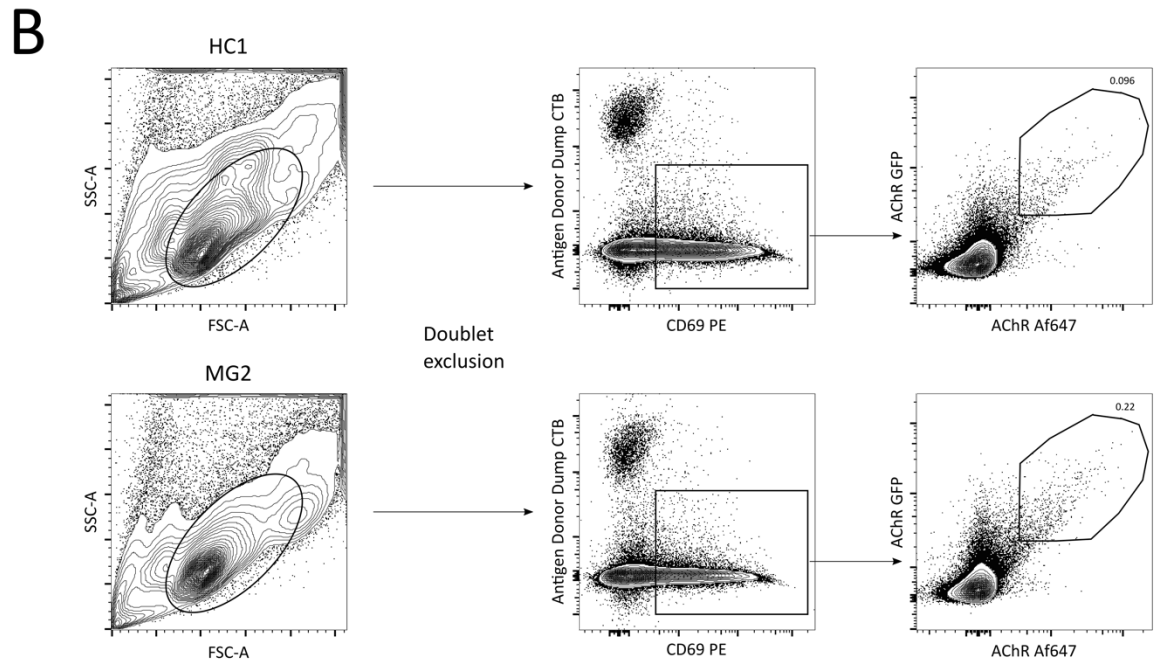
B
HC1
SSC-A
FSC-A
Doublet exclusion
Antigen Donor Dump CTB
CD69 PE
AChR GFP
AChR Af647
0.096
MG2
SSC-A
FSC-A
Antigen Donor Dump CTB
CD69 PE
AChR GFP
AChR Af647
0.22

Figure 3

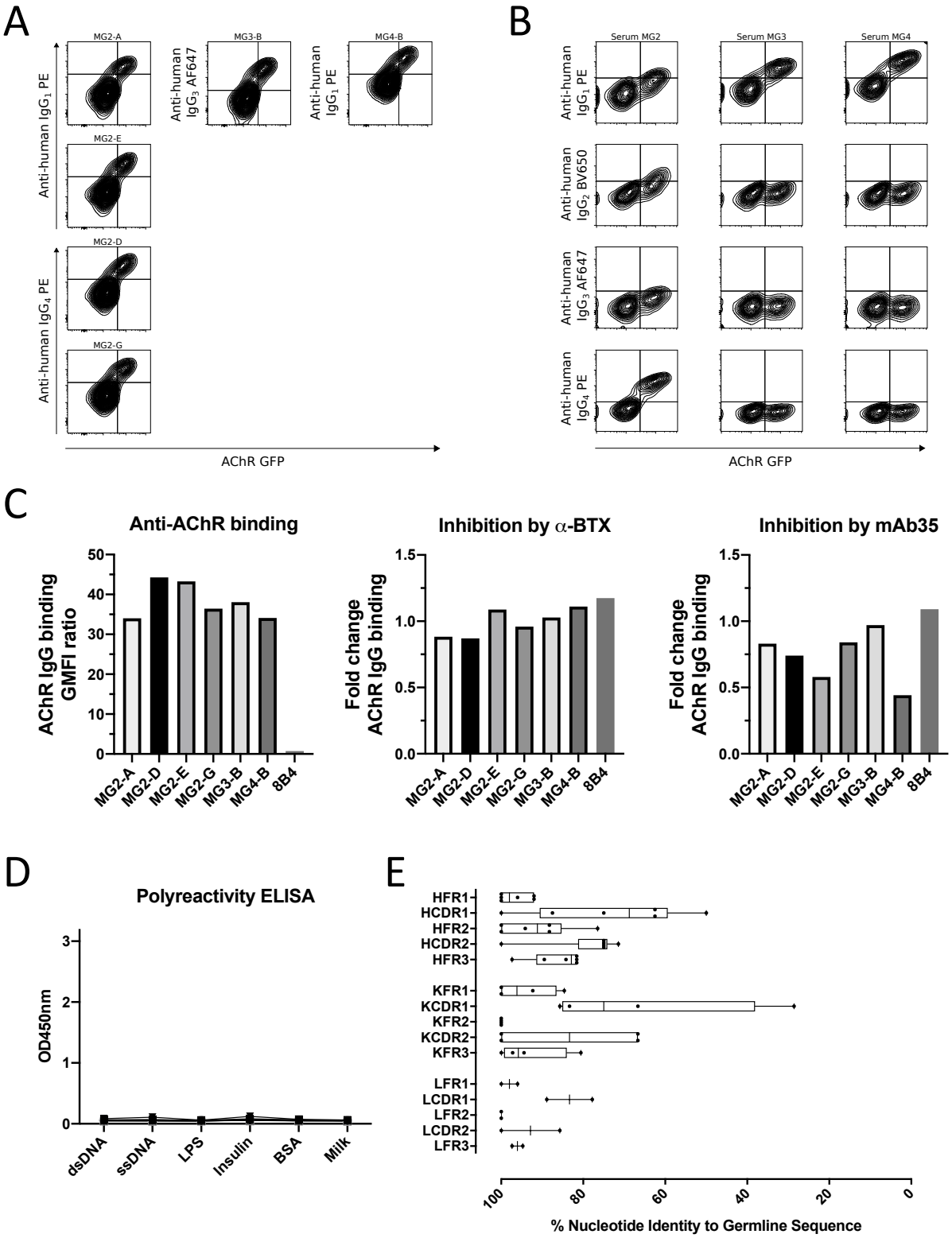
A
MG2-A
MG3-B
MG4-B
MG2-E
MG2-D
MG2-G
Anti-human IgG1 PE
Anti-human IgG3 AF647
Anti-human IgG1 PE
Anti-human IgG4 PE
AChR GFP
B
Serum MG2
Serum MG3
Serum MG4
Anti-human IgG1 PE
Anti-human IgG2 BV650
Anti-human IgG3 AF647
Anti-human IgG4 PE
AChR GFP
C
Anti-AChR binding
AChR IgG binding GMFI ratio
Inhibition by α-BTX
Fold change AChR IgG binding
Inhibition by mAb35
Fold change AChR IgG binding
MG2-A
MG2-D
MG2-E
MG2-G
MG3-B
MG4-B
8B4
D
Polyreactivity ELISA
OD450nm
dsDNA
ssDNA
LPS
Insulin
BSA
Milk
E
HFR1
HCDR1
HFR2
HCDR2
HFR3
KFR1
KCDR1
KFR2
KCDR2
KFR3
LFR1
LCDR1
LFR2
LCDR2
LFR3
% Nucleotide Identity to Germline Sequence

Figure 4

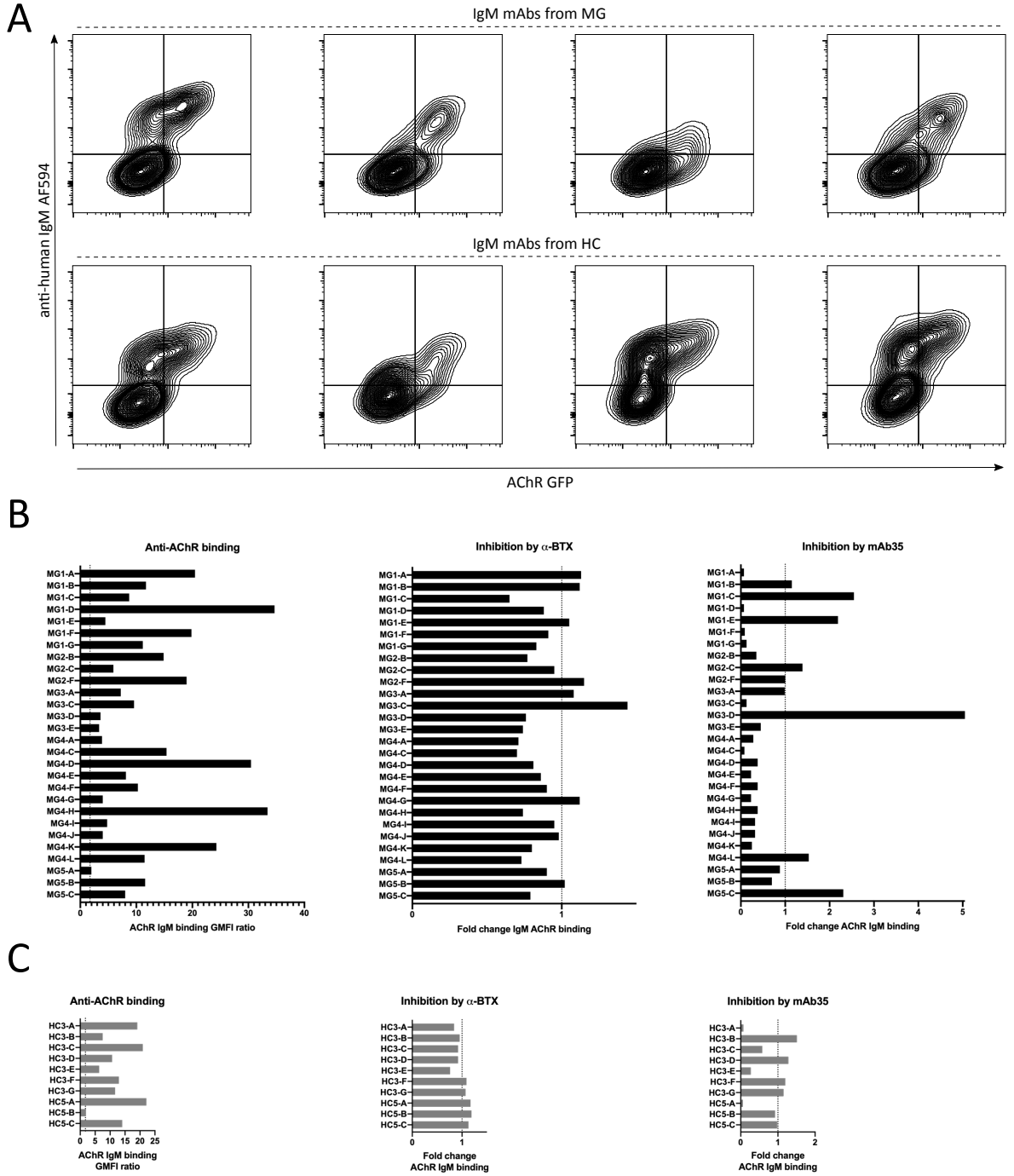
A
IgM mAbs from MG
IgM mAbs from HC
anti-human IgM AF594
AChR GFP
B
Anti-AChR binding
AChR IgM binding GMFI ratio
Inhibition by α-BTX
Fold change IgM AChR binding
Inhibition by mAb35
Fold change AChR IgM binding
C
Anti-AChR binding
AChR IgM binding GMFI ratio
Inhibition by α-BTX
Fold change AChR IgM binding
Inhibition by mAb35
Fold change AChR IgM binding

Figure 5

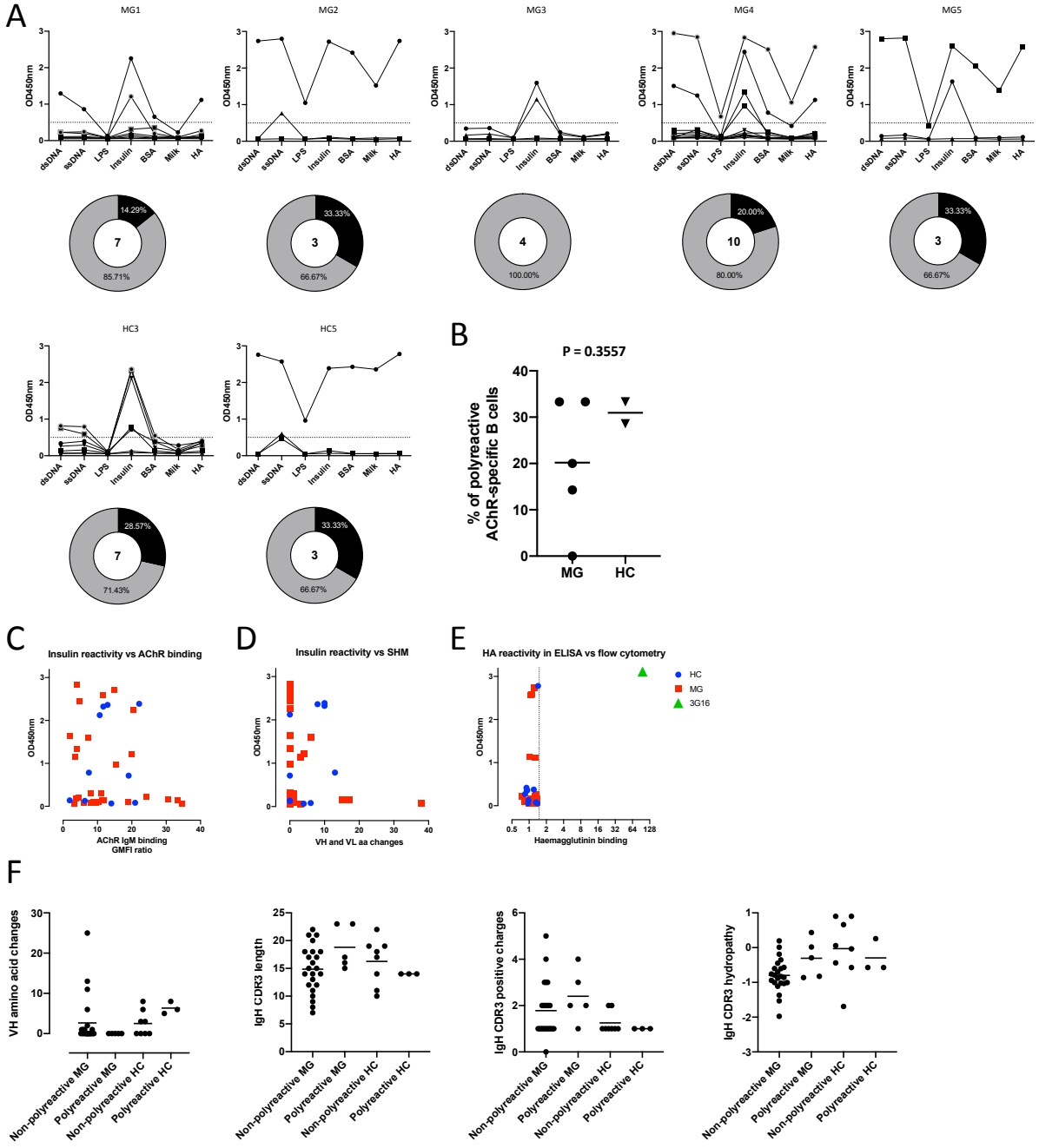
A
MG1
MG2
MG3
MG4
MG5
OD450nm
dsDNA
ssDNA
LPS
Insulin
BSA
Milk
HA
14.29%
7
85.71%
33.33%
3
66.67%
4
100.00%
20.00%
10
80.00%
33.33%
3
66.67%
HC3
HC5
28.57%
7
71.43%
33.33%
3
66.67%
B
P = 0.3557
% of polyreactive AChR-specific B cells
MG
HC
C
Insulin reactivity vs AChR binding
AChR IgM binding GMFI ratio
D
Insulin reactivity vs SHM
VH and VL aa changes
E
HA reactivity in ELISA vs flow cytometry
HC
MG
3G16
Haemagglutinin binding
F
VH amino acid changes
IgH CDR3 length
IgH CDR3 positive charges
IgH CDR3 hydropathy
Non-polyreactive MG
Polyreactive MG
Non-polyreactive HC
Polyreactive HC

Table 1

Participant	Sex	Age	Diagnosis	Thymus status	Disease onset	Besinger Score	Immuno-therapy	Serum AChR antibody titer (nmol/l)
MG1	M	45	Generalized AChR MG	Thymectomy (2000)	1998	3	None	850.9
MG2	M	63	Ocular AChR MG	No thymoma	02/2018	6	None	16.5
MG3	M	35	Generalized AChR MG	Thymoma	06/2018	8	None	27.4
MG4	F	39	Generalized AChR MG	Slight thymic hyperplasia	2014	6	None	366
MG5	F	60	Poly auto-immunity	n/a	n/a	n/a	None	193.7
HC1	F	38	Healthy control	-	-	-	-	-
HC2	F	36	Healthy control	-	-	-	-	-
HC3	M	44	Healthy control	-	-	-	-	-
HC4	M	65	Healthy control	-	-	-	-	-
HC5	F	63	Healthy control	-	-	-	-	-

Table 2

mAb	Isotype	V	D	J	aa replacements in V region	CDR3
MG2-A	IgG1	3-23*01	2-2*01	6*03	11	ATRRIFMDV
	κ	3-20*01		1*01	1	QQYGSSPRT
MG2-D†	IgG4	1-2*02	1-1*01	6*02	9	ARDRWVHLGSYYFGLDV
	λ3	5-45*02		3*02	3	**V**IWHSSAWV
MG2-E	IgG1	4-4*07	3-16*01	6*03	7	ARNVGASYYYEYYYMDV
	κ	1-12*01		1*01	7	QQANSFPWT
MG2-G†	IgG4	1-2*02	1-1*01	6*02	12	ARDRWVHVGSYYFGLDV
	λ3	5-45*02		3*02	7	**V**IWHSSAWV
MG3-B	IgG3	3-15*01	3-10*01	6*02	11	TAYPRGLRGVVIMGGEEFHYYGMDV
	κ	1-9*01		5*01	2	QQLNS
MG4-B	IgG1	3-33*03	6-13*01	6*02	19	**G**REMSAAYSSNWARGEFSYGIDV
	κ	3-20*01		1*01	16	QQYEPTPMWT

Table 3

mAb	Isotype	V	D	J	aa replacements in V region	CDR3	CDR3 positive charges	Hydropathy
MG1-A	IgM	3-74*01	3-10*01	3*02	0	ARAYGSGRFFVLEAFDI	2	0.44
	λ2	3-1*01		2*01	0	QAWDSSTVV	0	0.00
MG2-B	IgM	3-23*01	2-2*02	6*02	0	AKDRCSSTSCYNVRDYYYYGMDV	3	-0.86
	κ	3-20*01		1*01	0	QQYGSSLRRT	2	-1.62
MG4-H	IgM	4-30-2*01	6-6*01	3*02	0	ARHSSIAARPRAFDI	4	-0.29
	κ	1-39*01		4*01	0	QQSYSTVLT	0	-0.37
MG4-I	IgM	3-21*01	3-22*01	5*02	0	ARVALWYYYDSSGYYPRGNWFDP	2	-0.83
	λ2	1-40*01		2*01	0	QSYDSSLSGSV	0	-0.43
MG5-B	IgM	3-30*02	5-18*01	4*02	0	AKGLSGYSYGYISPIY	1	0.02
	κ	4-1*01		1*01	0	QQYYSTLWT	0	-0.99

Table 4

mAb	Isotype	V	D	J	aa replacements in V region	CDR3	CDR3 positive charges	Hydropathy
HC3-F‡	IgM	3-23*01	3-10*01	4*02	5	AKVSNYYASGNIDY	1	-0.57
	κ	1-6*01		1*01	3	LQHYNYPWT	1	-1.36
HC3-G‡	IgM	3-23*01	3-10*01	4*02	6	AKVSNYYASGNIDY	1	-0.57
	κ	1-6*01		1*01	4	LQHYNYPWT	1	-1.36
HC3-B‡	IgM	3-23*01	3-10*01	4*02	8	AKVSNYYASGNIDY	1	-0.57
	κ	1-6*01		1*01	5	LQHYNYPWT	1	-1.36
HC5-A	IgM	3-9*01	4-17*01	3*01	8	TKLTVTTSGGAFDF	1	0.26
	λ1	3-21*01		1*01	2	QVWDSSSDPYV	0	-0.75

Supplementary Figure 1

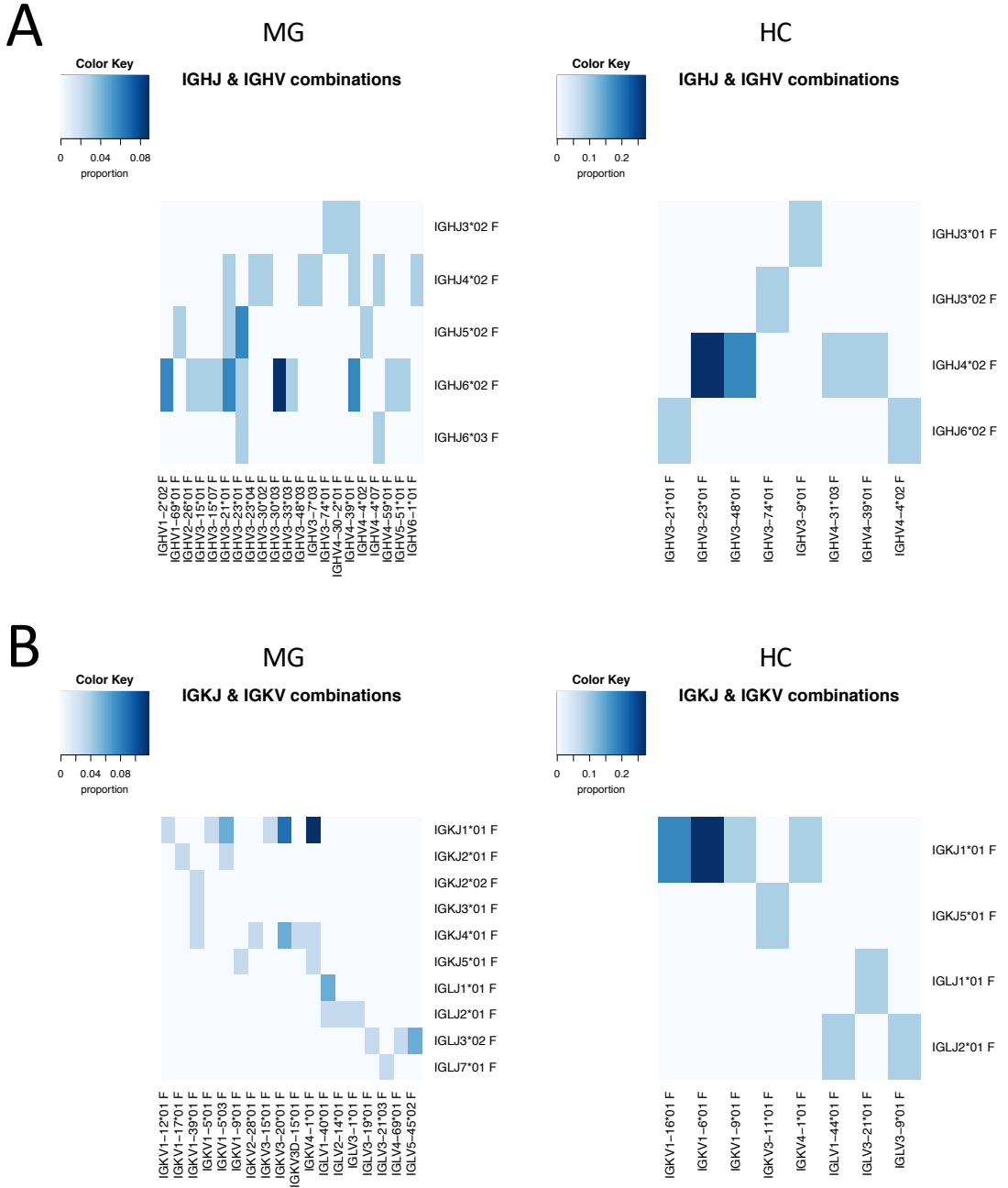

Supplementary Figure 2

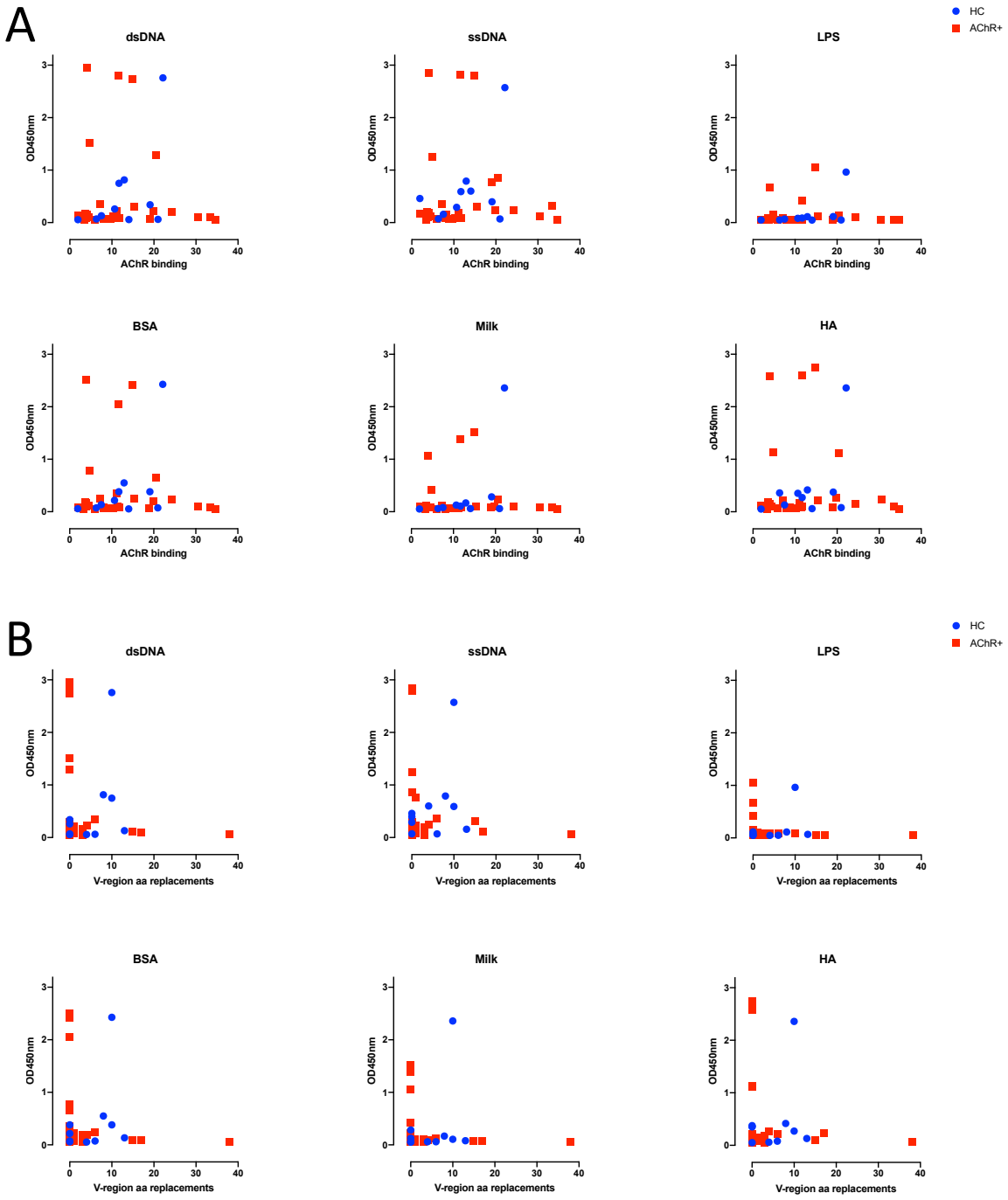

Supplementary Figure 3

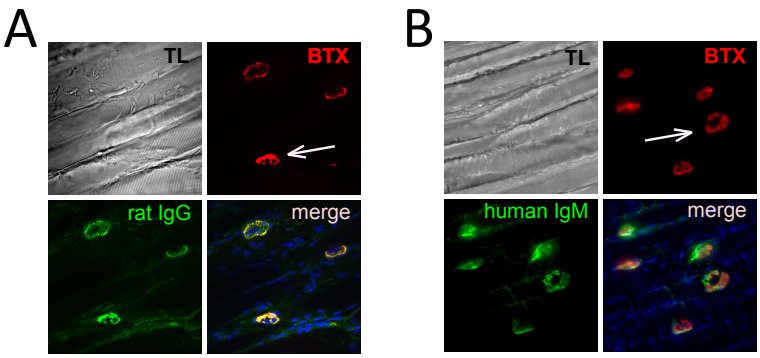

Supplementary Table 1

mAb	Isotype H	VH	DH	JH	aa replacements	Isotype L	VL	VJ	aa replacements
MG1-A	IgM	3-74*01	3-10*01	3*02	0	λ2	3-1*01	2*01	0
MG1-B	IgM	4-39*01	3-10*01	6*02	0	κ	4-1*01	1*01	0
MG1-C	IgM	4-4*02	3-22*01	5*02	0	λ2	2-14*01	2*01	1
MG1-D	IgM	3-48*03	3-10*01	4*02	0	κ	1-39*01	3*01	0
MG1-E	IgM	4-39*01	3-10*01	6*02	0	κ	4-1*01	5*01	0
MG1-F	IgM	4-39*01	3-3*01	3*02	1	λ2	3-19*01	3*02	3
MG1-G	IgM	3-21*01	1-26*01	6*02	0	κ	1-17*01	2*01	0
MG2-A	IgG1	3-23*01	2-2*01	6*03	11	κ	3-20*01	1*01	1
MG2-B	IgM	3-23*01	2-2*02	6*02	0	κ	3-20*01	1*01	0
MG2-C	IgM	3-7*03	4-23*01	4*02	25	κ	1-5*01	1*01	13
MG2-D†	IgG4	1-2*02	1-1*01	6*02	9	λ3	5-45*02	3*02	3
MG2-E	IgG1	4-4*07	3-16*01	6*03	7	κ	1-12*01	1*01	7
MG2-F	IgM	4-39*01	3-22*01	4*02	1	κ	4-1*01	1*01	0
MG2-G†	IgG4	1-2*02	1-1*01	6*02	12	λ3	5-45*02	3*02	7
MG3-A	IgM	4-4*07	6-13*01	4*02	6	κ	4-1*01	4*01	0
MG3-B	IgG3	3-15*01	3-10*01	6*02	11	κ	1-9*01	5*01	2
MG3-C	IgM	3-23*01	3-10*01	5*02	0	κ	1-39*01	2*02	0
MG3-D	IgM	6-1*01	6-6*01	4*02	1	κ	1-5*03	1*01	2
MG3-E	IgM	3-21*01	6-13*01	4*02	2	λ2	4-69*01	3*02	1
MG4-A	IgM	1-69*01	3-16*01	5*02	0	κ	4-1*01	1*01	0
MG4-B	IgG1	3-33*03	6-13*01	6*02	19	κ	3-20*01	1*01	16
MG4-C	IgM	2-26*01	3-22*01	6*02	0	κ	3-20*01	4*01	0
MG4-D‡	IgM	3-30*03	3-10*01	6*02	13	λ1	1-40*01	1*01	4
MG4-E	IgM	3-23*04	3-10*01	4*02	0	κ	1-5*03	2*01	1
MG4-F	IgM	3-15*07	3-16*02	6*02	0	κ	3-20*01	4*01	0
MG4-G‡	IgM	3-30*03	3-10*01	6*02	11	λ1	1-40*01	1*01	4
MG4-H	IgM	4-30-2*01	6-6*01	3*02	0	κ	1-39*01	4*01	0
MG4-I	IgM	3-21*01	3-22*01	5*02	0	λ2	1-40*01	2*01	0
MG4-J	IgM	4-59*01	6-19*01	6*02	0	κ	1-5*03	1*01	0
MG4-K	IgM	3-30*03	1-14*01	6*02	1	λ7	3-21*03	7*01	0
MG4-L	IgM	5-51*01	6-13*01	6*02	0	κ	3D-15*01	4*01	0
MG5-A	IgM	3-23*01	4-17*01	5*02	0	κ	3-15*01	1*01	0
MG5-B	IgM	3-30*02	5-18*01	4*02	0	κ	4-1*01	1*01	0
MG5-C	IgM	3-21*01	6-13*01	6*02	0	κ	2-28*01	4*01	0

Supplementary Table 2

mAb	Isotype H	VH	DH	JH	aa replacements	Isotype L	VL	VJ	aa replacements
HC3-A	IgM	4-31*03	2-21*02	4*02	0	λ2	3-9*01	2*01	0
HC3-B‡	IgM	3-23*01	3-10*01	4*02	8	κ	1-6*01	1*01	5
HC3-C	IgM	3-74*01	1-7*01	3*02	6	λ2	1-44*01	2*01	0
HC3-D	IgM	4-39*01	3-10*01	4*02	0	κ	4-1*01	1*01	0
HC3-E	IgM	3-21*01	2-15*01	6*02	0	κ	1-9*01	1*01	0
HC3-F‡	IgM	3-23*01	3-10*01	4*02	5	κ	1-6*01	1*01	3
HC3-G‡	IgM	3-23*01	3-10*01	4*02	6	κ	1-6*01	1*01	4
HC5-A	IgM	3-9*01	4-17*01	3*01	8	λ1	3-21*01	1*01	2
HC5-B	IgM	4-4*02	2-2*01	6*02	0	κ	3-11*01	5*01	0
HC5-C†	IgM	3-48*01	3-3*01	4*02	3	κ	1-16*01	1*01	1
HC5-D†	IgM	3-48*01	3-3*01	4*02	3	κ	1-16*01	1*01	1

Discussion

Extended from Results II

After establishing the membrane-antigen capture assay using HA as a model antigen, we focused on adapting the method to characterize autoreactive B cells in myasthenia gravis. Originally, we planned to label the autoreactive B cells with a large panel of antibodies directed against surface markers and perform index sorting. Subsequent analysis of the surface marker expression of AChR-specific B cells could have provided information about the phenotype of these B cells. Pilot experiments with HA-specific B cells showed that the addition of a large panel of antibodies to FACS staining solution significantly reduced the percentage of primary B cell cultures that secrete immunoglobulins (unpublished data). Furthermore, the abort rate of index sorting is comparatively large which reduces the yield of B cells that enter the culture phase. Another approach to gain insight into the phenotype is the single-cell RNA sequencing of AChR-specific B cells. Due to the low specificity of the assay when applied to AChR-specific B cells (69), this approach was deemed to be not economical and we proceeded with the B cell expansion and sequencing protocol as described.

Polyreactivity of monoclonal antibodies

Studies of B cells from patients with systemic lupus erythematosus (SLE), rheumatoid arthritis, or MG suggest that defects in central and peripheral tolerance checkpoints lead to the accumulation of autoreactive B cells in the periphery (70–72). The relationship between polyreactive and autoreactive antibodies has not yet been elucidated. Self-reactive IgG antibodies in SLE patients can arise from nonreactive or polyreactive precursors. The reversion of autoantibodies back to their germline sequence greatly reduces the affinity for self- and foreign-antigens (6) indicating that the autoreactive properties were acquired during a germinal center reaction.

ELISAs have been used to measure poly- and autoreactivity of antibodies, in particular of IgM antibodies, since the late 1980s (73–75). While the selection of antigens differs slightly between publications, the general principle remains the same. An antibody is considered polyreactive when it binds to two or more unrelated self or foreign antigens. Most commonly, dsDNA and ssDNA, insulin, and lipopolysaccharide are used to assess polyreactivity. Early experiments were mainly performed with unpurified supernatants of EBV-immortalized B

cells. Technological advances have facilitated the production and purification of recombinant human antibodies but IgM antibodies pose several problems. Human IgM binds to protein A only weakly and does not at all bind to protein G (76) and the harsh elution conditions can destroy the pentameric structure of secreted IgM. This means that many researchers have shifted to expressing variable region sequences gained from IgM B cells in an IgG backbone instead (3,72,77). Our collaborators have shown that this switching of the constant region from IgM to IgG actually can affect the affinity of a recombinant antibody drastically (10) and we thus chose to produce the antibodies sequenced from IgM B cells as recombinant IgM.

Our data suggest that most of the polyreactive antibodies also bind to bovine serum albumin (BSA). As BSA was used as a blocking agent in the preparation of the ELISA plate for all other antigens except for milk and is commonly used by other groups for blocking (78), we cannot conclude that the positive reactivity to wells coated with other antigens is not mediated by the residual presence of BSA. Whether the positive reactivity to a variety of self and foreign antigens in ELISA that is reported by so many groups is really facilitated by the interaction of the antigen-binding groove of the antibody with its epitope or interactions of other regions of the antibody with the plate-bound antigen is still unknown. While some claim that the polyreactivity is due to a higher flexibility of the antigen-binding pocket in polyreactive antibodies, there is not yet concrete evidence to support this hypothesis (79,80). We have shown that polyreactive IgM antibodies that have a high reactivity for HA in an ELISA do not bind to HA that is expressed on the surface of cells. While it could be argued that the sensitivity of the ELISA exceeds that of the flow cytometric assay, we hypothesize that the cell-based assay most likely presents the antigen in its native conformation and is thus more specific. Much emphasis has been placed on the length (81), hydrophobicity, and charge (82) of the CDR3 of the heavy chain of the antibody that supposedly confer polyreactivity. Neither we nor a group investigating the polyreactivity of antibodies specific for an HIV glycoprotein found any such correlation (83).

The discovery of B cells that co-express two different light chains has offered another possible mechanism for the emergence of autoreactive B cells. Receptor editing, the rearranging of a second light chain, is the most commonly employed process of the central tolerance checkpoint (31). In up to 5% of peripheral blood B cells, allelic exclusion after receptor editing is imperfect and more than one light chain is expressed (84). It was shown in mice that these dual light

chain expressing B cells often co-express an autoreactive and a non-autoreactive BCR (85). However, it is still unclear how relevant these B cells are in human autoimmunity.

Epitopes of AChR-specific antibodies

The epitope that an antibody binds to, but also the IgG subclass of the antibody can make the difference between raising an efficient immune response or succumbing to infection (86,87). While the IgG subclass is easily determined by sequencing or through the use of subclass specific secondary antibodies, the mapping of the binding of an antibody to a discrete region on the antigen remains challenging.

Despite the fact that 90% of antibodies are raised against discontinuous, conformation-dependent epitopes (50,88–91), most of the available methods for epitope mapping focus on continuous, also called linear epitopes. These methods comprise experimental approaches such as determining the binding of antibodies to short synthetic peptides (92) and computational approaches which make predictions based on algorithms (93). Structure based methods such as x-ray crystallography and nuclear magnetic resonance are more suited to investigate conformational epitopes, but are dependent on the antigen's ability to crystallize or go into solution respectively. They are expensive, technically challenging and require large amounts of antigen (94,95). Recent advances in mass-spectrometry have enabled the mapping of epitopes even on large proteins under non-denaturing conditions. Mass-spectrometry can deliver highly accurate information about the interactions between paratope and epitope atoms but remains an expensive approach that requires specialized equipment and personnel (96). In contrast, experimental approaches that introduce mutations or swap protein-subunits for related ones are cheaper alternatives that do not require much specialized equipment. The disadvantage of such experimental epitope mapping is that it often remains unclear whether the mutation is directly responsible for the loss of binding or whether this is due to a mutation-induced change in conformation of the antigen or steric hindrance. The same problem applies to the commonly used approach of preincubating AChR with the MIR-specific rat antibody mAb35. Concluding that a mAb35-induced inhibition of the binding of the investigated antibody means that both antibodies bind the same epitope ignores the complexities of the paratope-epitope interactions.

We envisage that the large panel of AChR-specific human mAbs that we have generated from patients with MG and from HC could be used for studies of affinity, epitope mapping, and pathogenicity, and thus provide essential clues on the etiology of the disease.

Conclusion and outlook

In the first part of this thesis, we reported a novel and highly sensitive and specific assay for the isolation of human B cells with specificity for any membrane-expressed antigen using influenza hemagglutinin as an example.

We then applied the membrane-antigen capture assay to the isolation of B cells specific for the autoantigen acetylcholine receptor in the rare autoimmune neurological disorder myasthenia gravis. Our findings indicate that AChR-specific B cells in MG patients can be clonally expanded, highly specific for AChR, somatically hypermutated, and mostly of the IgG_1 isotype. In contrast, IgM B cells with a BCR specificity for AChR were found both in patients with MG and in HCs. In both groups, clonally expanded IgM B cell clones with somatic hypermutations were present in the peripheral blood. Affinities of the recombinant IgM antibodies for AChR, as measured by binding to AChR in a cell-based assay, ranged from low to very high, and some recombinant IgM were polyreactive to unrelated antigens in an ELISA.

The presence of presumably antigen-experienced autoantigen-specific IgM B cells in HCs brings us back to the fundamental question of how an autoimmune disorder develops. Reverting the somatically hypermutated antibodies back to their original germline sequence and testing their specificity will provide information on whether the somatic hypermutations have increased, or perhaps even decreased the specificity of the antibody for AChR. In future experiments, the pathogenicity of the recombinant antibodies can be assessed in an animal model. First, cross-reactivity of the recombinant antibodies to rat AChR will be tested. Cross-reactive antibodies will then be transferred intravenously in a passive model of EAMG. To define the epitope specificity, chimeric AChRs will be expressed, where single subunits were exchanged with the corresponding subunit from a nonmammalian vertebrate such as zebrafish. The recombinant antibodies will then be tested for binding to the chimeric AChR.

References

1. Murphy KP. In: Janeway's Immunobiology. 8th ed. Garland Science; 2012. p. 275–90.

2. Van Regenmortel MHV. Mapping Epitope Structure and Activity: From One-Dimensional Prediction to Four-Dimensional Description of Antigenic Specificity. Methods. 1996 Jun;9(3):465–72.

3. Wardemann H. Predominant Autoantibody Production by Early Human B Cell Precursors. Science. 2003 Sep 5;301(5638):1374–7.

4. Goodnow CC, Crosbie J, Adelstein S, Lavoie TB, Smith-Gill SJ, Brink RA, et al. Altered immunoglobulin expression and functional silencing of self-reactive B lymphocytes in transgenic mice. Nature. 1988 Aug;334(6184):676–82.

5. Tiller T, Tsuiji M, Yurasov S, Velinzon K, Nussenzweig MC, Wardemann H. Autoreactivity in Human IgG+ Memory B Cells. Immunity. 2007 Feb;26(2):205–13.

6. Mietzner B, Tsuiji M, Scheid J, Velinzon K, Tiller T, Abraham K, et al. Autoreactive IgG memory antibodies in patients with systemic lupus erythematosus arise from nonreactive and polyreactive precursors. Proceedings of the National Academy of Sciences. 2008 Jul 15;105(28):9727–32.

7. De Silva NS, Klein U. Dynamics of B cells in germinal centres. Nat Rev Immunol. 2015 Mar;15(3):137–48.

8. Bannard O, Horton RM, Allen CDC, An J, Nagasawa T, Cyster JG. Germinal Center Centroblasts Transition to a Centrocyte Phenotype According to a Timed Program and Depend on the Dark Zone for Effective Selection. Immunity. 2013 Nov;39(5):912–24.

9. Klein U, Rajewsky K, Küppers R. Human Immunoglobulin IgM+IgD+ Peripheral Blood B Cells Expressing the CD27 Cell Surface Antigen Carry Somatically Mutated Variable Region Genes: CD27 as a General Marker for Somatically Mutated (Memory) B Cells. J Exp Med. 1998 Nov 2;188(9):1679–89.

10. Lindner JM, Cornacchione V, Sathe A, Be C, Srinivas H, Riquet E, et al. Human Memory B Cells Harbor Diverse Cross-Neutralizing Antibodies against BK and JC Polyomaviruses. Immunity. 2019 Mar;50(3):668-676.e5.

11. Benson MJ, Elgueta R, Schpero W, Molloy M, Zhang W, Usherwood E, et al. Distinction of the memory B cell response to cognate antigen versus bystander inflammatory signals. J Exp Med. 2009 Aug 31;206(9):2013–25.

12. Dogan I, Bertocci B, Vilmont V, Delbos F, Mégret J, Storck S, et al. Multiple layers of B cell memory with different effector functions. Nat Immunol. 2009 Dec;10(12):1292–9.

13. Pape KA, Taylor JJ, Maul RW, Gearhart PJ, Jenkins MK. Different B Cell Populations Mediate Early and Late Memory During an Endogenous Immune Response. Science. 2011 Mar 4;331(6021):1203–7.

14. Seifert M, Przekopowitz M, Taudien S, Lollies A, Ronge V, Drees B, et al. Functional capacities of human IgM memory B cells in early inflammatory responses and secondary germinal center reactions. Proc Natl Acad Sci USA. 2015 Feb 10;112(6):E546–55.

15. McHeyzer-Williams LJ, Milpied PJ, Okitsu SL, McHeyzer-Williams MG. Class-switched memory B cells remodel BCRs within secondary germinal centers. Nat Immunol. 2015 Mar;16(3):296–305.

16. Franz B, May KF, Dranoff G, Wucherpfennig K. Ex vivo characterization and isolation of rare memory B cells with antigen tetramers. Blood. 2011 Jul 14;118(2):348–57.

17. Wilson PC, Andrews SF. Tools to therapeutically harness the human antibody response. Nat Rev Immunol. 2012 Oct;12(10):709–19.

18. Marasco WA, Sui J. The growth and potential of human antiviral monoclonal antibody therapeutics. Nat Biotechnol. 2007 Dec;25(12):1421–34.

19. Traggiai E, Becker S, Subbarao K, Kolesnikova L, Uematsu Y, Gismondo MR, et al. An efficient method to make human monoclonal antibodies from memory B cells: potent neutralization of SARS coronavirus. Nat Med. 2004 Aug;10(8):871–5.

20. Matsumoto T, Yamada K, Noguchi K, Nakajima K, Takada K, Khawplod P, et al. Isolation and characterization of novel human monoclonal antibodies possessing neutralizing ability against rabies virus: Human mAb against rabies virus. Microbiology and Immunology. 2010 Nov;54(11):673–83.

21. Schieffelin JS, Costin JM, Nicholson CO, Orgeron NM, Fontaine KA, Isern S, et al. Neutralizing and non-neutralizing monoclonal antibodies against dengue virus E protein derived from a naturally infected patient. Virol J. 2010 Dec;7(1):28.

22. Morris L, Chen X, Alam M, Tomaras G, Zhang R, Marshall DJ, et al. Isolation of a Human Anti-HIV gp41 Membrane Proximal Region Neutralizing Antibody by Antigen-Specific Single B Cell Sorting. Nixon DF, editor. PLoS ONE. 2011 Sep 30;6(9):e23532.

23. Makino T, Nakamura R, Terakawa M, Muneoka S, Nagahira K, Nagane Y, et al. Analysis of peripheral B cells and autoantibodies against the anti-nicotinic acetylcholine receptor derived from patients with myasthenia gravis using single-cell manipulation tools. Saruhan-Direskeneli G, editor. PLoS ONE. 2017 Oct 17;12(10):e0185976.

24. Tiller T, Meffre E, Yurasov S, Tsuiji M, Nussenzweig MC, Wardemann H. Efficient generation of monoclonal antibodies from single human B cells by single cell RT-PCR and expression vector cloning. Journal of Immunological Methods. 2008 Jan;329(1–2):112–24.

25. Wykes M, Pombo A, Jenkins C, Gordon G. Dendritic Cells Interact Directly with Naive B Lymphocytes to Transfer Antigen and Initiate Class Switching in a Primary T-Dependent Response. JI. 1998 Aug 1;161(3):1313–9.

26. Carrasco YR, Batista FD. B cell recognition of membrane-bound antigen: an exquisite way of sensing ligands. Current Opinion in Immunology. 2006 Jun;18(3):286–91.

27. Batista FD, Iber D, Neuberger MS. B cells acquire antigen from target cells after synapse formation. Nature. 2001 May;411(6836):489–94.

28. Fleire SJ. B Cell Ligand Discrimination Through a Spreading and Contraction Response. Science. 2006 May 5;312(5774):738–41.

29. Natkanski E, Lee W-Y, Mistry B, Casal A, Molloy JE, Tolar P. B Cells Use Mechanical Energy to Discriminate Antigen Affinities. Science. 2013 Jun 28;340(6140):1587–90.

30. Spillane KM, Tolar P. B cell antigen extraction is regulated by physical properties of antigen-presenting cells. J Cell Biol. 2017 Jan 2;216(1):217–30.

31. Halverson R, Torres RM, Pelanda R. Receptor editing is the main mechanism of B cell tolerance toward membrane antigens. Nat Immunol. 2004 Jun;5(6):645–50.

32. Sanderson NSR, Zimmermann M, Eilinger L, Gubser C, Schaeren-Wiemers N, Lindberg RLP, et al. Cocapture of cognate and bystander antigens can activate autoreactive B cells. Proc Natl Acad Sci USA. 2017 Jan 24;114(4):734–9.

33. Boldingh MI, Maniaol AH, Brunborg C, Dekker L, Heldal AT, Lipka AF, et al. Geographical Distribution of Myasthenia Gravis in Northern Europe - Results from a Population-Based Study from Two Countries. Neuroepidemiology. 2015;44(4):221–31.

34. Gilhus NE, Skeie GO, Romi F, Lazaridis K, Zisimopoulou P, Tzartos S. Myasthenia gravis — autoantibody characteristics and their implications for therapy. Nat Rev Neurol. 2016 May;12(5):259–68.

35. Evoli A, Alboini PE, Damato V, Iorio R, Provenzano C, Bartoccioni E, et al. Myasthenia gravis with antibodies to MuSK: an update: An update on MuSK $^{+}$ MG. Ann NY Acad Sci. 2018 Jan;1412(1):82–9.

36. Higuchi O, Hamuro J, Motomura M, Yamanashi Y. Autoantibodies to low-density lipoprotein receptor-related protein 4 in myasthenia gravis. Ann Neurol. 2011 Feb;69(2):418–22.

37. Gilhus NE, Verschuuren JJ. Myasthenia gravis: subgroup classification and therapeutic strategies. The Lancet Neurology. 2015 Oct;14(10):1023–36.

38. Wolfe GI, Kaminski HJ, Aban IB, Minisman G, Kuo H-C, Marx A, et al. Randomized Trial of Thymectomy in Myasthenia Gravis. N Engl J Med. 2016 Aug 11;375(6):511–22.

39. Gilhus NE. Myasthenia Gravis. Longo DL, editor. N Engl J Med. 2016 Dec 29;375(26):2570–81.

40. Kerty E, Elsais A, Argov Z, Evoli A, Gilhus NE. EFNS/ENS Guidelines for the treatment of ocular myasthenia. Eur J Neurol. 2014 May;21(5):687–93.

41. Chiou-Tan FY, Gilchrist JM. Repetitive nerve stimulation and single-fiber electromyography in the evaluation of patients with suspected myasthenia gravis or Lambert-Eaton myasthenic syndrome: Review of recent literature: Electrodiagnosis in MG and LEMS. Muscle Nerve. 2015 Sep;52(3):455–62.

42. Chatzistefanou KI, Kouris T, Iliakis E, Piaditis G, Tagaris G, Katsikeris N, et al. The Ice Pack Test in the Differential Diagnosis of Myasthenic Diplopia. Ophthalmology. 2009 Nov;116(11):2236–43.

43. Unwin N. Refined Structure of the Nicotinic Acetylcholine Receptor at 4Å Resolution. Journal of Molecular Biology. 2005 Mar;346(4):967–89.

44. Görne-Tschelnokow U, Strecker A, Kaduk C, Naumann D, Hucho F. The transmembrane domains of the nicotinic acetylcholine receptor contain alpha-helical and beta structures. The EMBO Journal. 1994 Jan;13(2):338–41.

45. Liu Y, Padgett D, Takahashi M, Li H, Sayeed A, Teichert RW, et al. Essential roles of the acetylcholine receptor γ-subunit in neuromuscular synaptic patterning. Development. 2008 Apr 23;135(11):1957–67.

46. Yumoto N, Wakatsuki S, Sehara-Fujisawa A. The acetylcholine receptor γ-to-ε switch occurs in individual endplates. Biochemical and Biophysical Research Communications. 2005 Jun;331(4):1522–7.

47. Witzemann V, Schwarz H, Koenen M, Berberich C, Villarroel A, Wernig A, et al. Acetylcholine receptor epsilon-subunit deletion causes muscle weakness and atrophy in juvenile and adult mice. Proceedings of the National Academy of Sciences. 1996 Nov 12;93(23):13286–91.

48. Tindall RSA. Humoral immunity in myasthenia gravis: Biochemical characterization of acquired antireceptor antibodies and clinical correlations. Ann Neurol. 1981 Nov;10(5):437–47.

49. Rødgaard A, Nielsen FC, Djurup R, Somnier R, Gammeltoft S. Acetylcholine receptor antibody in myasthenia gravis: predominance of IgG subclasses 1 and 3. Clin exp Immunol. 1987;67(1):82–8.

50. Luo J, Taylor P, Losen M, de Baets MH, Shelton GD, Lindstrom J. Main Immunogenic Region Structure Promotes Binding of Conformation-Dependent Myasthenia Gravis Autoantibodies, Nicotinic Acetylcholine Receptor Conformation Maturation, and Agonist Sensitivity. Journal of Neuroscience. 2009 Nov 4;29(44):13898–908.

51. Ching KH, Burbelo PD, Kimball RM, Clawson LL, Corse AM, Iadarola MJ. Recombinant expression of the AChR-alpha1 subunit for the detection of conformation-dependent epitopes in Myasthenia Gravis. Neuromuscular Disorders. 2011 Mar;21(3):204–13.

52. Tzartos SJ, Sophianos D, Efthimiadis A. Role of the main immunogenic region of acetylcholine receptor in myasthenia gravis. An Fab monoclonal antibody protects against antigenic modulation by human sera. JI. 1985;134(4):2343–9.

53. Nastuk WL, Plescia OJ, Osserman KE. Changes in Serum Complement Activity in Patients with Myasthenia Gravis. Experimental Biology and Medicine. 1960 Oct 1;105(1):177–84.

54. Sahashi K, Engel AG, Lambert EH, Howard FM. Ultrastructural localization of the terminal and lytic ninth complement component (C9) at the motor endplate in myasthenia gravis. J Neuropathol Exp Neurol. 1979 Sep 17;(39):160–72.

55. Engel AG, Sahashi K, Fumagalli G. THE IMMUNOPATHOLOGY OF ACQUIRED MY ASTHENIA GRAVIS. Ann NY Acad Sci. 1981 Dec;377(1 Myasthenia Gr):158–74.

56. Howard JF. Myasthenia gravis: the role of complement at the neuromuscular junction: Role of complement in myasthenia gravis. Ann NY Acad Sci. 2018 Jan;1412(1):113–28.

57. Chamberlain-Banoub J, Neal JW, Mizuno M, Harris CL, Morgan BP. Complement membrane attack is required for endplate damage and clinical disease in passive experimental myasthenia gravis in Lewis rats. Clin Exp Immunol. 2006 Nov;146(2):278–86.

58. Tüzün E, Scott BG, Goluszko E, Higgs S, Christadoss P. Genetic Evidence for Involvement of Classical Complement Pathway in Induction of Experimental Autoimmune Myasthenia Gravis. J Immunol. 2003 Oct 1;171(7):3847–54.

59. Nakano S, Engel AG. Myasthenia gravis: Quantitative immunocytochemical analysis of inflammatory cells and detection of complement membrane attack complex at the end-plate in 30 patients. Neurology. 1993 Jun 1;43(6):1167–1167.

60. Howard JF, Barohn RJ, Cutter GR, Freimer M, Juel VC, Mozaffar T, et al. A randomized, double-blind, placebo-controlled phase II study of eculizumab in patients with refractory generalized myasthenia gravis: Eculizumab in Refractory MG. Muscle Nerve. 2013 Jul;48(1):76–84.

61. Howard JF, Utsugisawa K, Benatar M, Murai H, Barohn RJ, Illa I, et al. Safety and efficacy of eculizumab in anti-acetylcholine receptor antibody-positive refractory generalised myasthenia gravis (REGAIN): a phase 3, randomised, double-blind, placebo-controlled, multicentre study. The Lancet Neurology. 2017 Dec;16(12):976–86.

62. Iorio R, Damato V, Alboini PE, Evoli A. Efficacy and safety of rituximab for myasthenia gravis: a systematic review and meta-analysis. J Neurol. 2015 May;262(5):1115–9.

63. Topakian R, Zimprich F, Iglseder S, Embacher N, Guger M, Stieglbauer K, et al. High efficacy of rituximab for myasthenia gravis: a comprehensive nationwide study in Austria. J Neurol. 2019 Mar;266(3):699–706.

64. Sims GP, Shiono H, Willcox N, Stott DI. Somatic Hypermutation and Selection of B Cells in Thymic Germinal Centers Responding to Acetylcholine Receptor in Myasthenia Gravis. J Immunol. 2001 Aug 15;167(4):1935–44.

65. Vrolix K, Fraussen J, Losen M, Stevens J, Lazaridis K, Molenaar PC, et al. Clonal heterogeneity of thymic B cells from early-onset myasthenia gravis patients with antibodies against the acetylcholine receptor. Journal of Autoimmunity. 2014 Aug;52:101–12.

66. Gerli R, Paganelli R, Cossarizza A, Muscat C, Piccolo G, Barbieri D, et al. Long-term immunologic effects of thymectomy in patients with myasthenia gravis. J Allergy Clin Immunol. 1999 May;103(5):865–72.

67. Silvestri NJ, Wolfe GI. Treatment-Refractory Myasthenia Gravis: Journal of Clinical Neuromuscular Disease. 2014 Jun;15(4):167–78.

68. Gilhus NE, Tzartos S, Evoli A, Palace J, Burns TM, Verschuuren JJGM. Myasthenia gravis. Nat Rev Dis Primers. 2019 Dec;5(1):30.

69. Zimmermann M, Rose N, Lindner JM, Kim H, Gonçalves AR, Callegari I, et al. Antigen Extraction and B Cell Activation Enable Identification of Rare Membrane Antigen Specific Human B Cells. Front Immunol. 2019 Apr 16;10:829.

70. Yurasov S, Wardemann H, Hammersen J, Tsuiji M, Meffre E, Pascual V, et al. Defective B cell tolerance checkpoints in systemic lupus erythematosus. J Exp Med. 2005 Mar 7;201(5):703–11.

71. Menard L, Samuels J, Ng Y-S, Meffre E. Inflammation-independent defective early B cell tolerance checkpoints in rheumatoid arthritis. Arthritis & Rheumatism. 2011 May;63(5):1237–45.

72. Lee J-Y, Stathopoulos P, Gupta S, Bannock JM, Barohn RJ, Cotzomi E, et al. Compromised fidelity of B-cell tolerance checkpoints in AChR and MuSK myasthenia gravis. Ann Clin Transl Neurol. 2016 Jun;3(6):443–54.

73. Nakamura M, Burastero SE, Notkins AL, Casal P. Human monoclonal rheumatoid factor-like antibodies from CD5 (Leu-1)+ B cells are polyreactive. :8.

74. Lydyard PM, Quartey-Papafio R, Broker B, Mackenzie L, Jouquan J, Blaschek MA, et al. The Antibody Repertoire of Early Human B Cells I. High Frequency of Autoreactivity and Polyreactivity. Scand J Immunol. 1990 Jan;31(1):33–43.

75. Chen ZJ, Wheeler J, Notkins AL. Antigen-binding B cells and polyreactive antibodies. Eur J Immunol. 1995 Feb;25(2):579–86.

76. Huse K, Böhme H-J, Scholz GH. Purification of antibodies by affinity chromatography. Journal of Biochemical and Biophysical Methods. 2002 May;51(3):217–31.

77. Meffre E, Schaefer A, Wardemann H, Wilson P, Davis E, Nussenzweig MC. Surrogate Light Chain Expressing Human Peripheral B Cells Produce Self-reactive Antibodies. J Exp Med. 2004 Jan 5;199(1):145–50.

78. Robbiani DF, Bozzacco L, Keeffe JR, Khouri R, Olsen PC, Gazumyan A, et al. Recurrent Potent Human Neutralizing Antibodies to Zika Virus in Brazil and Mexico. Cell. 2017 May;169(4):597-609.e11.

79. Notkins AL. Polyreactivity of antibody molecules. Trends in Immunology. 2004 Apr;25(4):174–9.

80. Zhou Z-H, Tzioufas AG, Notkins AL. Properties and function of polyreactive antibodies and polyreactive antigen-binding B cells. Journal of Autoimmunity. 2007 Dec;29(4):219–28.

81. Meffre E, Milili M, Blanco-Betancourt C, Antunes H, Nussenzweig MC, Schiff C. Immunoglobulin heavy chain expression shapes the B cell receptor repertoire in human B cell development. The Journal of Clinical Investigation. 2001;108(6):9.

82. Aguilera I, Melero J, Nunez-Roldan A, Sanchez B. Molecular structure of eight human autoreactive monoclonal antibodies. Immunology. 2001 Mar;102(3):273–80.

83. Mouquet H, Scheid JF, Zoller MJ, Krogsgaard M, Ott RG, Shukair S, et al. Polyreactivity increases the apparent affinity of anti-HIV antibodies by heteroligation. Nature. 2010 Sep;467(7315):591–5.

84. Melchers F. Checkpoints that control B cell development. J Clin Invest. 2015 Jun 1;125(6):2203–10.

85. Li Y, Li H, Weigert M. Autoreactive B Cells in the Marginal Zone that Express Dual Receptors. J Exp Med. 2002 Jan 21;195(2):181–8.

86. Benhnia MR-E-I, McCausland MM, Laudenslager J, Granger SW, Rickert S, Koriazova L, et al. Heavily Isotype-Dependent Protective Activities of Human Antibodies against Vaccinia Virus Extracellular Virion Antigen B5. Journal of Virology. 2009 Dec 1;83(23):12355–67.

87. Hofmeister Y, Planitzer CB, Farcet MR, Teschner W, Butterweck HA, Weber A, et al. Human IgG Subclasses: In Vitro Neutralization of and In Vivo Protection against West Nile Virus. Journal of Virology. 2011 Feb 15;85(4):1896–9.

88. Huang J, Honda W. CED: A conformational epitope database. BMC Immunol. 2006;7(1):7.

89. Hadlock KG, Lanford RE, Perkins S, Rowe J, Yang Q, Levy S, et al. Human Monoclonal Antibodies That Inhibit Binding of Hepatitis C Virus E2 Protein to CD81 and Recognize Conserved Conformational Epitopes. Journal of Virology. 2000 Nov 15;74(22):10407–16.

90. Vinion-Dubiel AD, McClain MS, Cao P, Mernaugh RL, Cover TL. Antigenic Diversity among Helicobacter pylori Vacuolating Toxins. Infection and Immunity. 2001 Jul 1;69(7):4329–36.

91. Sun J, Kudahl UJ, Simon C, Cao Z, Reinherz EL, Brusic V. Large-Scale Analysis of B-Cell Epitopes on Influenza Virus Hemagglutinin – Implications for Cross-Reactivity of Neutralizing Antibodies. Front Immunol [Internet]. 2014 [cited 2019 Oct 28];5. Available from: http://journal.frontiersin.org/article/10.3389/fimmu.2014.00038/abstract

92. Bellone M, Tang F, Milius R, Conti-Tronconi BM. The main immunogenic region of the nicotinic acetylcholine receptor. Identification of amino acid residues interacting with different antibodies. :13.

93. Yao B, Zheng D, Liang S, Zhang C. Conformational B-Cell Epitope Prediction on Antigen Protein Structures: A Review of Current Algorithms and Comparison with Common Binding Site Prediction Methods. Fang D, editor. PLoS ONE. 2013 Apr 19;8(4):e62249.

94. Abbott WM, Damschroder MM, Lowe DC. Current approaches to fine mapping of antigen-antibody interactions. Immunology. 2014 Aug;142(4):526–35.

95. Rosenzweig R, Kay LE. Solution NMR Spectroscopy Provides an Avenue for the Study of Functionally Dynamic Molecular Machines: The Example of Protein Disaggregation. J Am Chem Soc. 2016 Feb 10;138(5):1466–77.

96. Opuni KFM, Al-Majdoub M, Yefremova Y, El-Kased RF, Koy C, Glocker MO. Mass spectrometric epitope mapping: ELUCIDATION OF ANTIGENIC DETERMINANT REGIONS BY MASS SPECTROMETRY. Mass Spec Rev. 2018 Mar;37(2):229–41.